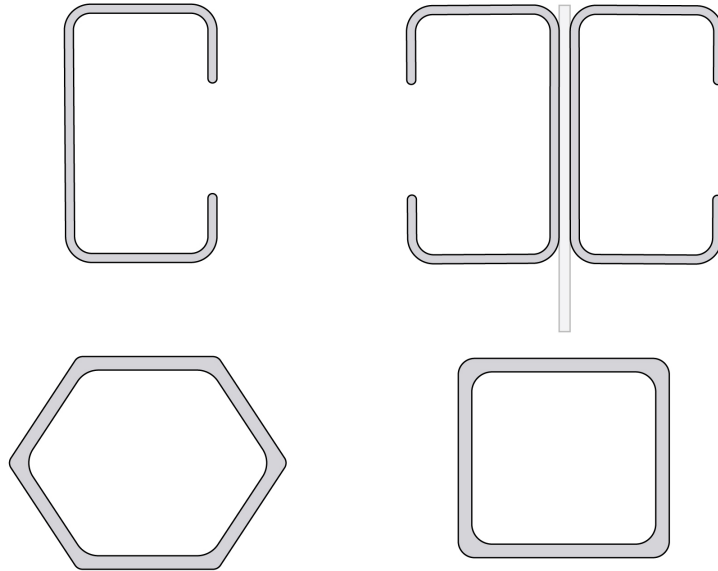




**CHALMERS**  
UNIVERSITY OF TECHNOLOGY



# Optimization of Cold-formed Steel Sections using Genetic Algorithm

Master's thesis in Master Program Structural Engineering and Building Technology

SARAH AREF

MAHDI MAHDI

---

Department of Architecture and Civil Engineering

CHALMERS UNIVERSITY OF TECHNOLOGY  
Gothenburg, Sweden 2022  
[www.chalmers.se](http://www.chalmers.se)



MASTER'S THESIS ACEX30 2022

# Optimization of Cold-formed Steel Sections using Genetic Algorithm

SARAH AREF  
MAHDI MAHDI



**CHALMERS**  
UNIVERSITY OF TECHNOLOGY

Department of Architecture and Civil Engineering  
*Division of Structural Engineering*  
Lightweight Structures  
CHALMERS UNIVERSITY OF TECHNOLOGY  
Gothenburg, Sweden 2022

Optimization of Cold-formed Steel Sections using Genetic Algorithm  
SARAH AREF  
MAHDI MAHDI

© SARAH AREF, MAHDI MAHDI, 2022.

Examiner: Professor Mohammad Al-Emrani, Department of Architecture and Civil Engineering  
Supervisor: Professor Mohammad Al-Emrani, Department of Architecture and Civil Engineering

Master's Thesis 2022  
Department of Architecture and Civil Engineering  
Division of Structural Engineering  
Lightweight Structures  
Chalmers University of Technology  
SE-412 96 Gothenburg  
Telephone +46 31 772 1000

Cover: An illustration of different cold-formed steel cross-sections.

Typeset in L<sup>A</sup>T<sub>E</sub>X  
Printed by Chalmers Reproservice  
Gothenburg, Sweden 2022



# Optimization of Cold-formed Steel Sections using Genetic Algorithm

SARAH AREF

MAHDI MAHDI

Department of Architecture and Civil Engineering

Chalmers University of Technology

## Abstract

Most research done on optimization of cold-formed steel members focuses on a single cross-section with set conditions and steel yield strengths. How would this optimization look if different cold-formed cross-sections are compared. Furthermore, how would different cold-formed cross-sections with varying steel yield strength behave in a global optimization.

The aim is to study how to reach optimized cross-sections (profiles) for roof trusses in different steel strength classes using a genetic algorithm and create a library of the most optimized cross-sections for certain spans and applied loads.

The four selected cross-sections to be analysed are C-section, double back-to-back C-section, hollow square-section and hollow hexagon-section. These profiles can act as diagonals in a roof truss and the compressed diagonals will be analysed. As for the upper chord which is subjected to both compression and bending, only double back-to-back C-sections will be optimized. `Matlab` functions were generated to calculate the required parameters, buckling modes and capacities for the selected sections. These functions were connected to a genetic algorithm to find the most optimized dimensions for each section. Lastly the most optimized cross-sections with respect to smallest area were selected for different load and span length combination to create a library.

The results of the genetic algorithm showed that for the upper chord the higher the steel strength the smaller the area becomes but the section with higher steel strength have a lower utilization ratio. The diagonals which were divided into two groups and were analysed separately showed that the most optimized shape to use is a hollow square-section. However, the connection between the upper chord and the diagonals will not be feasible with closed cross-sections used as diagonals. The chosen cross-section shape is therefore C-section.

Keywords: steel, cold-formed, cross-section, optimization, genetic algorithm, roof truss, Eurocode 3.



Optimering av kallformade stålsektioner med hjälp av genetisk algoritm  
SARAH AREF  
MAHDI MAHDI  
Institutionen för arkitektur och samhällsbyggnad  
Chalmers tekniska högskola

## Sammanfattning

Syftet med det här examensarbetet är att studera hur valet av lämpliga kallformade stålsektioner som ska användas i en takstolsbalk sker med hjälp av en genetisk algoritm. Stålsektionerna ska även optimeras med avseende på olika sträckgränser för stålet. Efter körningen av optimeringen ska ett bibliotek med olika stålsektioner skapas för olika spannlängder och krafter.

De fyra valda tvärsnitten är; C-sektion, dubbel C-sektion, kvadratisk hålprofil och hexagon hålprofil. Alla dessa fyra profiler kommer att analyseras som diagonaler i takstolen medan endast dubbel C-sektionen kommer att analyseras som överramstång. `Matlab` har använts för att skapa funktioner som beräknar olika parametrar och kapacitet för de valda profilerna. Med hjälp av genetisk algoritm hittades de mest optimala dimensionerna för de valda lasterna och spannlängderna av takstolsbalken.

Examensarbetet resulterade i att de mest optimala tvärsektionerna för övre ramstången är dubbla C-sektioner med sträckgränsen 460 MPa. Lägsta arean erhöles för stål med sträckgräns 690 MPa men tvärsnittet utnyttjades inte fullt ut och därför valdes stål av typen S460 för de olika tvärsnitten för överramstången. Optimeringen av diagonalerna medförde att kvadratiske hålprofiler är de mest optimala. I praktiken är det dock mer lämpligt att fästa en öppen tvärsektion med dubbel C-profilen för övre ramstången. Därav väljs öppen C-profil för de tryckta diagonalerna.

Nyckelord: stål, kallformning, tvärsektioner, optimering, genetisk algoritm, takstol, Eurocode 3.



# Acknowledgements

This master's thesis was written at Chalmers University of Technology during spring 2022 and was carried out at the division of Structural Engineering and Building Technology. The thesis is a part of a research project that is carried out by Chalmers University of Technology and different companies from the construction industry.

We would like to thank our examiner and supervisor Mohammad Al-Emrani, full professor in steel structures at Chalmers, for his great support and guidance through the project. His knowledge and feedback have helped us greatly. A big thank you to our opponent group, Alaa Achour and Ziad Mlli, for their valuable feedback during the project.

Sarah Aref & Mahdi Mahdi, Gothenburg, June 2022



# Contents

<b>List of Figures</b>	<b>xv</b>
<b>List of Tables</b>	<b>xvii</b>
<b>Nomenclature</b>	<b>xix</b>
<b>1 Introduction</b>	<b>1</b>
1.1 Background . . . . .	1
1.2 Aim . . . . .	2
1.3 Scope and limitation . . . . .	2
1.4 Methodology . . . . .	2
<b>2 Cold-formed steel sections</b>	<b>3</b>
2.1 Introduction to cold-formed steel sections . . . . .	3
2.2 Method of production . . . . .	5
2.2.1 Roll forming . . . . .	5
2.2.2 Folding and press braking . . . . .	6
2.3 Applications . . . . .	7
<b>3 Structural behaviour of cold-formed steel elements</b>	<b>11</b>
3.1 Material limitations . . . . .	11
3.2 Dimension limitations . . . . .	12
3.2.1 Cross-section analysis and classification . . . . .	12
3.2.2 Effective width method . . . . .	15
3.2.3 Ratios of interest . . . . .	18
3.3 Imperfections . . . . .	20
3.3.1 Global imperfection for frames and bracing systems . . . . .	20
3.3.2 Local imperfections for individual members . . . . .	22
3.4 Local instability . . . . .	23
3.5 Members buckling resistance . . . . .	26
3.5.1 Roof truss girders: assumptions and buckling modes . . . . .	26
3.5.2 Compression . . . . .	28
3.5.2.1 Flexural buckling resistance . . . . .	28
3.5.2.2 Torsional and torsional-flexural buckling resistance . . . . .	29
3.5.3 Bending moment . . . . .	30
3.5.4 Combined load action . . . . .	32
3.5.4.1 Cross-section load carrying capacity criterion . . . . .	32

3.5.4.2	Interaction of bending and compression for buckling resistance . . . . .	34
<b>4</b>	<b>Roof truss girders</b>	<b>37</b>
4.1	Loads and spans . . . . .	38
4.1.1	Upper chord . . . . .	38
4.1.2	Compressed diagonals . . . . .	40
4.2	Cross-sections . . . . .	43
<b>5</b>	<b>Optimization of cross-sections in Matlab</b>	<b>45</b>
5.1	Matlab implementation . . . . .	45
5.1.1	Cross-section idealization . . . . .	45
5.1.2	Matlab implementation of cross-section resistance . . . . .	48
5.2	Cross-section optimization using genetic algorithm . . . . .	50
5.2.1	What is a genetic algorithm? . . . . .	51
5.2.2	Genetic algorithm implementation . . . . .	51
<b>6</b>	<b>Results and discussion</b>	<b>55</b>
6.1	Upper chord . . . . .	56
6.2	Compressed diagonals . . . . .	59
6.2.1	Diagonal group 1 . . . . .	59
6.2.1.1	Square cross-section vs hexagon cross-section . . . . .	63
6.2.1.2	Single C-section vs double C-section . . . . .	65
6.2.2	Diagonal group 2 . . . . .	66
<b>7</b>	<b>Conclusion</b>	<b>73</b>
7.1	Upper chord . . . . .	73
7.2	Compressed diagonals . . . . .	74
7.3	Further studies . . . . .	75
	<b>Bibliography</b>	<b>77</b>
<b>A</b>	<b>Appendix: Matlab functions</b>	<b>I</b>
A.1	Cross-section classification . . . . .	I
A.2	Distance to centroid . . . . .	V
A.3	Second moment of area . . . . .	VII
A.4	Flange reduction . . . . .	X
A.5	Distorsional buckling . . . . .	XV
A.6	Reduction of hexagon . . . . .	XXIII
A.7	Web reduction . . . . .	XXVIII
A.8	Torsion constant . . . . .	XXXIV
A.9	Warping constant . . . . .	XXXVI
A.10	Flexural buckling . . . . .	XXXVII
A.11	Torsional buckling . . . . .	XL
A.12	Flexural-torsional buckling . . . . .	XLII
A.13	Lateral-torsional buckling . . . . .	XLV
A.14	Interaction of combined bending and axial compression . . . . .	XLVIII



<b>B</b>	<b>Appendix: Example of cross-section resistance calculations</b>	<b>LIII</b>
<b>C</b>	<b>Appendix: Genetic Algorithm</b>	<b>LIX</b>



# List of Figures

2.1	Typical cross-sections for cold-formed steel sections. . . . .	3
2.2	Roll forming production setup at Bendirol. . . . .	5
2.3	Roll forming production machines at Bendirol. . . . .	6
2.4	Example of complex cross-sections produced by Bendirol. . . . .	6
2.5	Steel framing made of cold-formed steel elements (Dubina et al., 2012) (p.35). . . . .	7
2.6	Wall partitioning made of cold-formed steel elements (Dubina et al., 2012) (p.36). . . . .	8
2.7	Large panels for housing (Dubina et al., 2012) (p.37). . . . .	8
2.8	Roof trusses made of cold-formed steel-sections (Dubina et al., 2012) (p.40). . . . .	9
2.9	Roof purlins made of cold-formed Z-section (Dubina et al., 2012) (p.411). . . . .	9
3.1	Behaviour of a cross-section in different cross-section classifications, figure inspired by Al-Emrani et al. (2013). . . . .	13
3.2	Effective width of plate under compression (Al-Emrani et al., 2013) . . . . .	16
3.3	Equivalent sway imperfection (Eurocode 1993-1-1 (2005) figure 5.2) . . . . .	20
3.4	Replacement of initial sway imperfection by system of horizontal forces (Eurocode 1993-1-1 (2005) figure 5.4) . . . . .	21
3.5	Equivalent stabilizing force (Eurocode 1993-1-1 (2005) figure 5.6) . . . . .	22
3.6	Initial imperfection ( $e_{0,d}$ ) of a column with length $L$ and compressive force $N_{Ed}$ (Eurocode 1993-1-1 (2005) figure 5.4). . . . .	22
3.7	Illustrative figures for different buckling modes, created in the software Abaqus. . . . .	24
3.8	Equivalent stabilizing force (Eurocode 1993-1-3 (2006) figure 5.6). . . . .	25
3.9	Example of analysed roof truss girder. . . . .	27
3.10	Moment due to eccentricity of the shifted natural axis. . . . .	33
3.11	Moment diagram for upper chord of a roof truss girder with evenly distributed load. . . . .	36
4.1	Dimensions and load for analysed roof truss girder. . . . .	37
4.2	Mid span moments for top chord elements. . . . .	39
4.3	Ratios between mid span moments, start moments and end moments for top chord elements. . . . .	39
4.4	Moment distribution for upper chord. . . . .	39
4.5	Axial forces for top chord elements. . . . .	40

4.6	Length for diagonal elements. . . . .	41
4.7	Axial forces for diagonal elements (only compression is shown). . . . .	42
4.8	Scatter of lengths vs axial force for diagonals. . . . .	42
4.9	C-section for diagonals. . . . .	43
4.10	Double back-to-back c-section for diagonals and upper chord. . . . .	44
4.11	Connection between upper chord and diagonals. . . . .	44
4.12	Square cross-section for diagonals. . . . .	44
4.13	Hexagon cross-section for diagonals. . . . .	44
5.1	The chosen cold-formed cross-sections. . . . .	45
5.2	Idealization of C cross-section. . . . .	46
5.3	Coordinates for idealized C cross-section. . . . .	47
5.4	Bending axis and distance to neutral axis. . . . .	48
5.5	Flowchart for procedure to obtain cross-sectional parameters. . . . .	49
5.6	Flowchart for procedure to obtain cross-section capacity. . . . .	50
5.7	Flowchart for GA-optimization of cross-sections . . . . .	52
5.8	Convergence study for variables with different population sizes. . . . .	53
6.1	Area needed to obtain enough load carrying resistance for different steel qualities; Upper chord $L = 3\text{ m}$ . . . . .	56
6.2	Cross-section of upper chord element. . . . .	56
6.3	Moment distribution over the upper chord. . . . .	56
6.4	Ratios between areas needed to obtain enough load carrying resistance for different steel yield strengths; Upper chord $L = 3\text{ m}$ . . . . .	57
6.5	Dimensions of upper chord cross-section vs applied force. . . . .	58
6.6	Area needed to obtain enough load carrying capacity for different cross-sections; diagonal 1. . . . .	60
6.7	Cross-section of diagonal 1. . . . .	61
6.8	Back-to-back C-section used as diagonal. . . . .	62
6.9	Square cross-section shape for different span lengths in group diagonal 1. Cross-section capacity determined by local buckling if cross-section area is reduced (class 4). . . . .	63
6.10	Hexagon cross-section shape for different span lengths in group diagonal 1. Cross-section capacity determined by local buckling if cross-section area is reduced (class 4). . . . .	64
6.11	Second moment of area for C-section and double C-section. . . . .	66
6.12	Area needed to obtain enough load carrying capacity for different cross-sections; diagonal 2, $f_y = 355\text{ MPa}$ . . . . .	67
6.13	Area needed to obtain enough load carrying capacity for different cross-sections; diagonal 2, $f_y = 460\text{ MPa}$ . . . . .	68
6.14	Area needed to obtain enough load carrying capacity for different cross-sections; diagonal 2, $f_y = 690\text{ MPa}$ . . . . .	69
6.15	Hexagon cross-section for diagonal 2 . . . . .	70
6.16	Square cross-section for diagonal 2 . . . . .	70
7.1	Bolt connection between upper chord and diagonal. Upper chord consist of a double back-to-back C-section with a gap. . . . .	75

# List of Tables

3.1	Maximum width-to-thickness ratios for compression parts: internal compression parts (Eurocode 1993-1-1 (2005) table 5.2). . . . .	14
3.2	Maximum width-to-thickness ratios for compression parts: Outstand flanges (Eurocode 1993-1-1 (2005) table 5.2). . . . .	15
3.3	Effective width for internal compression elements subjected to compression (Eurocode 1993-1-5 (2006)). . . . .	17
3.4	Effective width for outstand compression elements subjected to compression (Eurocode 1993-1-5 (2006)). . . . .	18
3.5	Conditions for welding cold-formed steel elements zones and adjacent material (Eurocode 1993-1-8 (2005) table 4.2). . . . .	19
3.6	Loading and support coefficients as seen in Dubina et al. (2012). . . .	32
3.7	Interaction factors for members susceptible to torsional deformations, (Eurocode 1993-1-1 (2005), table B.2). . . . .	34
3.8	Interaction factors for members not susceptible to torsional deformations, (Eurocode 1993-1-1 (2005), table B.1). . . . .	35
3.9	Equivalent uniform moment factors $C_m$ , (Eurocode 1993-1-1 (2005), table B.3). . . . .	36
4.1	Analysed spans, heights and evenly distributed loads for the roof truss girders. . . . .	37
4.2	Forces used to optimize the cross-section of the upper chord. . . . .	40
4.3	Axial forces and lengths to be used for cross-section optimization. . .	43
5.1	Lower and upper bounds for the variables. . . . .	52
5.2	Input data for GA-options. . . . .	53
5.3	Geometrical constraints applied from Eurocode 1993-1-3 (2006). . . .	53
6.1	Optimized cross-sections for different applied loads; upper chord $f_y = 460 \text{ MPa}$ . . . . .	57
6.2	Cross-section dimensions for applied normal force $N_{Ed} = 700 \text{ kN}$ and different steel strengths. . . . .	59
6.3	Optimized cross-sections for different length of diagonal elements with applied force $N_{Ed} = 100 \text{ kN}$ ; diagonal 1 $f_y = 690 \text{ MPa}$ (square cross-section). . . . .	61
6.4	Library for diagonal group 1 with applied force $N_{Ed} = 100 \text{ kN}$ consisting of C-section with S690 steel ( $f_y = 690 \text{ MPa}$ ). . . . .	61

6.5	Square cross-section vs hexagon cross-section effective area and second moment of area for different length of diagonals $f_y = 690 \text{ MPa}$ . . . . .	64
6.6	Optimized cross-sections type for different length and applied forces of diagonal elements; diagonal 2. . . . .	70
6.7	Dimension of optimized cross-sections described in table 6.6. . . . .	71
6.8	Library for diagonal group 2 with consisting of C-section with S690 steel ( $f_y = 690 \text{ MPa}$ ). . . . .	72
7.1	Library for upper chord consisting of back-to-back double C-section, $f_y = 460 \text{ MPa}$ . . . . .	73
7.2	Library for compressed diagonals consisting of C-section, $f_y = 690 \text{ MPa}$	74







# Nomenclature

## Greek letters

$\alpha$	Imperfection factor dependent on the buckling curves
$\alpha_h$	Reduction factor for height h applicable to columns
$\alpha_m$	Reduction factor for the number of columns in a row
$\alpha_{cr}$	Factor by which the design loads would have to be increased to cause elastic instability in a global mode
$\bar{\lambda}$	Relative slenderness
$\beta$	Correction factor for the lateral
$\chi$	Reduction factor for the relevant buckling mode
$\Delta M_{y.Ed}$	Additional moment due to shift in centroid
$\delta$	Deflection of the stiffener due to unit load u
$\delta_q$	In-plane deflection of a bracing system
$\epsilon$	Strain ratio
$\epsilon_u$	Ultimate strain
$\epsilon_y$	Yield strain
$\gamma_{M1}$	Partial factor for resistance of members to instability assessed by member checks
$\lambda$	Non dimensional slenderness
$\phi$	Global initial sway imperfection
$\phi_0$	Basic value for global initial sway imperfection
$\psi$	Stress distribution
$\rho$	Reduction factor for width of an element
$\sigma_{cr}$	Elastic critical buckling stress
$\theta$	Angle of deformation

## Roman letters

$A$	Cross-sectional area
$A_0$	Original cross-sectional area
$A_g$	Gross cross-sectional area

$A_s$	Effective cross-sectional area of the edge stiffener
$A_{eff}$	Reduced cross-sectional area
$b_1$	Distance from web to the center of the effective area of the edge stiffener
$b_f$	Width of flange
$b_p$	Notional flat width of plane element
$b_{eff}$	Effective width
$C_1, C_2, C_3$	Coefficients dependent on the loading conditions and support conditions
$C_\theta$	Spring stiffness for rotation
$C_{my}, C_{mLT}$	Equivalent uniform moment factors
$E$	Modulus of elasticity (for steel $E=210$ GPa)
$e_0$	Maximum amplitude of a member imperfection
$e_{Ny}$	shift of centroid in z-z axis
$f_u$	Tensile strength or ultimate strength for steel
$f_y$	Yield strength
$F_{cr}$	Elastic critical buckling load for global instability mode based on initial elastic stiffnesses
$F_{Ed}$	Design load on the structure
$f_{ya}$	Average yield strength
$f_{yb}$	Basic yield strength
$G$	Shear modulus
$H$	Height of roof truss girder
$h$	Height of the structure
$h_w$	Height of web
$i$	Radius of gyration about the relevant axis, using the properties of the gross cross-section
$I_s$	Effective second moment of area of the stiffener
$I_T$	Torsion constant
$I_W$	Warping constant
$K$	Spring stiffness for displacement
$k$	Numerical coefficient that depends on the type of forming
$k_f$	Ratio of length for top and bottom flange
$k_\sigma$	Buckling factor
$k_{yy}, k_{zy}$	Interaction factors
$L$	Length of the bracing system
$L_{cr}$	Buckling length of the member

$m$	Number of columns in a row
$M_{c.Rd}$	Design resistance of the cross-section for uniform bending
$M_{cr}$	Elastic critical moment for lateral-torsional buckling
$M_{Ed}$	Design bending moment
$n$	Number of 90 bends in the cross-section with an internal radius $r \leq 5$
$N_{b,Rd}$	Design buckling resistance of compression member
$N_{c.Rd}$	Design resistance of the cross-section for uniform compression
$N_{cr}$	Elastic critical force for the relevant buckling mode based on the gross cross sectional properties
$N_{Ed}$	Design value of the applied axial force
$N_{vars}$	Number of variables
$Q$	Uniformly distributed load
$q_d$	Equivalent design force per unit length
$r$	Internal bend radius
$t$	Design core thickness of the steel material before cold-forming, exclusive of metal and organic coating
$t_0$	Thickness of element
$u$	Unit load per unit length
$\nu$	Poisson's ratio in elastic stage
$W$	Section modulus
$W_{eff}$	Section modulus of effective cross-section
$y_o, z_o$	Shear centre coordinates with respect to to the centroid of gross cross-section
$y_{tp}, z_{tp}$	Distance to centroid of cross-section

# 1

## Introduction

### 1.1 Background

Steel is a commonly used material in structural elements and withing steel construction there are many ways to shape the steel cross-sections, for instance through welding, hot-rolling and cold-forming. Steel members that are shaped by cold-forming is widely used in industrial buildings as framing and as storage rack systems (Yu et al., 2010). As well as for highway products, sheeting, piping and it has a broad application in the car industry.

A possible way to optimize steel members is through cold-forming of thin steel plates. These members can be used in truss structures in different applications. Various shapes and dimensions can be achieved through cold-forming sections with different yield strength. More complex sections can be produced through cold-forming when it is compared to hot-rolled (Dubina et al., 2012) and this gives a wide potential to the material. Furthermore, cold-formed steel members can be produced through a process called roll-forming, where steel sheets are run through a series of rolls to produce the desired cross-section. Roll-forming means more complex cross-section can be mass produced in a rather inexpensive way (Rhodes, 1991).

In design, local buckling and different types of global instabilities become critical and various failure modes need to be checked, for such thin-walled members. Moreover, Dubina et al. (2012) describes that thin-walled cold-formed steel members of high yield strengths are not widely used in roof truss girders due to the lack of knowledge on the behaviour of these members. In particular the buckling of thin-walled cold-formed are more complicated to consider in comparison to hot-rolled members. This is due to the complexity of the cold-formed cross-sections (Dubina et al., 2012).

Most research done on optimization of cold-formed steel members focuses on a single cross-section with set conditions and steel yield strengths. Tran, Li (2006) method of global optimization for channeled cold-formed steel sections gives a good point to start. However, as mentioned before the global optimization done by Tran, Li (2006) is for a single cross-section. How would this optimization look if different cold-formed cross-sections are compered? Furthermore, how would different cold-formed cross-sections with varying steel yield strength behave in a global optimization?

### 1.2 Aim

The aim is to study how to reach optimized cross-sections (profiles) for roof trusses in different steel strength classes using a genetic algorithm and create a library of the most optimized cross-sections for certain spans and applied loads. The different cross-sections are also to be compared. This master's thesis is a part of an ongoing research project, including Chalmers and companies from the industry, which focuses on roof trusses, pedestrian and bicycle bridges.

### 1.3 Scope and limitation

This study will focus on thin-walled steel members not thicker than  $5\text{ mm}$ . The different steel yield strengths that are of interest in this project are  $S355$ ,  $S460$ ,  $S690$ , other steel yield strengths will not be considered in this master thesis. The number of cross-section shapes will be confined to 4. Further limitations are to consider roof trusses in spans from  $30\text{ m}$  up to  $40\text{ m}$  which are common length of the investigated roof truss girders in the research project.

The project will be limited to only consider one load case with uniformly distributed load on roof trusses and the calculations and checks will only be done for ultimate limit state, ULS, and not for service limit state, SLS. The length of the spans as well as the magnitudes of the loads to be applied on the steel members are provided through the research project. the values are obtained from a set of parametric design studies with various conditions, such as span lengths, loads and truss geometries.

### 1.4 Methodology

This master's thesis will be carried out in four phases. The first phase is to study the design aspects of thin-walled, cold-formed steel members. Reference is made to Eurocode and available literature on the topic. Moreover, in this phase there will also be a study done on the limitations of the cold-formed cross-sections shape and dimensions. This information is used to set the limitations and constraints for the optimization.

The second phase is to set up design procedures in **Matlab** to calculate all necessary cross-sectional parameters and checks according to Eurocode.

The third phase is to connect the **Matlab** procedure to different cold-formed cross-sections with different steel yield strengths. The outputs from **Matlab** design procedures will then be run through the genetic algorithm to get the most optimized cross-sections.

The last phase is to analyse the results of the genetic algorithm optimization and create a library for the most optimized cross-sections for given parameters.

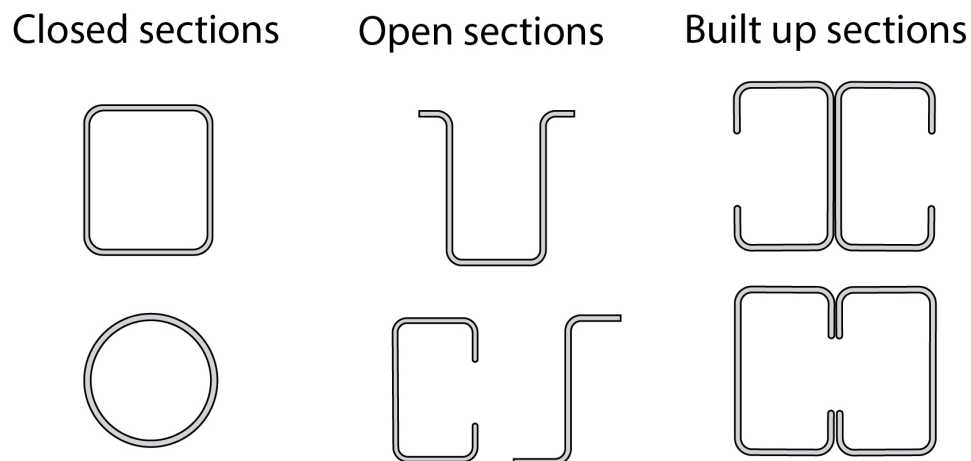
# 2

## Cold-formed steel sections

Cold-formed steel is a common product used in structures and there are some differences between cold-formed and hot-rolled steel products. The manufacturing process of cold-formed steel is also described in detail. The different manufacturing requirements on the material, such as radius-to-thickness ratios and width-to-thickness ratios, are also explained and presented. Furthermore,

### 2.1 Introduction to cold-formed steel sections

One way of shaping a steel members cross-section is by hot-rolling. Another common way of shaping a steel members cross-section is by cold-forming. The hot-rolled process forms steel plates into various shapes, such as I-section, by heating the steel and shaping it. The cold-formed steel elements are shaped at room temperature out of steel sheets, plates or bars and forms structural shapes or panels (Yu et al., 2010). The shapes can be closed sections such as box sections, or open sections, U-, C- and Z-sections, or built-up sections which consists of multiple sections put together as one. The steel sheets can be formed to panels or decks, and with a large range of dimensions these can serve as floors, roofs or walls.



**Figure 2.1:** Typical cross-sections for cold-formed steel sections.

An advantage of cold-forming is that more complex sections can be formed compared

to hot-rolled, this will be described in chapter 2.2. Another advantage of cold-forming is an increase of the yield strength of the steel due to the cold working, however, this results in a reduced ductility (Dubina et al., 2012). This increase of strength is due to strain hardening and is mainly influenced by the material that is used. Dubina et al. (2012) further explain that the residual stresses are less of a problem for cold-formed sections as the residual stresses occur when hot-rolled sections are cooling down which changes the stress-strain curve for material. The process of coiling and uncoiling the steel sheet causes residual stresses in the material along with the flattening of the sheet before it is formed to the desired shape (Quach et al., 2004). According to Eurocode 1993-1-3 (2006) the average increase of the yield strength for cold-formed members can be determined as follows in equation 2.1.

$$f_{ya} = f_{yb} + (f_u - f_{yb}) \frac{knt^2}{A_g} \quad \text{but} \quad f_{ya} \leq \frac{f_u + f_{yb}}{2} \quad (2.1)$$

Where:

$f_{ya}$ : average yield strength     $f_{yb}$ : basic yield strength     $f_u$ : tensile strength

$A_g$ : gross cross-sectional area

$k$ : numerical coefficient that depends on the type of forming as follows:

$k = 7$  for roll forming

$k = 5$  for other methods of forming

$n$ : number of 90 bends in the cross-section with an internal radius  $r \leq 5t$  (fractions of 90 bends should be counted as fractions of  $n$ )

$t$ : design core thickness of the steel material before cold-forming, exclusive of metal and organic coating

However, certain requirements need to be met for equation 2.1, as stated in chapter 3.2 in Eurocode 1993-1-3 (2006). An alternative way to find the increased yield strength is through testing which is also listed in the previously named chapter in Eurocode.

Additional advantages of cold-formed steel elements in comparison to hot-rolled are listed below (Yu et al., 2010):

- For light forces and/or short spans, cold-formed steel structures can be produced in contrast to thicker hot-rolled sections.
- The sections can be manufactured in such a way that they are easily packed within one another which lead to less need of shipping due to the compact packing.
- Cold-forming can be used to manufacture steel sections that are unique. The production is economically favourable, hence this can result in efficient strength-to-weight ratios.

- Flat hollow sections such as decks and panels, can be utilized to run electrical wiring through the hollow section and the flat surfaces can be used as supports for construction of floors, roofs and walls.
- If panels and decks are mounted in a certain way, they can act as rigid shear diaphragms.

## 2.2 Method of production

In comparison to hot-rolled steel members, cold-formed steel members can be manufactured at a faster rate and into more complex cross-sections. The cold-formed steel members can generally be manufactured by roll forming or by folding and press braking (Dubina et al., 2012). Depending on the cross-section complexity one or the other method may be used.

### 2.2.1 Roll forming

The roll forming method consists of a series of rolls that gradually deform a flat sheet of steel until the required shape is achieved. An example of roll forming machine series can be seen in figure 2.2. The deformation allowed at each stage is generally decided by the material properties. Furthermore, more complex cross-sections need to go through a larger number of rolling stages (Rhodes, 1991). Some of these complex cross-sections can be seen in figure 2.4. An advantage of roll forming is that all necessary holes that a cross-section need can be done to a flat sheet of metal before roll forming starts. The hole stamping machine can be seen in figure 2.2 placed before the roll forming series. This saves time and means that more complex cross-sections are possible (Dubina et al., 2012).

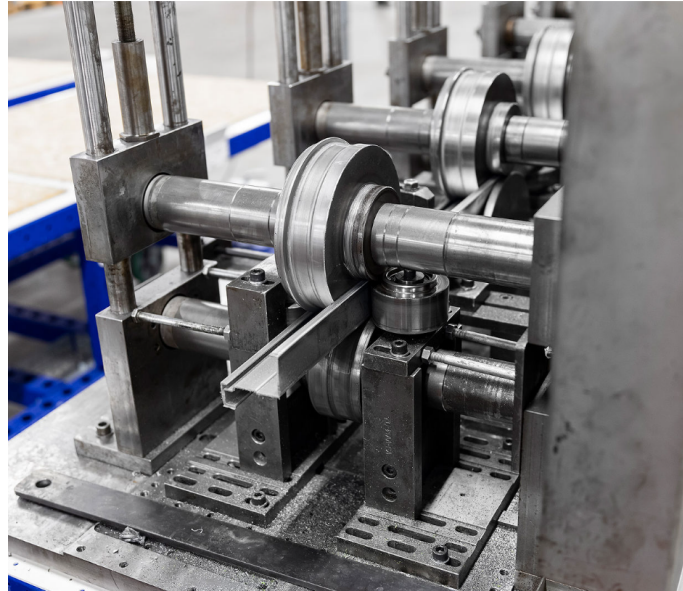


**Figure 2.2:** Roll forming production setup at Bendiro.

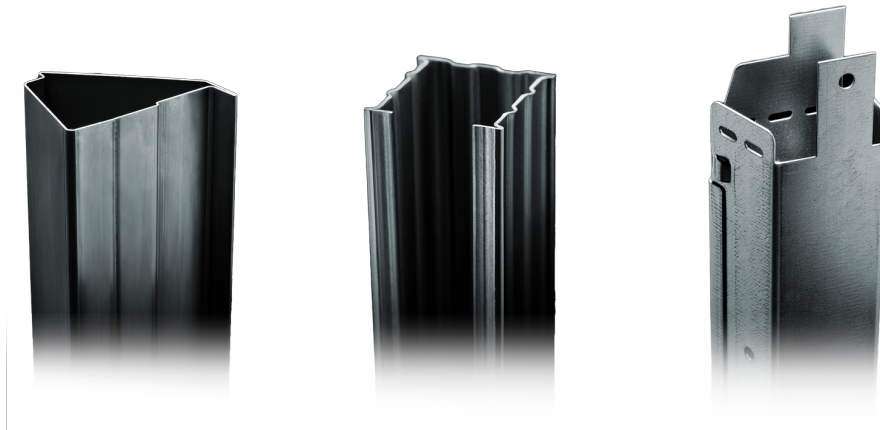
Roll forming can be a very effective and fast method of manufacturing for a standard profile cross-section. This is mainly due to the very automated process of production



as can be seen in figure 2.3. However, to produce a different cross-section the roll forming setup needs to be changed or altered, which is a time-consuming process (Rhodes, 1991). The initial cost of rolls and machines also implies that roll forming is generally only used for large volume production.



**Figure 2.3:** Roll forming production machines at Bendirol.



**Figure 2.4:** Example of complex cross-sections produced by Bendirol.

### 2.2.2 Folding and press braking

As the name suggests, folding is a method where sheet material is folded in different directions to produce a cross-section. Folding has however its limitations where only simple cross-sections from short length sheet material can be produced in an effective manner. For more complex cross-sections press braking is commonly used (Dubina et al., 2012). Press braking is a method where larger sections of sheet material is placed between a press and a shape. The press forces the sheet material to deform

and mimic the shape profile. Using this method, the sheet material can be rotated and replaced to produce complex cross-sections. Press braking is generally used to produce custom shapes that are not widely available whereas roll forming is used to produce standard shapes and cross-sections (Yu et al., 2010).

## 2.3 Applications

The use of cold-formed steel members varies widely and is applied in the car industry, highway products, railway carriages, storage rack systems, sheeting, piping in different industries, bridge construction and structural members in buildings, (Yu et al., 2010).

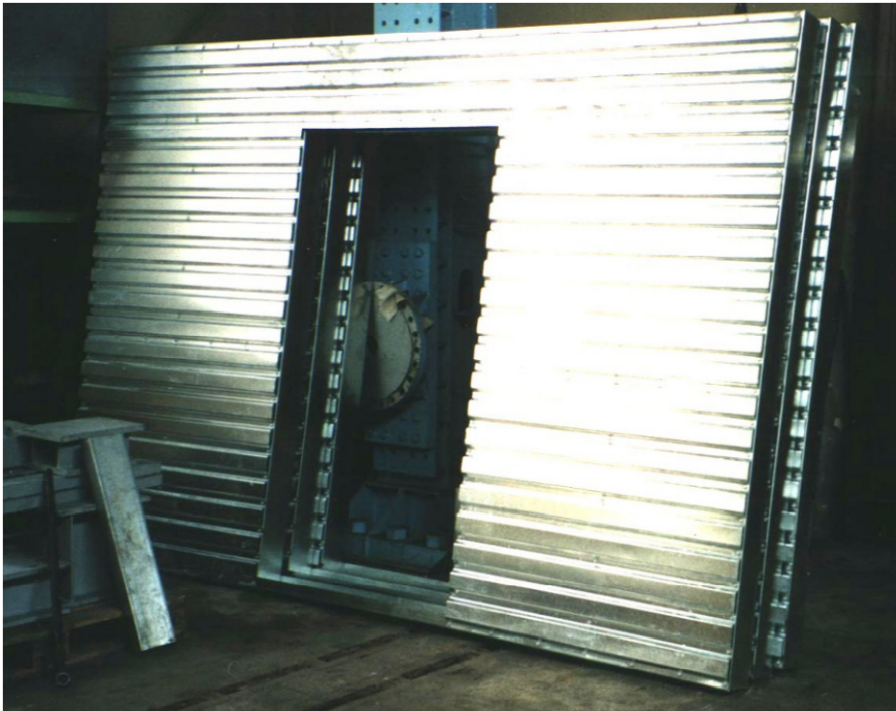
The production of standardized buildings is easily made with cold-formed steel elements and with the following advantages, fast construction and low maintenance, it is commonly used in applications of agriculture and industrial halls, (Yu et al., 2010). It can be used as steel framing, see figure 2.5, wall partitioning, see figure 2.6, as large panels for housing, see figure 2.7 or in truss systems such as a roof truss, see figure 2.8, (Dubina et al., 2012).



**Figure 2.5:** Steel framing made of cold-formed steel elements (Dubina et al., 2012) (p.35).



**Figure 2.6:** Wall partitioning made of cold-formed steel elements (Dubina et al., 2012) (p.36).



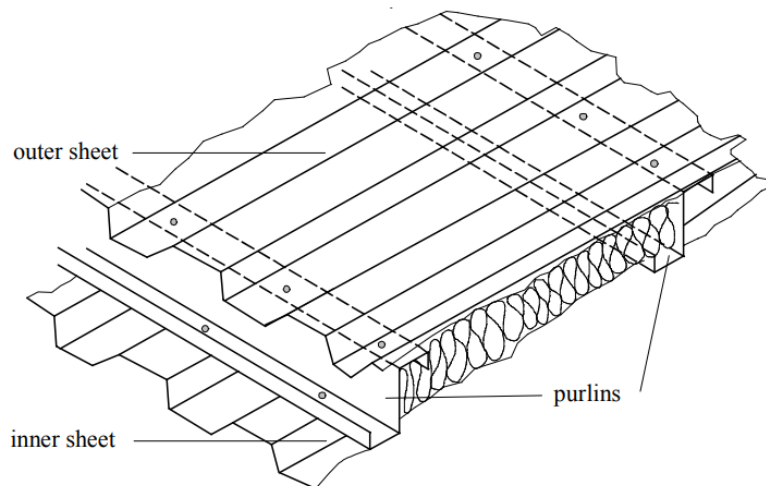
**Figure 2.7:** Large panels for housing (Dubina et al., 2012) (p.37).





**Figure 2.8:** Roof trusses made of cold-formed steel-sections (Dubina et al., 2012) (p.40).

Cold-formed Z-sections are usually used in today's market mostly in roof purlins, flooring and wall studs. The shape of the Z-section is optimal for having anchor point on both sides, as can be seen in figure 2.9 (Yu et al., 2010). The advantage of roll forming in this case is that all necessary holes and anchorage point can be done to a flat sheet of metal before rolling. This reduced the complexity of production compered to hot rolled. Moreover, the installation time is reduced which saves money (Halmos, 1983).



**Figure 2.9:** Roof purlins made of cold-formed Z-section (Dubina et al., 2012) (p.411).



# 3

## Structural behaviour of cold-formed steel elements

During design of thin-walled members the structural behaviour needs to be considered. The main buckling types for cold-formed steel sections are local, global, distortional and shear buckling (Dubina et al., 2012). The global instability includes various forms of buckling, namely flexural (Euler) and flexural-torsional buckling of columns, as well as lateral-torsional buckling of beams. All the previously mentioned buckling types will be checked according to Eurocode.

### 3.1 Material limitations

There are some requirements on the material properties of the steel with regard to ductility, these are stated in Eurocode 1993-1-1 (2005). The requirements are limits for certain ratios and values according to National Annex which must be fulfilled. The first ratio, as seen in equation 3.1 shows the ratio for tensile strength and yield strength. Equation 3.2 calculates the elongation at failure and should not be lower than 15 % and the third requirement states the recommended ratio for the strains as seen in equation 3.3.

$$\frac{f_u}{f_y} \geq 1.10 \quad (3.1)$$

Where:

$f_u$ : ultimate strength

$f_y$ : yield strength

$$5.65\sqrt{A_0} \geq 15 \% \quad (3.2)$$

Where:

$A_0$ : the original cross-sectional area

$$\epsilon_u \geq 15\epsilon_y \quad (3.3)$$

Where:

$\epsilon_u$ : ultimate strain

$\epsilon_y$ : yield strain

## 3.2 Dimension limitations

As described in chapter 2.2 cold-formed cross-sections can be built up to become very complex. To avoid manufacturing processes that are economically unsound the built-up cross-sections need to meet some requirements concerning dimensions and shape. The manufacturing process of cold-formed cross-sections is often limited by the number of folds or bends; therefore, the radius of each bend need to be considered. Moreover, the cold-forming process induces, in comparison to hot-rolled process, small amounts of residual stresses (Quach et al., 2004). These residual stresses are for the most part in the bends of the cold-formed cross-sections. Consequently, the radius-to-thickness ratio is important for the characteristics of the cross-section. According to Rondal (2000) the type of analysis of the cross-section is heavily influenced by the material choice, the thickness of the material and the width. Another ratio to consider is therefore the width-to-thickness ratio for each part in the cross-section. The width-to-thickness of each part in the cross-section ratio also determines the risk for or susceptibility to local buckling for webs, flanges and edge folds. By reducing the width of elements in the cross-section that may buckle locally under compression, the susceptibility of local buckling can be reduced. This is explained further in chapter 3.2.1. determines the risk for or susceptibility to local buckling

### 3.2.1 Cross-section analysis and classification

To choose a method of global analysis the cross-section of a frame or structure can be analysed for a classification. In Eurocode 1993-1-1 (2005) there are four different classes to choose from. To determine a classification of the cross-section two parameters need to be considered:

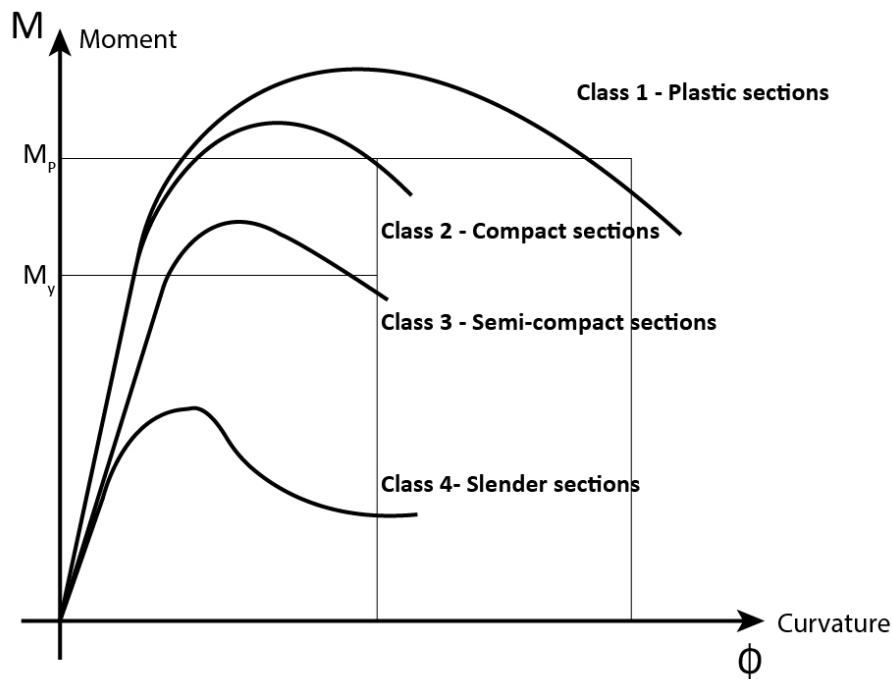
- Slenderness (width-to-thickness ratio) of each element in the cross-section
- Type of compressive stress distribution

Depending on the classification of the cross-section and the stress distribution a method of analysis can be chosen as described in Eurocode 1993-1-1 (2005) chapter 5.5. For this Master's thesis only the elastic analysis is of interest. The four classes of a cross-section are defined as the following:

- **Class 1:** A cross-section that can form a plastic hinge with the required rotational capacity for plastic analysis.
- **Class 2:** A cross-section that can develop their plastic moment resistance but have limited rotation capacity because of local buckling.

- **Class 3:** A cross-section that the stress in the extreme compression fibre can reach yield however due to the slenderness buckling occurs before development of the plastic moment resistance.
- **Class 4:** A cross-section that will buckle before reaching yielding in one or more members of the cross-section.

This is visualised in figure 3.1.



**Figure 3.1:** Behaviour of a cross-section in different cross-section classifications, figure inspired by Al-Emrani et al. (2013).

For cold-formed steel members the thickness is much smaller than the width which consequently means that the cross-section is in class 4 or class 3 (Dubina et al., 2012). Only elastic global analysis can be carried out for cross-sections in class 4 or class 3 (Eurocode 1993-1-1 (2005)). For first order elastic global analysis to be carried out the internal forces or any other structural behaviour that is changed due to deformation must be negligible (Dubina et al., 2012). The changes can be neglected if the condition in equation 3.4 is fulfilled.

The cross-section class can be checked using the table 3.1 for internal compression parts and table 3.2 for outstand compression parts.



### 3. Structural behaviour of cold-formed steel elements

**Table 3.1:** Maximum width-to-thickness ratios for compression parts: internal compression parts (Eurocode 1993-1-1 (2005) table 5.2).

Internal compression parts			
Class	Part subjected to bending	Part subjected to compression	Part subjected to bending and compression
Stress distribution in parts (compression positive)			
1	$c/t \leq 72\epsilon$	$c/t \leq 33\epsilon$	when $\alpha > 0,5$ : $c/t \leq \frac{396\epsilon}{13\alpha-1}$ when $\alpha \leq 0,5$ : $c/t \leq \frac{36\epsilon}{4-5\alpha}$
2	$c/t \leq 83\epsilon$	$c/t \leq 38\epsilon$	when $\alpha > 0,5$ : $c/t \leq \frac{496\epsilon}{13\alpha-1}$ when $\alpha \leq 0,5$ : $c/t \leq \frac{41,5\epsilon}{\alpha}$
Stress distribution in parts (compression positive)			
3	$c/t \leq 124\epsilon$	$c/t \leq 42\epsilon$	when $\psi > -1$ : $c/t \leq \frac{42\epsilon}{0,67+0,33\psi}$ when $\psi \leq -1$ : $c/t \leq 42\epsilon(1-\psi)\sqrt{-\psi}$
$\epsilon = \sqrt{235/f_y}$			

**Table 3.2:** Maximum width-to-thickness ratios for compression parts: Outstand flanges (Eurocode 1993-1-1 (2005) table 5.2).

Outstand flanges			
Rolled sections		Welded sections	
Class	Part subjected to bending	Part subjected to bending and compression	
		Tip in compression	Tip in tension
Stress distribution in parts (compression positive)			
1	$c/t \leq 9\epsilon$	$c/t \leq \frac{9\epsilon}{\alpha}$	$c/t \leq \frac{9\epsilon}{\alpha\sqrt{\alpha}}$
2	$c/t \leq 10\epsilon$	$c/t \leq \frac{10\epsilon}{\alpha}$	$c/t \leq \frac{10\epsilon}{\alpha\sqrt{\alpha}}$
Stress distribution in parts (compression positive)			
3	$c/t \leq 14\epsilon$	$c/t \leq 42\epsilon$	$c/t \leq 21\epsilon\sqrt{k_\sigma}$ for $k_\sigma$ see table 3.4
$\epsilon = \sqrt{235/f_y}$			

$$\alpha_{cr} = \frac{F_{cr}}{F_{Ed}} \geq 10 \quad (3.4)$$

Where:

$\alpha_{cr}$ : load factor which the design load needs to be multiplied by to achieve elastic instability in global mode.

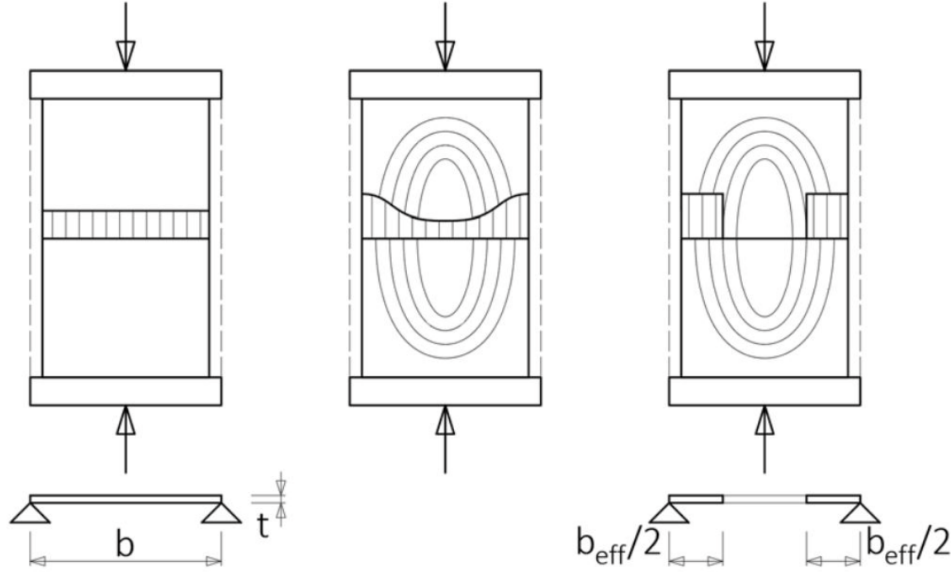
$F_{cr}$ : elastic critical buckling load for the global instability mode.

$F_{Ed}$ : design load on the structure.

### 3.2.2 Effective width method

As mentioned before a cross-section in class 4 will buckle locally before reaching yielding. To take this into account in the analysis, the cross-section members that are in class 4 need to be reduced to an effective width (Hansen et al., 2010). The idea is that members under compression can be seen like plates and have plate like behaviour. The stresses will be redistributed when the plate reaches the buckling

stress. The redistribution will be to an effective width, therefore only the effective width is considered (Al-Emrani et al., 2013). This can be seen in figure 3.2.



**Figure 3.2:** Effective width of plate under compression (Al-Emrani et al., 2013)

The effective width,  $b_{eff}$ , of a member subjected to compression can be calculated according to Eurocode 1993-1-5 (2006) as seen in table 3.3 and table 3.4. Where  $\rho$  is the reduction factor for the width,  $\psi$  is the stress ratio and  $k_\sigma$  is the buckling factor.

For internal compression elements the reduction factor,  $\rho$ , can be calculated as seen in equation 3.5 and equation 3.6

$$\rho = 1,0 \quad \text{for } \bar{\lambda}_p \leq 0,673 \quad (3.5)$$

$$\rho = \frac{\bar{\lambda}_p - 0,055(3 + \psi)}{\bar{\lambda}_p^2} \leq 1,0 \quad \text{for } \bar{\lambda}_p > 0,673, \text{ where } (3 + \psi) \geq 0 \quad (3.6)$$

For outstand compression elements the reduction factor,  $\rho$ , can be calculated as seen in equation 3.7 and equation 3.8

$$\rho = 1,0 \quad \text{for } \bar{\lambda}_p \leq 0,748 \quad (3.7)$$

$$\rho = \frac{\bar{\lambda}_p - 0,188}{\bar{\lambda}_p^2} \leq 1,0 \quad \text{for } \bar{\lambda}_p > 0,748 \quad (3.8)$$

Where:

$$\bar{\lambda}_p : \frac{\bar{b}/t}{28,4\epsilon\sqrt{k_\sigma}}$$

$$\epsilon = \sqrt{235/f_y}$$

$k_\sigma$ : buckling factor

To calculate the effective width of edge folds the same process as described above is used. However, the buckling factor,  $k_\sigma$ , is calculated as stated in equation 3.9 and equation 3.10

$$k_\sigma = 0.5 \quad \text{for} \quad b/c \leq 0.35 \quad (3.9)$$

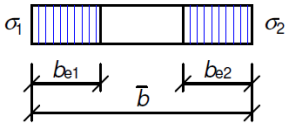
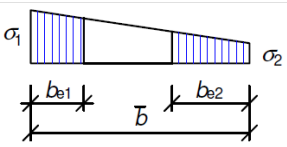
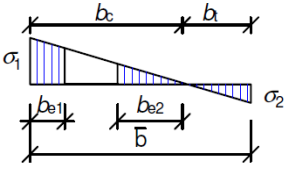
$$k_\sigma = 0.5 + 0.83\sqrt[3]{(b/c - 0.35)^2} \quad \text{for} \quad 0.35 < b/c \leq 0.6 \quad (3.10)$$

Where:

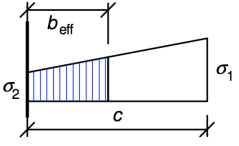
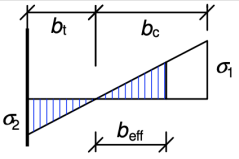
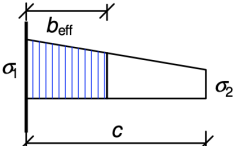
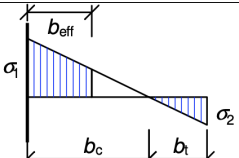
$c$ : edge fold width

$b$ : flange width

**Table 3.3:** Effective width for internal compression elements subjected to compression (Eurocode 1993-1-5 (2006)).

Stress distribution (compression positive)				Effective width $b_{eff}$		
				$\psi = 1 :$ $b_{eff} = \rho \bar{b}$ $b_{e1} = 0,5b_{eff} \quad b_{e2} = 0,5b_{eff}$		
				$1 > \psi \geq 0$ $b_{eff} = \rho \bar{b}$ $b_{e1} = \frac{2}{5-\psi} b_{eff} \quad b_{e2} = b_{eff} - b_{e1}$		
				$\psi < 0$ $b_{eff} = \rho b_c = \rho \bar{b} / (1 - \psi)$ $b_{e1} = 0,4b_{eff} \quad b_{e2} = 0,6b_{eff}$		
$\psi = \sigma_2/\sigma_1$	1	$1 > \psi > 0$	0	$0 > \psi > -1$	-1	$-1 > \psi > -3$
Buckling factor $k_\sigma$	4,0	$8,2/(1,05 + \psi)$	7,81	$7,81 - 6,29\psi + 9,78\psi^2$	23,9	$5,98(1 - \psi)^2$

**Table 3.4:** Effective width for outstand compression elements subjected to compression (Eurocode 1993-1-5 (2006)).

Stress distribution (compression positive)			Effective width $b_{eff}$	
			$1 > \psi \geq 0 :$ $b_{eff} = \rho c$	
			$\psi < 0 :$ $b_{eff} = \rho b_c = \rho c / (1 - \psi)$	
$\psi = \sigma_2 / \sigma_1$	1	0	-1	$1 \geq \psi \geq -3$
Buckling factor $k_\sigma$	0,43	0,57	0,85	$0,57 - 0,21\psi + 0,07\psi^2$
			$1 > \psi \geq 0 :$ $b_{eff} = \rho c$	
			$\psi < 0 :$ $b_{eff} = \rho b_c = \rho c / (1 - \psi)$	
$\psi = \sigma_2 / \sigma_1$	1	$1 > \psi > 0$	$0 > \psi > -1$	-1
Buckling factor $k_\sigma$	0,43	$0,578 / (\psi + 0,34)$	$1,7 - 5\psi + 17,1\psi^2$	23,8

### 3.2.3 Ratios of interest

To assure that the cross-section can be manufactured the radius-to-thickness ratio needs to be evaluated. According to Eurocode 1993-1-3 (2006) there are two different requirements for radius-to-thickness ratio that are of interest for this thesis. The first requirement states that if the radius-to-thickness ratio is less or equal to 5 then the influence of rounded corners can be neglected in the calculations, as seen in equation 3.11.

$$\frac{r}{t} \leq 5 \quad (3.11)$$

Where:

$r$ : radius of internal bend

$t$ : thickness

The other requirement states that if equation 3.12 is true then the resistance of the cross-section should be determined by test. Moreover, Eurocode 1993-1-3 (2006) states that the angle between two plane elements,  $\theta$ , should be between 45°-135°.

$$\frac{r}{t} > 0.04 \frac{E}{f_y} \quad (3.12)$$

Where:

$E$ : modulus of elasticity

$f_y$ : yield strength

As stated in chapter 3.2.1 cold-formed thin-walled steel members have often reduced post-elastic strength and ductility. In practice this means that the cross-section is in class 4 or class 3 and only elastic analysis is of interest. To determine the cross-section class the width-to-thickness ratio needs to be considered for all the parts of the cross-section which is stated in Eurocode 1993-1-1 (2005) chapter 5.6. Moreover, for practical reasons the ratios stated above should be sought after to neglect the effects of rounded corners in the calculations.

The radius-to-thickness ratio is also important for cold-formed sections when welding is used to connect the cross-section members. As described in Eurocode 1993-1-8 (2005) chapter 4.14 welding can be used within a distance of  $5t$  either side of the rounded corner if the radius-to-thickness ratio satisfy the relevant value from table 3.5.

**Table 3.5:** Conditions for welding cold-formed steel elements zones and adjacent material (Eurocode 1993-1-8 (2005) table 4.2).

r/t	Strain due to cold forming [%]	Maximum thickness [mm]		
		Generally		Fully killed Aluminium-killed steel (Al >0,02 %)
		Predominantly static loading	Where fatigue predominates	
>25	<2	any	any	any
>10	<5	any	16	any
>3	<14	24	12	24
>2	<20	12	10	12
>1,5	<25	8	8	10
>1	<33	4	4	6

The diagram illustrates a corner of a cold-formed steel section. It shows a vertical leg and a horizontal leg meeting at a rounded corner with radius  $r$ . The thickness of the steel is denoted by  $t$ . Two dimension lines indicate a distance of  $5t$  from the corner along both the vertical and horizontal legs, defining the zones where welding is permitted according to the table.

### 3.3 Imperfections

In every structure there are initial imperfections, shortcomings in the material or the assembled parts that contributes to second-order effects. According to the Eurocode 1993-1-1 (2005) there are two main sources of imperfection that the designer needs to account for in the global analysis:

- Global imperfections for frames and bracing systems.
- Local imperfections for individual members.

#### 3.3.1 Global imperfection for frames and bracing systems

For frames the initial imperfections are often in form of sway and can be accounted for using equation 3.13. Sway can be described as the inclination of the whole frame as seen in figure 3.3.

$$\phi = \phi_0 \alpha_h \alpha_m \quad (3.13)$$

Where:

$\phi$ : global initial sway imperfection

$\phi_0$ : basic value:  $\phi_0 = 1/200$

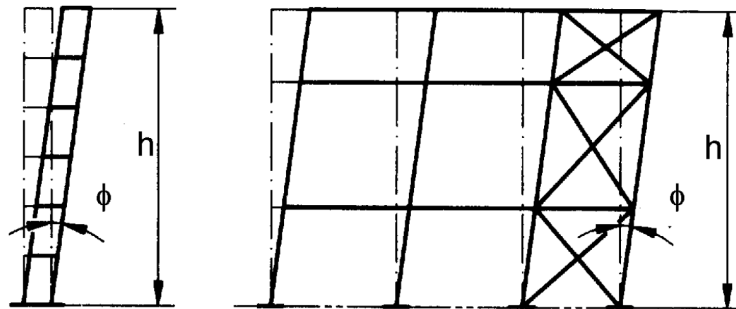
$\alpha_h$ : reduction factor for height  $h$  applicable to columns:

$$\alpha_h = \frac{2}{\sqrt{h}} \text{ but } \frac{2}{3} \leq \alpha_h \leq 1,0$$

$h$ : height of the structure

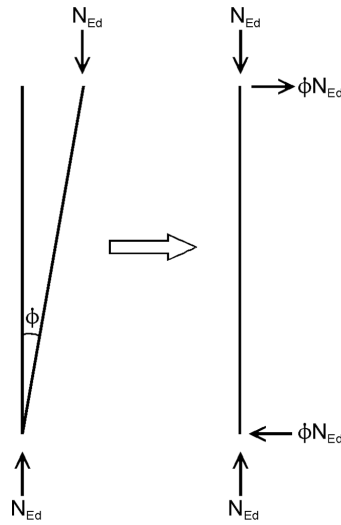
$\alpha_m$ : reduction factor for the number of columns in a row:  $\alpha_m = \sqrt{0,5 \left(1 + \frac{1}{m}\right)}$

$m$ : number of columns in a row including only those columns which carry a vertical load.  $N_{Ed}$  not less than 50% of the average value of the column in the vertical plane considered.



**Figure 3.3:** Equivalent sway imperfection (Eurocode 1993-1-1 (2005) figure 5.2)

The initial sway imperfection can also be replaced by a system of horizontal forces to account for in the global analysis as described in Eurocode 1993-1-1 (2005) chapter 5.3.1. See figure 3.4.



**Figure 3.4:** Replacement of initial sway imperfection by system of horizontal forces (Eurocode 1993-1-1 (2005) figure 5.4)

For bracing systems, the initial imperfections can be accounted for by a geometric imperfection of the members to be restrained. This is done in the form of initial bow imperfection that can be calculated using equation 3.14.

$$e_0 = \alpha_m L / 500 \quad (3.14)$$

Where:

$L$ : length of the bracing system

However, for convenience the effects may be replaced by an equivalent stabilizing force as shown in figure 3.5. The stabilizing force,  $q_d$ , can be calculated using equation 3.15 (Eurocode (1993-1-1, 2005)).

$$q_d = \sum N_{Ed} 8 \frac{e_0 + \delta_q}{L^2} \quad (3.15)$$

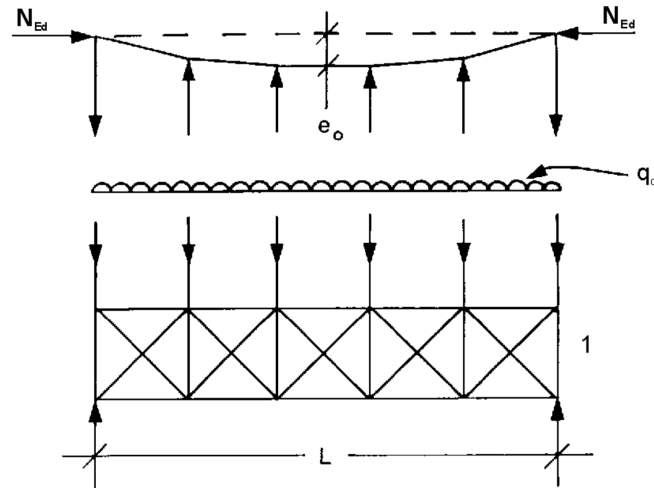
Where:

$N_{Ed}$ : design value of the compression force

$e_0$ : initial bow imperfection

$\delta_q$ : in-plane deflection of the bracing system due to  $q$  plus any external loads calculated from first order analysis (may be taken as 0 if second-order analysis is used)

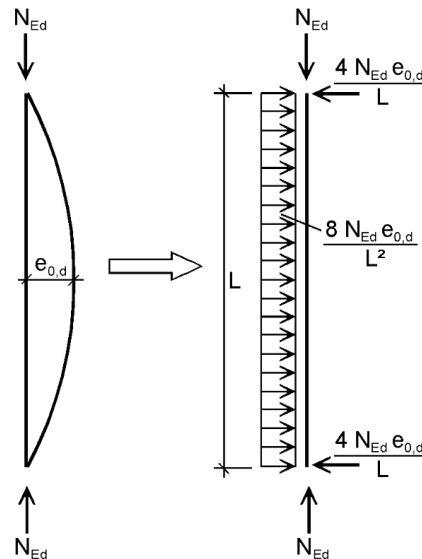




**Figure 3.5:** Equivalent stabilizing force (Eurocode 1993-1-1 (2005) figure 5.6)

#### 3.3.2 Local imperfections for individual members

Local imperfection for steel members can, as the global imperfections, also alter the capacity of a steel structure and needs to be accounted for in the design procedure. The first type of local imperfections is due to the sway of individual columns (Dubina et al., 2012). Dubina et al. (2012) further explains that columns are not completely straight and the initial imperfection will give an extra moment. This is shown in figure 3.6 where the extra moment is derived from the eccentricity of the bowed column.



**Figure 3.6:** Initial imperfection ( $e_{0,d}$ ) of a column with length  $L$  and compressive force  $N_{Ed}$  (Eurocode 1993-1-1 (2005) figure 5.4).

The effect of the initial imperfection of a column is accounted for in Eurocode's buckling curves. However, in some cases where the second-order effects of bow initial imperfection is sensitive an additional factor of safety must be introduced. This is done for cases where the condition in equation 3.16 is met.

$$\bar{\lambda} > 0.5 \sqrt{\frac{Af_y}{N_{Ed}}} \quad (3.16)$$

Where:

$N_{Ed}$ : design value of the compression force.

$\bar{\lambda}$ : in-plane non-dimensional slenderness calculated for the member considered as hinged at its ends

$A$ : cross-sectional area

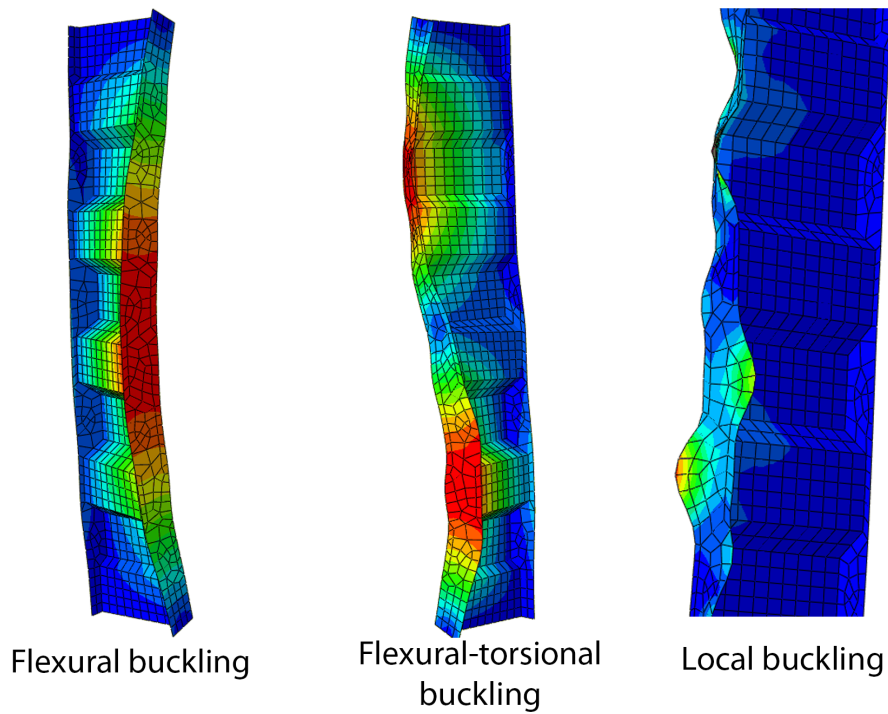
$f_y$ : yield strength

The initial bow imperfection can be replaced with a system of equivalent horizontal forces as shown in figure 3.6.

### 3.4 Local instability

The term "sectional" instability modes include local and distortional buckling since mainly the shape and the resistance of the cross-section is influenced (Ungureanu, Dubina, 1999). Either of these two buckling types can act independently or interact with global buckling i.e., flexural or flexural-torsional buckling (Dubina et al., 2012). Dubina et al. (2012) further describes that even though the two modes, local and distortional buckling, can interact the calculations can be performed separately.

Distorsional buckling can be calculated by linear buckling analysis according to Eurocode (1993-1-3, 2006) which uses a simplified approach.



**Figure 3.7:** Illustrative figures for different buckling modes, created in the software Abaqus.

The distortional buckling for plane elements with either edge or intermediate stiffeners is calculated by the following procedure:

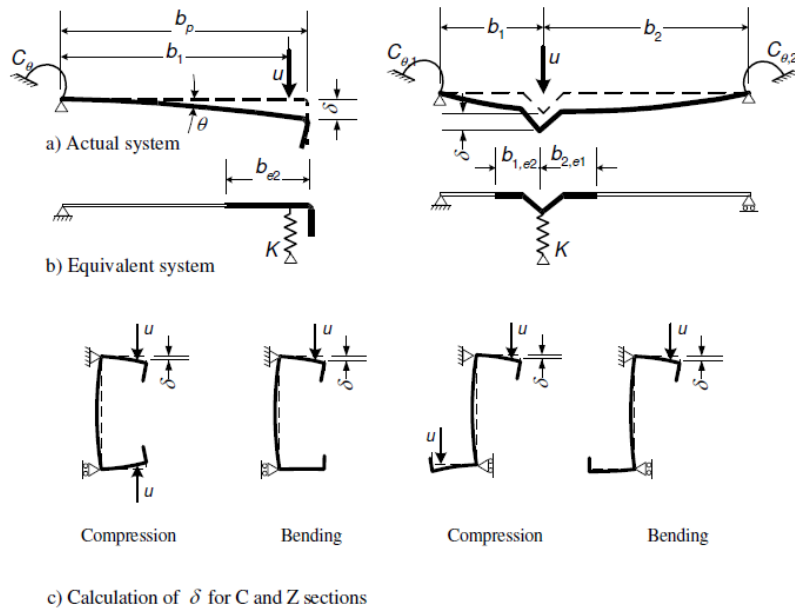
$$K = \frac{u}{\delta} \quad (3.17)$$

Where:

$K$ : spring stiffness per unit length

$u$ : unit load per unit length

$\delta$ : deflection of the stiffener due to  $u$



**Figure 3.8:** Equivalent stabilizing force (Eurocode 1993-1-3 (2006) figure 5.6).

The deflection,  $\delta$ , of an edge stiffener is calculated according to equation 3.18

$$\delta = \theta b_p + \frac{ub_p^3}{3} \frac{12(1-v^2)}{Et^3} \quad (3.18)$$

With

$$\theta = \frac{ub_p}{C_\theta} \quad (3.19)$$

Where:

$b_p$ : notional flat width of a plane element

$\theta$ : angle of deformed member as illustrated in figure 3.8

$C_\theta$ : spring stiffness for rotation

The elastic critical buckling stress is calculated according to equation 3.20

$$\sigma_{cr,s} = \frac{2\sqrt{KEI_s}}{A_s} \quad (3.20)$$

Where:

$K$ : is the spring stiffness

$I_s$ : is the effective second moment of area of the stiffener

$A_s$ : effective cross-sectional area of the edge stiffener

The thickness of the edge stiffener, as seen in figure 3.8, can be reduced to accommodate for distortional buckling with a factor  $\chi_d$ . The reduction factor is obtained from the relative slenderness  $\bar{\lambda}_d$  according to equation 3.22 to 3.24. In the case of

C-sections and back-to-back double C-sections the spring stiffness,  $K$ , is defined as seen in equation 3.21.

$$K = \frac{Et^3}{4(1 - \nu^2)} \cdot \frac{1}{b_1^2 h_w + b_1^3 + 0,5b_1 b_2 h_w k_f} \quad (3.21)$$

Where:

$b_1$ : Distance from web to the centre of the effective area of the edge stiffener

$b_1 = b_2$ : for cross-sections with same length flanges

$h_w$ : Web height

$k_f$ : Ratio of top and bottom flange widths.  $k_f = 1$  for same length flanges

$$\chi_d = 1,0 \quad \text{if} \quad \bar{\lambda}_d \leq 0,65 \quad (3.22)$$

$$\chi_d = 1,47 - 0,723\bar{\lambda}_d \quad \text{if} \quad 0,65 < \bar{\lambda}_d < 1,38 \quad (3.23)$$

$$\chi_d = \frac{0,66}{\bar{\lambda}_d} \quad \text{if} \quad \bar{\lambda}_d \geq 1,38 \quad (3.24)$$

Where:

$$\bar{\lambda}_d = \sqrt{\frac{f_{yb}}{\sigma_{cr,s}}} \quad (3.25)$$

## 3.5 Members buckling resistance

Members buckling resistance can be seen as the members resistance against buckling due to compression and bending. These cases can also be combined and the buckling resistance can be calculated as a combined case. If the applied force is greater than the buckling resistance of the member than the member will yield (or buckle). The effects of buckling are considered by reducing the cross-section as described in the chapter 3.2.1 for local analysis, however for global analysis there are different types of buckling modes.

### 3.5.1 Roof truss girders: assumptions and buckling modes

This study will analyse roof truss girders subjected to uniformly distributed loads which consist of snow and wind loads. As seen in figure 3.9 the roof truss girder can be divided into three groups of elements: upper chord, diagonals and lower chord. For this study only elements subjected to compression is of interest. In this case the upper chord and compressed diagonals. For these two groups of elements (upper chord and compressed diagonals) the following assumptions and buckling modes will

be analysed:

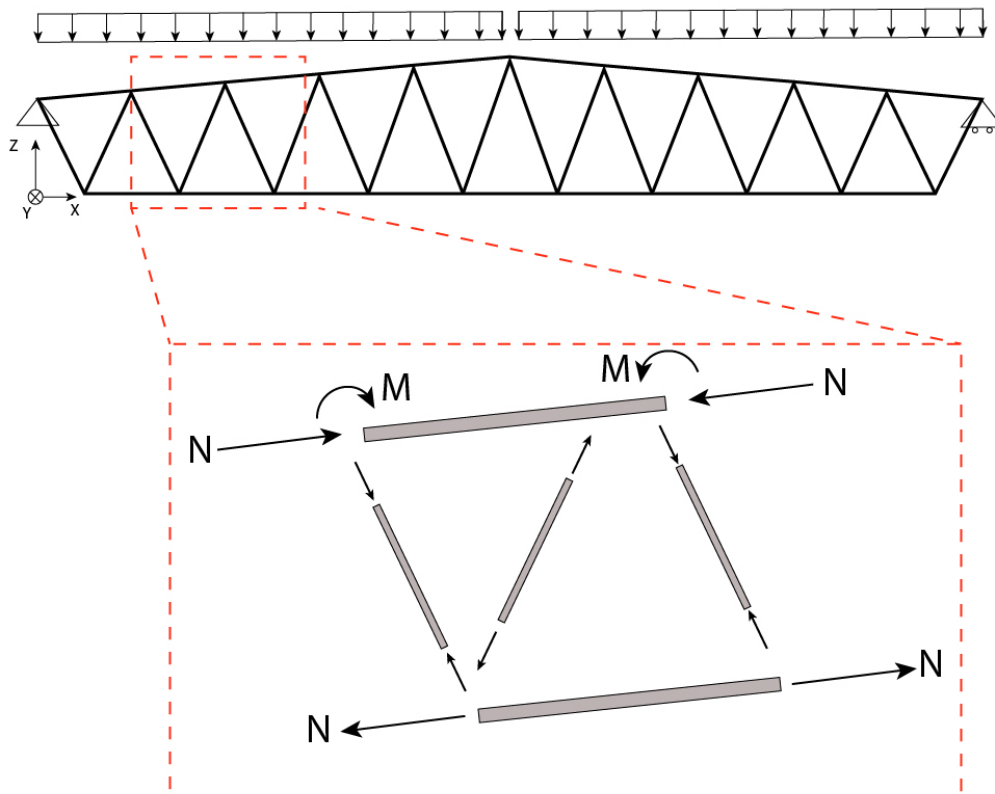
- **Upper chord:**

- Subjected to compression and bending
- Buckling modes: Flexural buckling (only in y-y plane as the z-z plane is restrained), torsional buckling, flexural-torsional buckling and lateral-torsional buckling

- **Diagonals:**

- Carries only axial force, seen as hinged elements. In the real case the diagonals will also be subjected to moment which is not considered in this study.
- Buckling modes: Flexural buckling, torsional buckling and flexural-torsional buckling

For the cross-section to have enough carrying capacity, both the cross-section resistance and buckling resistance criterion must be fulfilled. These criteria are dependent on the load case. The diagonals are only in pure compression or tension while the upper chord is both in compression and bending. This can be seen in figure 3.9.



**Figure 3.9:** Example of analysed roof truss girder.

#### 3.5.2 Compression

For a member to have enough resistance for axial force the following criterion need to be fulfilled:

$$\frac{N_{Ed}}{N_{c,Rd}} + \frac{\Delta M_{y,Ed}}{W f_y} \leq 1 \quad (3.26)$$

Where:

$N_{Ed}$ : design compression force

$N_{c,Rd}$ : design resistance of the cross-section for uniform compression

$N_{c,Rd} = \frac{A f_y}{\gamma_{M0}}$  for class 1,2 and 3

$N_{c,Rd} = \frac{A_{eff} f_y}{\gamma_{M0}}$  for class 4

$\Delta M_{y,Ed}$ : additional moment due to shift in centroid as seen in figure 3.10

For the member subjected to pure compression to have enough buckling resistance the following criterion need to be fulfilled:

$$\frac{N_{Ed}}{N_{b,Rd}} \leq 1 \quad (3.27)$$

Where:

$N_{b,Rd}$ : design buckling resistance of the compression member

The design buckling resistance of the compression member is calculated dependent on the relevant buckling mode. For the compressed diagonals there are three possible buckling modes, flexural buckling, torsional buckling and flexural-torsional buckling. Each mode reduces the resistance by a reduction factor  $\chi$ . The minimal design buckling resistance will therefore be for the case with the minimal reduction factor  $\chi$ .

##### 3.5.2.1 Flexural buckling resistance

The flexural buckling resistance of a cross-section can be calculated as stated in Eurocode 1993-1-1 (2005) chapter 6.3. The buckling resistance of a compression member is calculated as stated in equation 3.28. The reduction factor  $\chi$  is calculated as seen in equation 3.30 where the buckling curve used determines the imperfection factor  $\alpha$ .

$$N_{b,Rd} = \frac{\chi A f_y}{\gamma_{M1}} \quad \text{For Class 1, 2 and 3 cross-sections} \quad (3.28)$$

$$N_{b,Rd} = \frac{\chi A_{eff} f_y}{\gamma_{M1}} \quad \text{For Class 4 cross-sections} \quad (3.29)$$

Where:

$\chi$ : reduction factor

$A$ : cross-section area

$A_{eff}$ : reduced cross-section area

$f_y$ : yield strength

$\gamma_{M1}$ : safety factor

$$\chi = \frac{1}{\Phi + \sqrt{\Phi - \bar{\lambda}^2}} \quad (3.30)$$

Where:

$$\Phi = 0.5[1 + \alpha(\bar{\lambda} - 0.2) + \bar{\lambda}^2]$$

$$\bar{\lambda} = \sqrt{\frac{Af_y}{N_{cr}}} \quad \text{for class 1, 2 and 3 cross-sections}$$

$$\bar{\lambda} = \sqrt{\frac{A_{eff}f_y}{N_{cr}}} \quad \text{for class 4 cross-sections}$$

$\alpha$ : imperfection factor dependent on buckling curves

$N_{cr}$ : the elastic critical force for the relevant buckling mode based on the gross cross sectional properties

For flexural buckling the slenderness can be evaluated according to 1993-1-1 (2005):

$$\bar{\lambda} = \sqrt{\frac{Af_y}{N_{cr}}} = \frac{L_{cr}}{i} \frac{1}{\lambda_1} \quad \text{for class 1, 2 and 3 cross-sections} \quad (3.31)$$

$$\bar{\lambda} = \sqrt{\frac{A_{eff}f_y}{N_{cr}}} = \frac{L_{cr}}{\sqrt{\frac{A_{eff}}{A}}} \frac{1}{\lambda_1} \quad \text{for class 4 cross-sections} \quad (3.32)$$

Where:

$$\lambda_1 = \pi \sqrt{E/f_y}$$

The flexural buckling can be calculated in two directions, in y-y and z-z planes which will generate two reduction factors:  $\chi_y$  &  $\chi_z$ . The Design buckling resistance for flexural buckling mode is therefore in the weak axis of the cross-section

### 3.5.2.2 Torsional and torsional-flexural buckling resistance

The torsional-flexural buckling resistance can be calculated using the same method as for flexural buckling resistance, 1993-1-3 (2006). However, the elastic critical force,  $N_{cr}$ , is modified to compensate for twisting of the cross-section (Zahn,



Iwankiw, 1989). The elastic critical force for torsional buckling of a simply supported beam,  $N_{cr,T}$ , is calculated as seen in equation 3.33. The elastic critical torsional-flexural buckling force,  $N_{cr,TF}$ , is calculated using equation 3.34.

$$N_{cr,T} = \frac{1}{i_o^2} \left( GI_t + \frac{\pi^2 EI_W}{L_{cr}^2} \right) \quad (3.33)$$

With:

$$i_o^2 = i_y^2 + i_z^2 + y_o^2 + z_o^2$$

Where:

$G$ : shear modulus

$I_T$ : torsion constant of the gross cross-section

$I_W$ : warping constant of the gross cross-section

$i_y$ : radius of gyration of the gross-section about the y - y axis

$i_z$ : radius of gyration of the gross-section about the z - z axis

$L_{cr}$ : buckling length of the member for torsional buckling

$y_o, z_o$ : shear centre coordinates with respect to the centroid of the gross cross-section (for doubly symmetric cross-section  $y_o = z_o = 0$ )

For cross-sections that are symmetrical about the y - y axis, the torsional-flexural buckling elastic critical force can be calculated as:

$$N_{cr,TF} = \frac{N_{cr,T}}{2\beta} \left[ 1 + \frac{N_{cr,T}}{N_{cr,y}} - \sqrt{\left( 1 - \frac{N_{cr,T}}{N_{cr,y}} \right)^2 + 4 \left( \frac{y_o}{i_o} \right)^2 \frac{N_{cr,T}}{N_{cr,y}}} \right] \quad (3.34)$$

With:

$$\beta = 1 - \left( \frac{y_o}{i_o} \right)^2$$

#### 3.5.3 Bending moment

To have enough load carrying capacity for members subjected to uniform bending the following criterion needs to be fulfilled:

$$\frac{M_{Ed}}{M_{c,Rd}} \leq 1 \quad (3.35)$$

Where:

$M_{Ed}$ : Design bending moment

$M_{c,Rd}$ : Design resistance of the cross-section for uniform bending

$$M_{c,Rd} = \frac{W_{f_y}}{\gamma_{M1}} \text{ for class 1, 2 and 3}$$

$$M_{c,Rd} = \frac{W_{eff} f_y}{\gamma_{M1}} \text{ for class 4}$$

For the cross-section to have enough buckling resistance the following criterion needs to be fulfilled:

$$\frac{M_{Ed}}{M_{b.Rd}} \leq 1 \quad (3.36)$$

Where:

$M_{b.Rd}$  is the design buckling resistance of the cross-section for uniform bending calculated as:

$$M_{b.Rd} = \chi_{LT} \frac{W f_y}{\gamma_{M1}} \quad \text{For class 1,2 and 3} \quad (3.37)$$

$$M_{b.Rd} = \chi_{LT} \frac{W_{eff} f_y}{\gamma_{M1}} \quad \text{For class 4} \quad (3.38)$$

Where:

$W$ : section modulus

$\chi_{LT}$ : reduction factor for lateral-torsional buckling

$$\chi_{LT} = \frac{1}{\Phi_{LT} + \sqrt{\Phi_{LT} - \lambda_{LT}^{-2}}} \quad (3.39)$$

Where:

$$\Phi_{LT} = 0.5[1 + \alpha_{LT}(\lambda_{LT}^{-} - 0.2) + \lambda_{LT}^{-2}]$$

$$\lambda_{LT}^{-} = \sqrt{\frac{W f_y}{M_{cr}}} \quad \text{for class 1, 2 and 3 cross-sections}$$

$$\lambda_{LT}^{-} = \sqrt{\frac{W_{eff} f_y}{M_{cr}}} \quad \text{for class 4 cross-sections}$$

$\alpha_{LT}$ : imperfection factor dependent on buckling curves

$M_{cr}$ : elastic critical moment for lateral-torsional buckling

The critical moment shown in equation 3.39 is dependent on the shape of the moment diagram. As a result of this the critical moment is therefore dependent on the loading conditions, support conditions and point of application for the load.

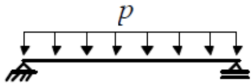

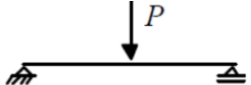

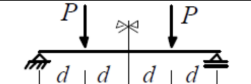

$$M_{cr} = C_1 \frac{\pi^2 E I_z}{(k_z L)^2} \left\{ \left[ \left( \frac{k_z}{k_w} \right)^2 \frac{I_w}{I_z} + \frac{(k_z L)^2 G I_T}{\pi^2 E I_z} + (C_2 z_g - C_3 z_j)^2 \right]^{0.5} \right\} \quad (3.40)$$

Where:

$C_1, C_2$  and  $C_3$ : coefficients dependent on the loading conditions and support conditions as can be seen in table 3.6

$k_z$  and  $k_w$ : effective length factors for rotation and warping, for the roof truss girder both values are set to 1

**Table 3.6:** Loading and support coefficients as seen in Dubina et al. (2012).

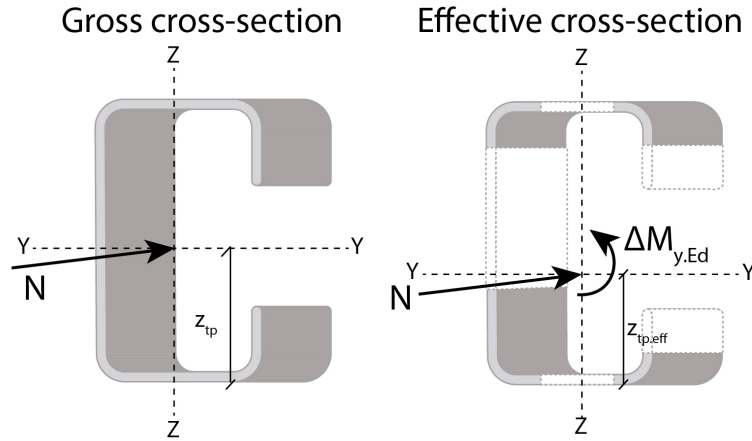
Loading and support conditions	Moment diagram	$k_z$	$C_1$	$C_2$	$C_3$
		1,000 0,500	1,127 0,970	0,454 0,360	0,525 0,478
		1,000 0,500	1,348 1,050	0,630 0,480	0,411 0,338
		1,000 0,500	1,040 0,950	0,420 0,310	0,562 0,539

#### 3.5.4 Combined load action

As seen in figure 3.9 the upper chord is subjected to both bending and compression. To see if the upper chord has enough buckling resistance both the compression and bending criterion must be fulfilled with regard to interaction. Moreover, for the buckling resistance the interaction of bending and compression is also taken into consideration as both flexural buckling and lateral-torsional buckling.

##### 3.5.4.1 Cross-section load carrying capacity criterion

When the cross-section is not symmetrical, the shift of the neutral axis from the gross cross-section to the effective cross-section will result in moment around the y-axis. This is illustrated in figure 3.10. This will yield in a case of both bending and compression with added moment ( $\Delta M_{y.Ed}$ ) due to the shift in centroid.



**Figure 3.10:** Moment due to eccentricity of the shifted natural axis.

For a cross-section subjected to compression the only additional moment will be from the shifted centroid. The shift can be in both z-z axis and y-y axis. The same principle is applied for a cross-section subjected to bending and compression. therefore, the criterion that needs to be fulfilled is:

$$\frac{N_{Ed}}{A_{eff} f_y / \gamma_{M0}} + \frac{M_{y,Ed} + \Delta M_{y,Ed}}{W_{eff,y,min} f_y / \gamma_{M0}} \leq 1 \quad (3.41)$$

Where:

$$\Delta M_{y,Ed} = N_{Ed} e_{Ny} \quad (3.42)$$

Where:

$e_{Ny} = y_{tp,eff} - y_{tp}$ : the shift of y-y axis

$N_{Ed}$ : the applied compression load

$M_{y,Ed}$ : the applied bending load

$\Delta M_{y,Ed}$ : moment due to eccentricity

$W_{eff,y,min}$ : sectional modulus for a cross-section in class 4

### 3.5.4.2 Interaction of bending and compression for buckling resistance

To calculate the interaction of bending moment and axial compression acting on a member the requirement stated in equation 3.43 and 3.44 from Eurocode 1993-1-1 (2005) must be fulfilled.

$$\frac{\frac{N_{Ed}}{\frac{\chi_y N_{Rk}}{\gamma_{M1}}}}{1} + k_{yy} \frac{M_{y,Ed} + \Delta M_{y,Ed}}{\chi_{LT} \frac{M_{y,Rk}}{\gamma_{M1}}} \leq 1 \quad (3.43)$$

$$\frac{\frac{N_{Ed}}{\frac{\chi_z N_{Rk}}{\gamma_{M1}}}}{1} + k_{zy} \frac{M_{y,Ed} + \Delta M_{y,Ed}}{\chi_{LT} \frac{M_{y,Rk}}{\gamma_{M1}}} \leq 1 \quad (3.44)$$

Where:

$$N_{Rk} = f_y A_i \quad (3.45)$$

$A_i$ : area of the cross-section

$A_{eff}$  for class 4 and  $A$  for class 3

$$M_{y,Rk} = f_y W_i \quad (3.46)$$

$W_i$ : section modulus

$W_{eff}$  for class 4 and  $W$  for class 3

In Eurocode 1993-1-1 (2005) there are two methods to obtain the interaction factors  $k_{yy}$  and  $k_{zy}$ . Method 1 requires the deformation and since this master thesis only considers ULS and not SLS, method 2 is used to determine the interaction factors. The factors are obtained from table 3.7 for  $k_{zy}$  and table 3.8 for  $k_{yy}$ .

**Table 3.7:** Interaction factors for members susceptible to torsional deformations, (Eurocode 1993-1-1 (2005), table B.2).

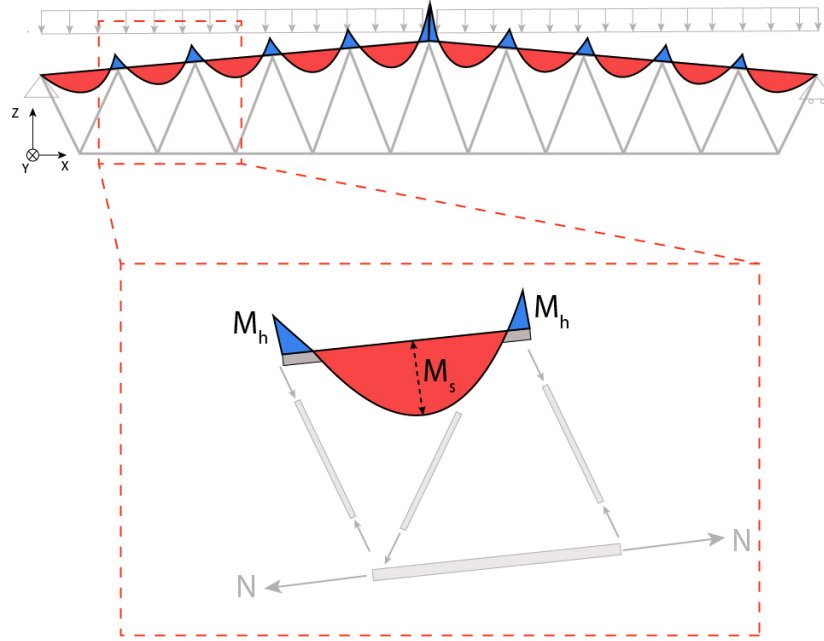
Interaction factors	Design assumptions	
	elastic cross-sectional properties class 3, class 4	plastic cross-sectional properties class 1, class 2
$k_{yy}$	$k_{yy}$ from Table 3.8	$k_{yy}$ from Table 3.8
$k_{yz}$	$k_{yz}$ from Table 3.8	$k_{yz}$ from Table 3.8
$k_{zy}$	$\left[ 1 - \frac{0,05 \bar{\lambda}_z}{(C_{mLT} - 0,25)} \frac{N_{Ed}}{\chi_z N_{Rk} / \gamma_{M1}} \right]$ $\geq \left[ 1 - \frac{0,05}{(C_{mLT} - 0,25)} \frac{N_{Ed}}{\chi_z N_{Rk} / \gamma_{M1}} \right]$	$\left[ 1 - \frac{0,1 \bar{\lambda}_z}{(C_{mLT} - 0,25)} \frac{N_{Ed}}{\chi_z N_{Rk} / \gamma_{M1}} \right]$ $\geq \left[ 1 - \frac{0,1}{(C_{mLT} - 0,25)} \frac{N_{Ed}}{\chi_z N_{Rk} / \gamma_{M1}} \right]$ <p>for <math>\bar{\lambda}_z &lt; 0,4</math>:</p> $k_{zy} = 0,6 + \bar{\lambda}_z \leq 1 - \frac{0,1 \bar{\lambda}_z}{(C_{mLT} - 0,25)} \frac{N_{Ed}}{\chi_z N_{Rk} / \gamma_{M1}}$
$k_{zz}$	$k_{zz}$ from Table 3.8	$k_{zz}$ from Table 3.8

**Table 3.8:** Interaction factors for members not susceptible to torsional deformations, (Eurocode 1993-1-1 (2005), table B.1).

Interaction factors	Type of sections	Design assumptions	
		elastic cross-sectional properties class 3, class 4	plastic cross-sectional properties class 1, class 2
$k_{yy}$	I-sections RHS-sections	$C_{my} \left( 1 + 0,6 \bar{\lambda}_y \frac{N_{Ed}}{\chi_y N_{Rk} / \gamma_{M1}} \right)$ $\leq C_{my} \left( 1 + 0,6 \frac{N_{Ed}}{\chi_y N_{Rk} / \gamma_{M1}} \right)$	$C_{my} \left( 1 + (\bar{\lambda}_y - 0,2) \frac{N_{Ed}}{\chi_y N_{Rk} / \gamma_{M1}} \right)$ $\leq C_{my} \left( 1 + 0,8 \frac{N_{Ed}}{\chi_y N_{Rk} / \gamma_{M1}} \right)$
$k_{yz}$	I-sections RHS-sections	$k_{zz}$	$0,6k_{zz}$
$k_{zy}$	I-sections RHS-sections	$0,8k_{yy}$	$0,6k_{yy}$
$k_{zz}$	I-sections	$C_{mz} \left( 1 + 0,6 \bar{\lambda}_z \frac{N_{Ed}}{\chi_z N_{Rk} / \gamma_{M1}} \right)$ $\leq C_{mz} \left( 1 + 0,6 \frac{N_{Ed}}{\chi_z N_{Rk} / \gamma_{M1}} \right)$	$C_{mz} \left( 1 + (2\bar{\lambda}_z - 0,6) \frac{N_{Ed}}{\chi_z N_{Rk} / \gamma_{M1}} \right)$ $\leq C_{mz} \left( 1 + 1,4 \frac{N_{Ed}}{\chi_z N_{Rk} / \gamma_{M1}} \right)$
	RHS-sections		$C_{mz} \left( 1 + (\bar{\lambda}_z - 0,2) \frac{N_{Ed}}{\chi_z N_{Rk} / \gamma_{M1}} \right)$ $\leq C_{mz} \left( 1 + 0,8 \frac{N_{Ed}}{\chi_z N_{Rk} / \gamma_{M1}} \right)$
For I- and H-sections and rectangular hollow sections under axial and uniaxial bending $M_{y,Ed}$ the coefficient $k_{zy}$ may be $k_{zy}=0$ .			


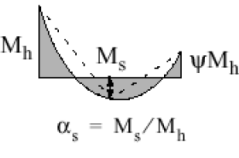
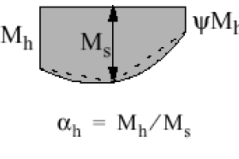
### 3. Structural behaviour of cold-formed steel elements

The parameter  $\Psi$  in table 3.9 is equal to 1 which indicates that the two support moments are of the same magnitude as seen in figure 3.11. As mentioned previously the upper chord will be both in compression and bending and the moment diagram will have the shape as the middle diagram in table 3.9 where the ratio  $\alpha_s$  is calculated to determine  $C_{my}$  and  $C_{mLT}$ .



**Figure 3.11:** Moment diagram for upper chord of a roof truss girder with evenly distributed load.

**Table 3.9:** Equivalent uniform moment factors  $C_m$ , (Eurocode 1993-1-1 (2005), table B.3).

Moment diagram	range		$C_{my}$ and $C_{mz}$ and $C_{mLT}$	
			uniform loading	concentrated load
 $\psi M$	$-1 \leq \Psi \leq 1$		$0,6 + 0,4\Psi \geq 0,4$	
 $\alpha_s = M_s/M_h$	$0 \leq \alpha_s \leq 1$	$-1 \leq \Psi \leq 1$	$0,2 + 0,8\alpha_s \geq 0,4$	$0,2 + 0,8\alpha_s \geq 0,4$
	$-1 \leq \alpha_s \leq 0$	$0 \leq \Psi \leq 1$	$0,1 - 0,8\alpha_s \geq 0,4$	$-0,8\alpha_s \geq 0,4$
		$-1 \leq \Psi \leq 0$	$0,1(1 - \Psi) - 0,8\alpha_s \geq 0,4$	$0,2(-\Psi) - 0,8\alpha_s \geq 0,4$
 $\alpha_h = M_h/M_s$	$0 \leq \alpha_h \leq 1$	$-1 \leq \Psi \leq 1$	$0,95 + 0,05\alpha_h$	$0,90 + 0,10\alpha_h$
	$-1 \leq \alpha_h \leq 0$	$0 \leq \Psi \leq 1$	$0,95 + 0,05\alpha_h$	$0,90 + 0,10\alpha_h$
		$-1 \leq \Psi \leq 0$	$0,95 + 0,05\alpha_h(1 + 2\Psi)$	$0,90 - 0,10\alpha_h(1 + 2\Psi)$

# 4

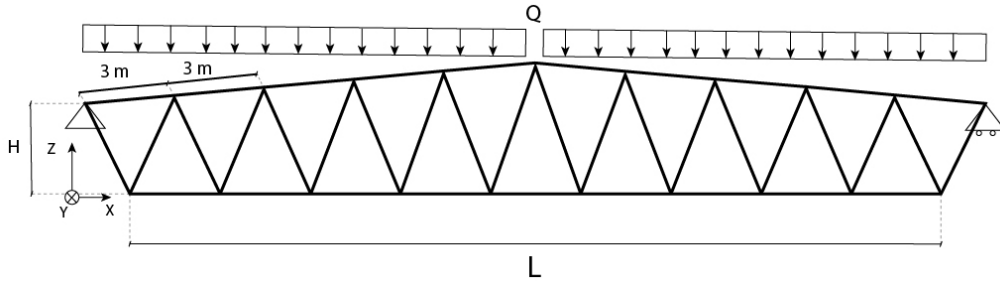
## Roof truss girders

In this study, cross-section optimization is done for a large number of truss members. Only elements in compression are considered (top chord and diagonals as seen in figure 3.9). Load effects (axial forces and bending moments) were obtained from a large parametric analysis of roof trusses with different input values. The parametric analysis was conducted in the frame of an ongoing research project "LightSpan" with the following parameters:  $L$ ,  $H$  and  $Q$ .

The span length,  $L$ , of the roof truss girder analysed varies between 30 m and 40 m with steps of 2 m and with a height,  $H$ , that varies as a function of the span length. The height,  $H$ , varies from  $L/30$  to  $L/20$  with increments of  $L/300$ . Along with the evenly distributed load,  $Q$ , that varies from 10 kN/m to 25 kN/m with increments of 2 kN/m. The dimensions are shown in figure 4.1 and presented in table 4.1.

**Table 4.1:** Analysed spans, heights and evenly distributed loads for the roof truss girders.

Span length $L$ [m]	30, 32, 34, ..., 40
Height of roof truss girder $H$ [m]	$L/30 : L/300 : L/20$
Evenly distributed load $Q$ [kN/m]	10, 12, 14, ..., 25



**Figure 4.1:** Dimensions and load for analysed roof truss girder.

To analyse all possible combinations of dimensions and loads some assumptions were made to limit the project. The pitch angle of the roof is set to  $3^\circ$  while the distance between two diagonals at the upper chord is fixed to 3m as shown in figure



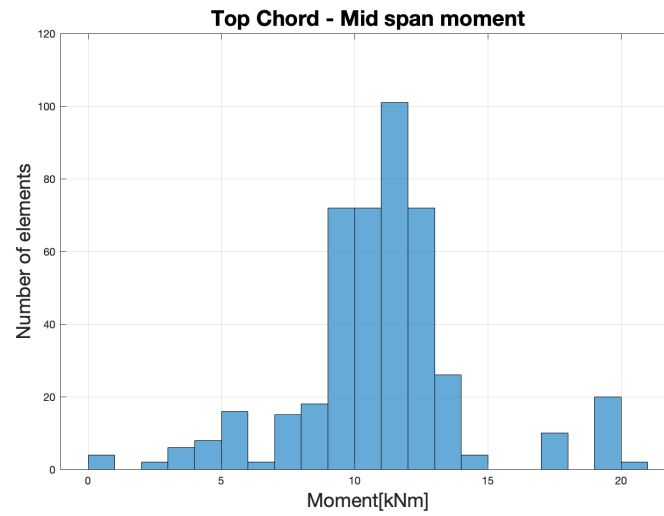
4.1. The possible combinations of span length, roof truss girder's height and evenly distributed load were analysed in a parametric study with the purpose to find the most optimized roof truss girders.

### 4.1 Loads and spans

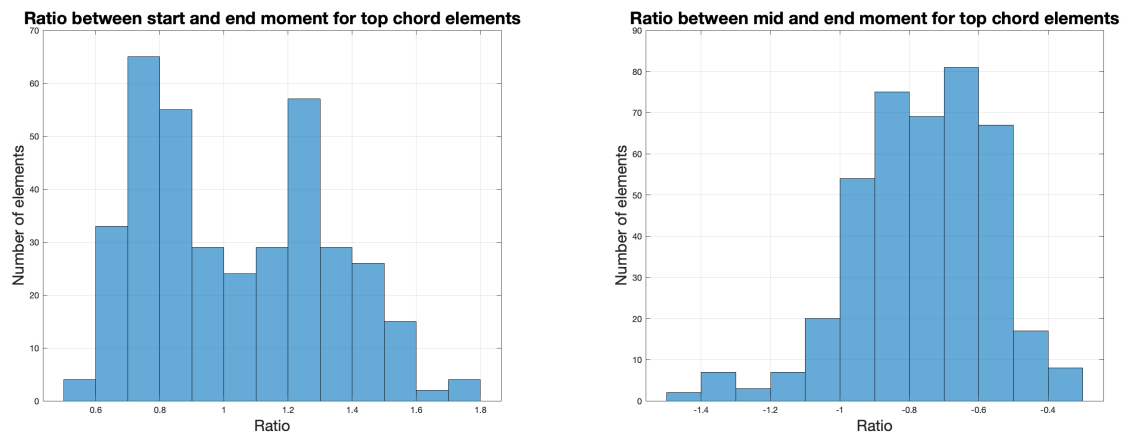
To achieve as optimized cross-sections as possible the analysis for the upper chord and the diagonal will be performed separately. This is mainly because the load acting on the two different members varies and therefore two analyses performed individually will be more favourable.

#### 4.1.1 Upper chord

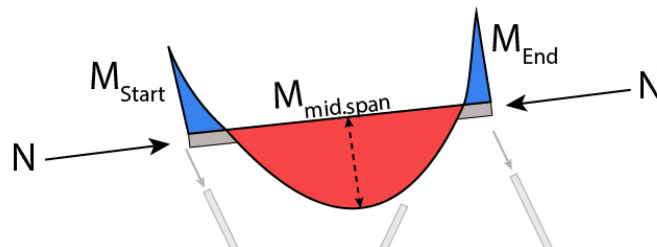
The analysis of the roof truss girder, which is performed in the parametric study of the ongoing project "LightSpan", is done to all possible combinations of  $L$ ,  $H$  and  $Q$  that are shown in table 4.1. The results of the forces acting on the upper chord, which has the length  $3m$ , are presented below. Figure 4.2 shows the number of elements that has a certain mid span moment. The mid span moment does not have a major distribution along the  $x$ -axis and is concentrated between the moments  $8 - 14 \text{ kNm}$ . Furthermore, the ratio between mid span moments and end moments for top chord elements is also very narrow as seen in figure 4.3. The ratio varies between 0.6 to 1.5 for 90 % of all analysed top chords. The same results can be viewed in figure 4.3 for the ratios between start and end moments for the top chord elements. As a result of the minor ratio differences the mid span moments, start moments and end moments are set to be of the same magnitude. The outcome of this is that the parameter  $\Psi$  in table 3.9, which is the ratio between start and end moment is set to 1. The parameter  $\alpha_s$  in the same table, which indicates the ratio between the span and support moment is set to a constant value of -1. Figure 4.4 shows the moment distribution for the upper chord.



**Figure 4.2:** Mid span moments for top chord elements.

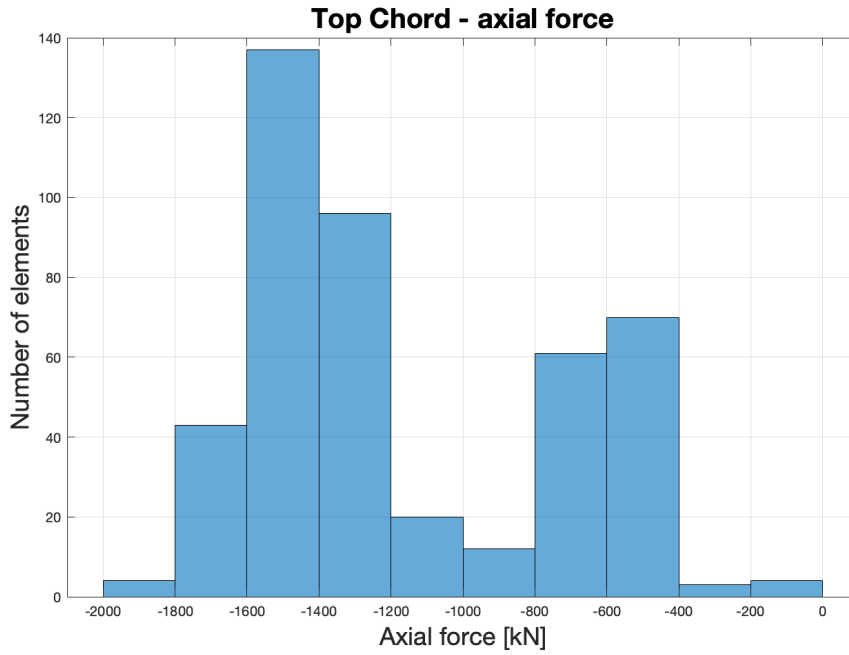


**Figure 4.3:** Ratios between mid span moments, start moments and end moments for top chord elements.



**Figure 4.4:** Moment distribution for upper chord.

The mid span moments in figure 4.2 is compared to the axial forces for the upper chord seen in figure 4.5. The axial forces are greater than the moments and as a result the axial forces will have the major effect on the system. For the cross-section optimization the mid span moment is set to  $14 \text{ kNm}$  for all the upper chord. This value will cover over 90 % of all the cases. For the axial force the values presented in table 4.2 will be analysed to find one optimized cross-section for each force. These values are steps as seen in the histogram illustrated in figure 4.5 to cover 90 % all axial forces. For each axial force an optimized upper chord cross-section will be created and added to a library.



**Figure 4.5:** Axial forces for top chord elements.

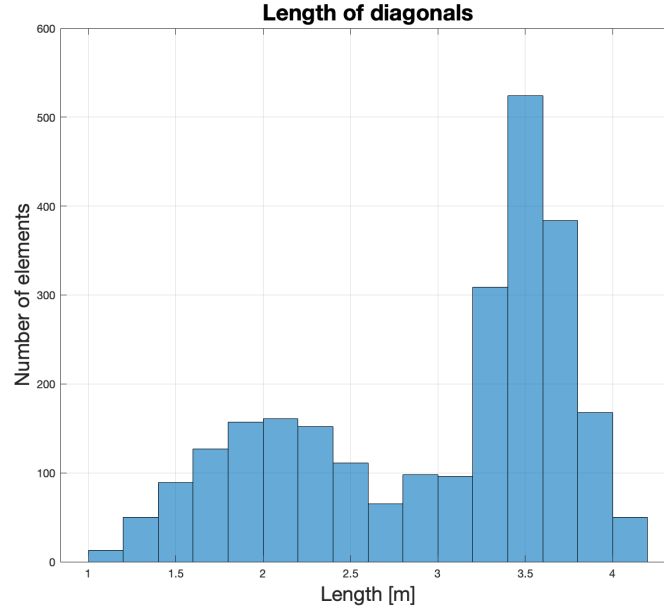
**Table 4.2:** Forces used to optimize the cross-section of the upper chord.

Forces acting on upper chord						
$N \text{ [kN]}$	-700	-900	-1300	-1400	-1500	-1600
$M_{Start} \text{ [kNm]}$	14					
$M_{Mid.span} \text{ [kNm]}$	-14					
$M_{End} \text{ [kNm]}$	14					

#### 4.1.2 Compressed diagonals

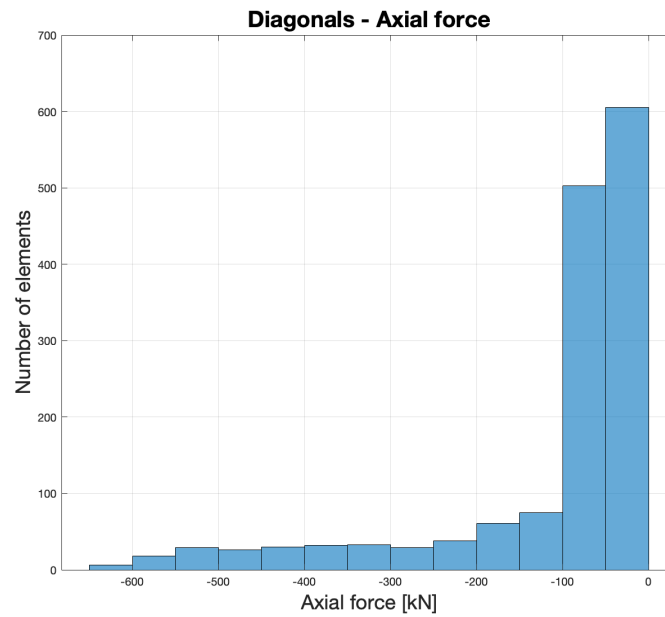
The compressed diagonals are analysed in the same way as the upper chord. For the diagonals the length of the elements is not fixed and varies with regard to span length and roof truss girder height. The parametric analysis done in the research

project "LightSpan" is presented in figure 4.6 and shows that there are two main groups for diagonals. The first group is diagonals between the lengths  $1.5\text{ m}$  to  $3\text{ m}$  while the other group is made of diagonals with lengths between  $3\text{ m}$  to  $4\text{ m}$ .

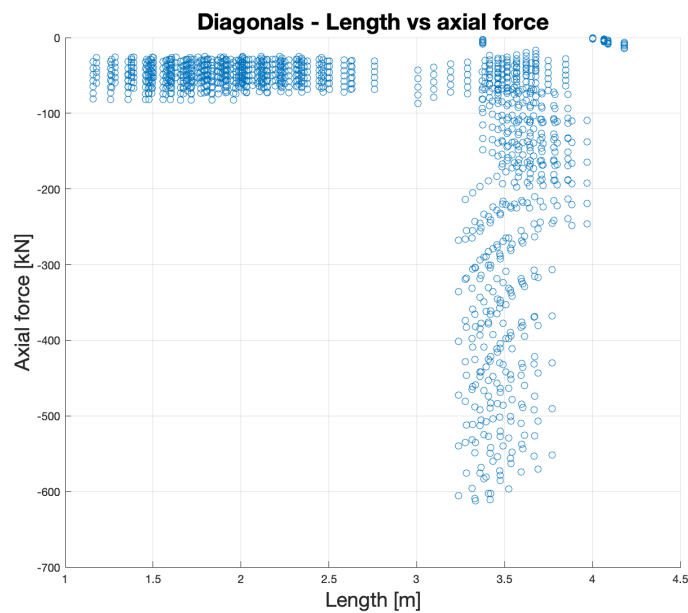


**Figure 4.6:** Length for diagonal elements.

For the compressing axial forces there is a variation from  $-100\text{ kN}$  to  $-600\text{ kN}$  as seen in figure 4.7. However, figure 4.7 does not give a clear picture of how the axial force is distributed over the diagonal lengths. Figure 4.8 shows a scatter plot for the diagonal lengths vs diagonals axial forces. From figure 4.8 it can be confirmed that the behaviour of two groups as seen in figure 4.6 also stands for the axial force. The first group has lengths between  $1\text{ m}$  to  $3\text{ m}$  with axial forces between  $0\text{ kN}$  to  $-100\text{ kN}$ . The Second group consists of lengths between  $3\text{ m}$  to  $4\text{ m}$  with axial forces between  $0$  to  $-600\text{ kN}$ .



**Figure 4.7:** Axial forces for diagonal elements (only compression is shown).



**Figure 4.8:** Scatter of lengths vs axial force for diagonals.

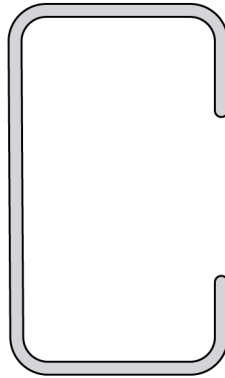
As a result of the two groups of diagonals two different analysis of optimization for cross-sections needs to be made. The first analysis will be made for "diagonal group 1" while the second analysis for "diagonal group 2" as presented in table 4.3. This will cover over 90 % of all possible cases. For each axial force an optimized cross-section will be created and added to a library.

**Table 4.3:** Axial forces and lengths to be used for cross-section optimization.

Forces and spans for diagonals											
Diagonal group 1					Diagonal group 2						
$N [kN]$	-100				$N [kN]$	-100	-200	-300	-400	-500	-600
$L [m]$	1,5	2	2,5	3	$L [m]$	3,5			4		

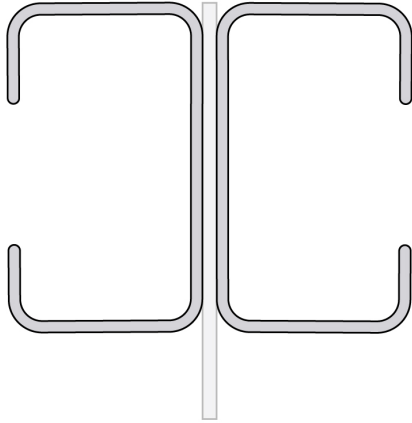
## 4.2 Cross-sections

A variety of cross-section types is aimed at and therefore one open, one built-up and two closed profiles were chosen. The open cross-section was chosen to a lipped C profile as seen in figure 4.9 because it is a common cross-section and it can be used as a diagonal for the truss girder. The C-section will be used as a diagonal and can be subjected to flexural, distortional, torsional buckling and flexural-torsional buckling. An additional moment is also acting on this section due to shift of centroid if the flanges are reduced.

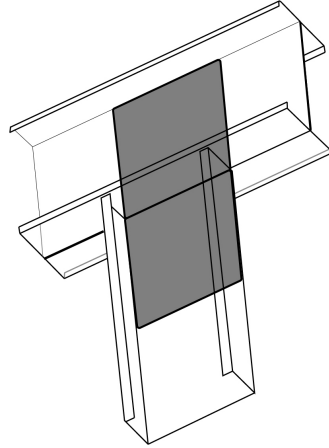
**Figure 4.9:** C-section for diagonals.

A double back-to-back lipped C-section as seen in figure 4.10 was selected as the built-up profile as to increase the capacity of a section, with an increased area, and it can be used both as a diagonal and upper chord. Since the upper chord is subjected to rather large loads with high magnitudes this cross-section will be the only section used as an upper chord. Another reason for this choice is that the diagonals easily can be mounted on the upper chord through the steel plate that runs through the C-sections, see figure 4.10. The two webs of the two C-section will also be connected with the steel plate. An assumption made for these cross-sections are that the webs are rigidly connected throughout the length of the upper chord. In the real case the webs are only rigidly connected where plates are placed as seen in figure 4.11. As a result of this assumption the second moment of area will be lower for the real case. In this study the difference will be neglected. For this case there will be no flexural buckling in the  $z$  (see coordinate system in figure 4.1) direction since it is restrained

due to the roof sheeting. As a result, the criteria showcased in equation 3.44 will have a reduction factor,  $\chi_z = 1$ .

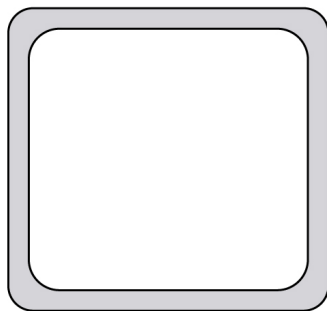


**Figure 4.10:** Double back-to-back c-section for diagonals and upper chord.

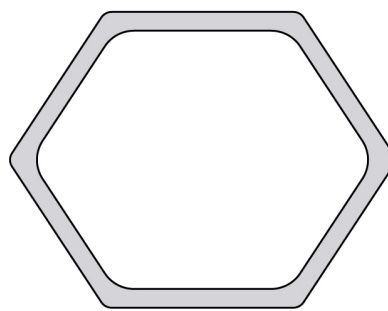


**Figure 4.11:** Connection between upper chord and diagonals.

The two closed sections are a hollow square section, see figure 4.12 and a hollow hexagon, see figure 4.13. The purpose of the selected profiles is to compare the square, which is a common profile, to a less used profile such as a hollow hexagon and to learn about the potential of this shape. The risk for local buckling is less for the hexagon if the same thickness is used. This might prove to be a more efficient choice particularly for steels with higher strength. These two sections will serve as diagonals and will therefore be subjected to compression and the following buckling modes can occur: flexural buckling and torsional buckling. The distortional buckling will not be considered for the closed sections as it will not occur.



**Figure 4.12:** Square cross-section for diagonals.



**Figure 4.13:** Hexagon cross-section for diagonals.

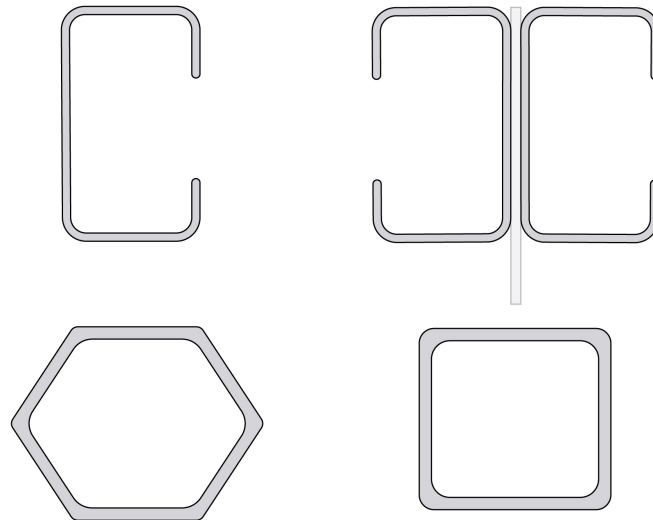
# 5

## Optimization of cross-sections in Matlab

To perform the calculations and checks described in Eurocode, **Matlab** is used. Several **Matlab** functions were created to obtain the different parameters of a cross-section as well as calculating the required checks. **Matlab** is also used to run the genetic algorithm to obtain the results of the optimized cross-sections.

### 5.1 Matlab implementation

The different limitations and checks will be performed according to Eurocode, which are described in chapter 3 and chapter 4. Each major calculation is performed in a **Matlab** function and totally 14 functions were created and can be seen in Appendix A. For the chosen cross-sections, see figure 5.1, various parameters will be calculated as well as the cross-sectional capacity and buckling resistance.



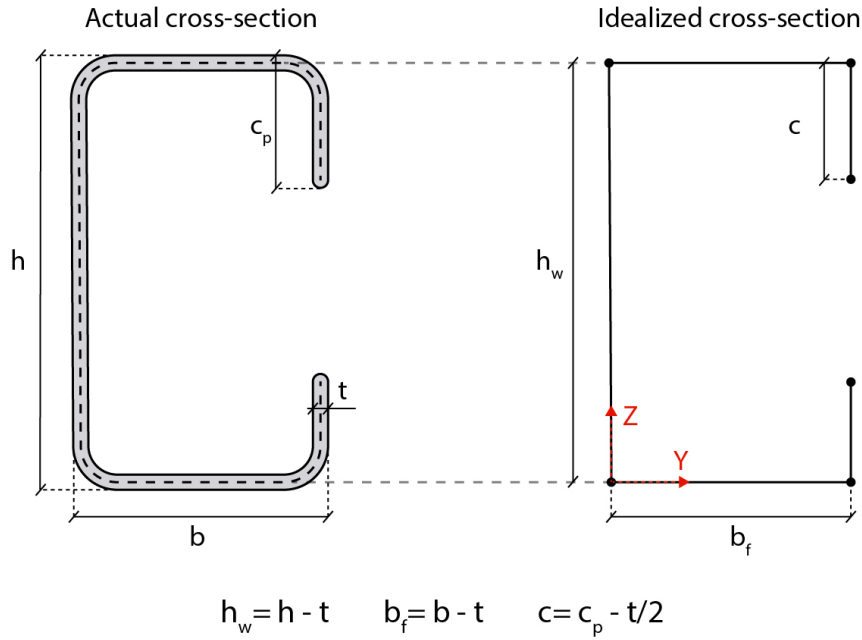
**Figure 5.1:** The chosen cold-formed cross-sections.

#### 5.1.1 Cross-section idealization

The **Matlab** functions created takes the idealized cross-section as input. An example of an idealized lipped C-section is shown in figure 5.2. For rolled cold-formed steel



sections the thickness is constant for all parts of the cross-section. This is also almost always the case for built up cross-sections. As seen in figure 5.2 the idealized dimensions therefore depends on the nominal thickness of the steel.



**Figure 5.2:** Idealization of C cross-section.

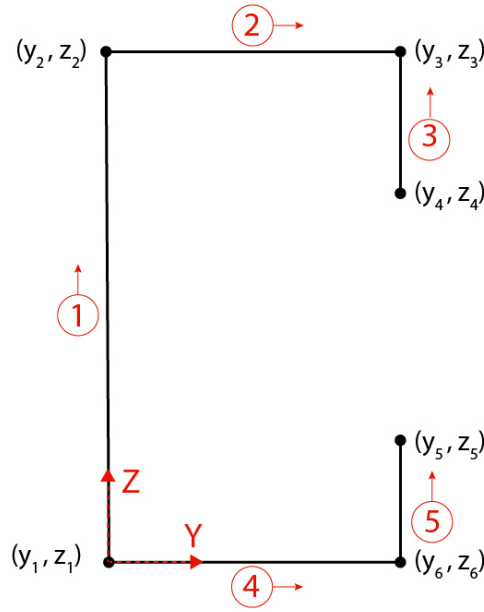
As input for the functions four matrices are required:

- $E_y$  &  $E_z$ : coordinate matrices containing each parts coordinates in y and z axis
- $t$ : thickness vector containing the thickness of each part
- $es$ : matrix that contains each parts' position, type and stress distribution

It is important to consider the numbering of the vectors  $E_y$  and  $E_z$ , they should be defined as shown in figure 5.3 and the flange should be defined before the nearby edgefold.

Some rules for how to number and give coordinates for each element in a cross-section:

- all vertical elements should be oriented from bottom to top.
- all horizontal elements should be oriented from left to right.
- if the cross-section has edge folds (lips), the nearest flange coordinates should always be presented before the coordinates of the edge fold. Example of that is element 4 and 5 in figure 5.3.
- the origin of the coordinate system should always be at the bottom leftmost part of the cross-section as seen in figure 5.2.



**Figure 5.3:** Coordinates for idealized C cross-section.

$$E_y = \begin{bmatrix} y_1 & y_2 \\ y_2 & y_3 \\ y_4 & y_3 \\ y_1 & y_6 \\ y_6 & y_5 \end{bmatrix} \quad E_z = \begin{bmatrix} z_1 & z_2 \\ z_2 & z_3 \\ z_4 & z_3 \\ z_1 & z_6 \\ z_6 & z_5 \end{bmatrix}$$

$$es = \begin{bmatrix} StressDistribution_1 & PartPosition_1 & PartType_1 \\ \vdots & \vdots & \vdots \\ StressDistribution_5 & PartPosition_5 & PartType_5 \end{bmatrix}$$

*StressDistribution:*

- 1 for compression
- 2 for bending
- 3 for bending and compression

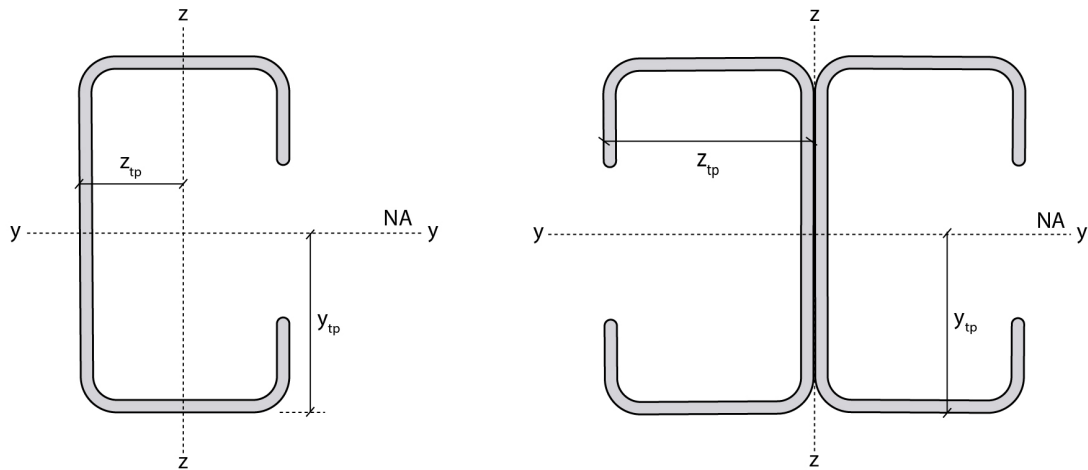
*PartPosition:*

- 1 for internal compression element
- 2 for outstand compression element

*PartType:*

- 1 for web
- 2 for flange
- 3 for edge fold

The axis for the cross-sections in the `Matlab` functions are defined as in Eurocode and are shown in figure 5.4. This is important to consider when calculations are made for plane buckling around the weak and strong axis as well as for calculations of the cross-section capacity. Furthermore, the centre of gravity in the `Matlab` functions are defined as shown in figure 5.4. The centre of gravity of the two cross-sections coincides at the intersection point of the  $y$  and  $z$  axis.  $y_{tp}$  is defined from the bottom of the element to the centre of gravity and  $z_{tp}$  is the distance from the left of the cross-section to the centre of gravity.



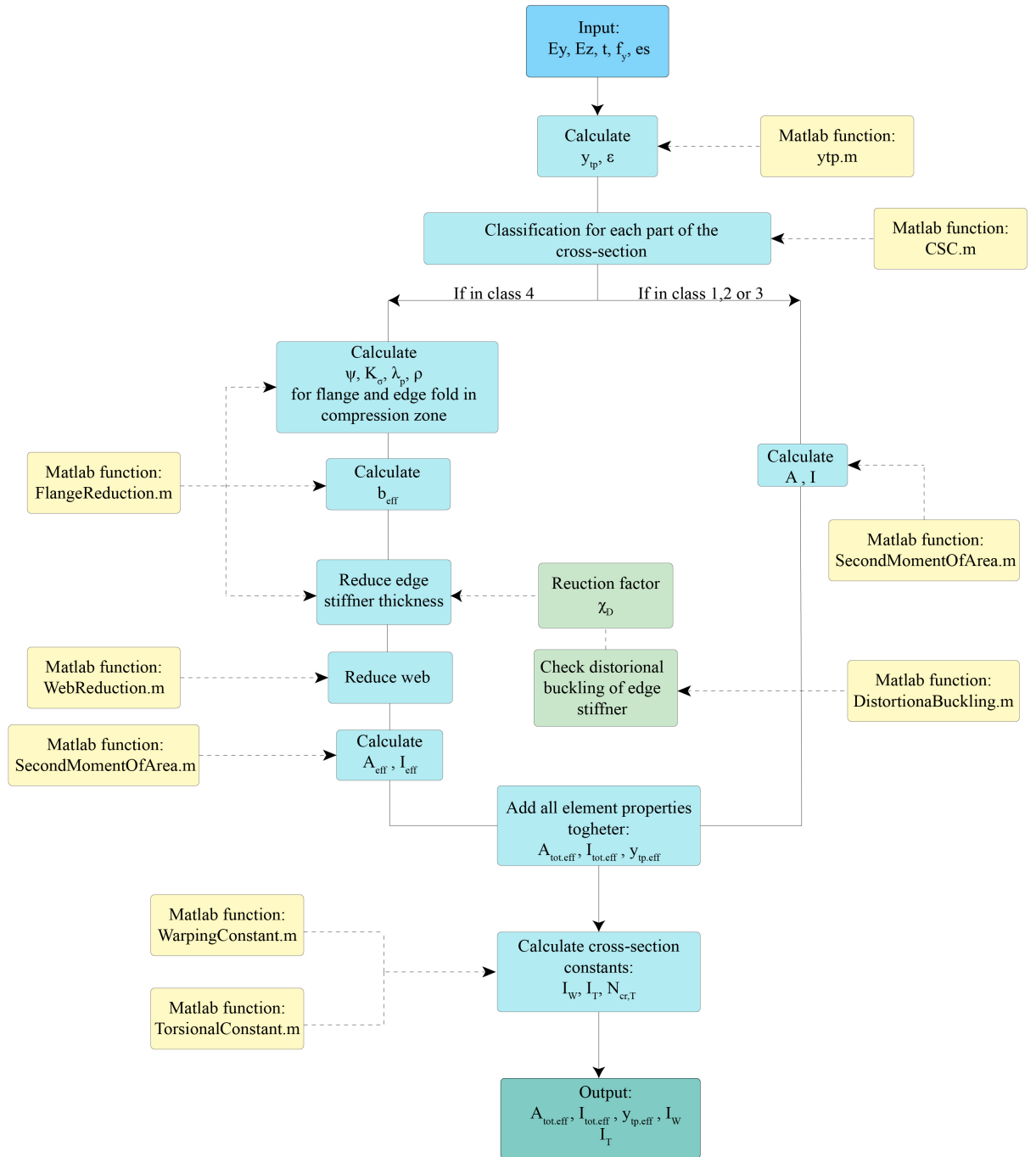
**Figure 5.4:** Bending axis and distance to neutral axis.

### 5.1.2 Matlab implementation of cross-section resistance

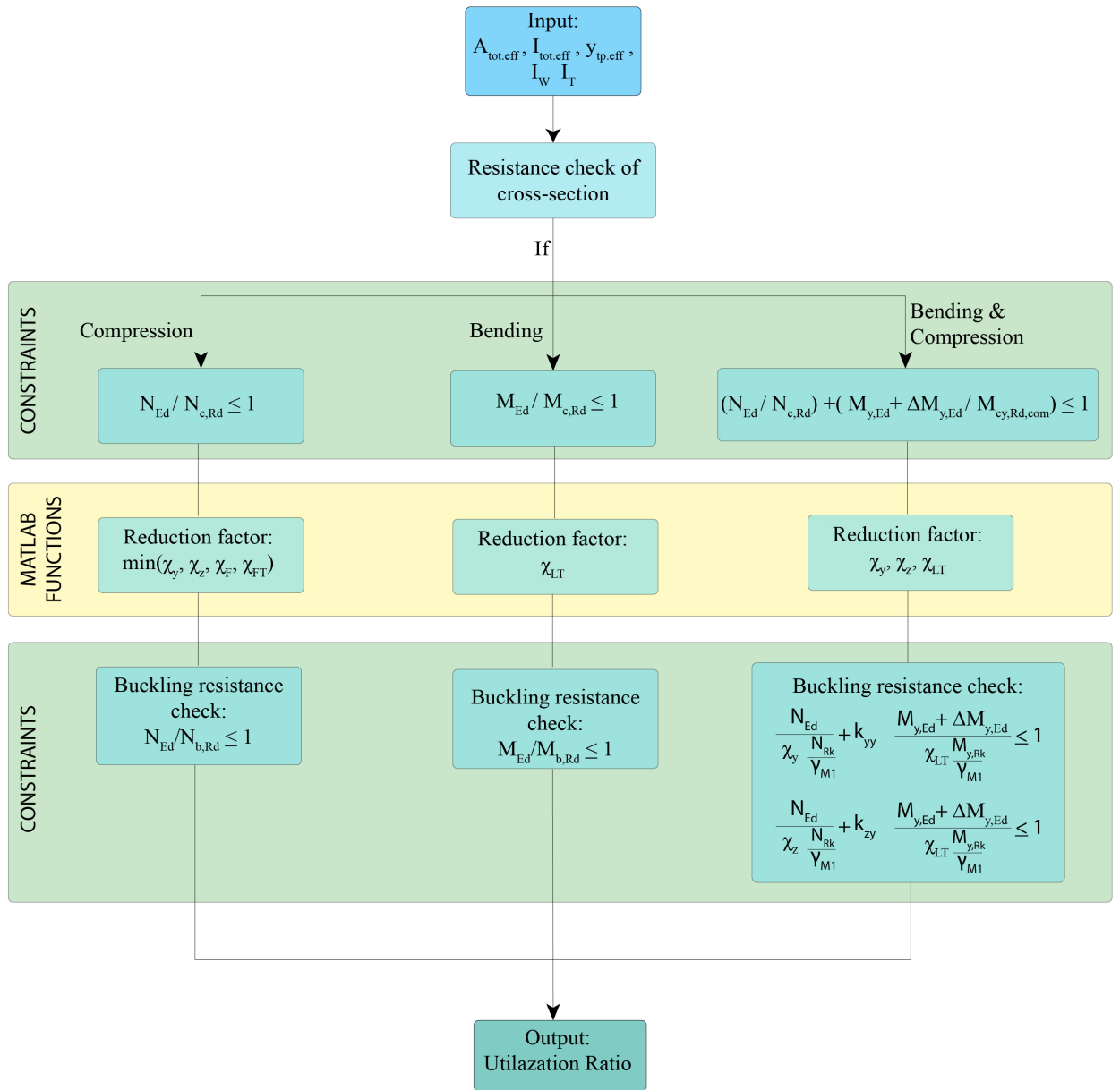
The main procedure to calculate the cross-sectional parameters is shown in the flowchart presented in figure 5.5. The outputs from this procedure can then be used to calculate the cross-section buckling capacity and the checks required as seen in figure 5.6.

As seen in figure 5.5 the first step is to calculate the distance from the bottom of the cross-section to the neutral axis and check all elements for cross-section classification. The `Matlab` functions used are seen in Appendix A.2 and Appendix A.1. The outputs from these functions can further be used as inputs to calculate the cross-sectional parameters needed to reduce all elements in class 4. The reduction functions can be seen in Appendix A.4, Appendix A.7 and Appendix A.5 while the cross-sectional parameters, second moment of area, torsional constant and warping constant, can be calculated with `Matlab` functions presented in Appendix A.3, Appendix A.8 and Appendix A.9.

An example of the procedure to calculate the cross-section load carrying capacity and all necessary checks as stated in Eurocode can be seen in Appendix B.



**Figure 5.5:** Flowchart for procedure to obtain cross-sectional parameters.



**Figure 5.6:** Flowchart for procedure to obtain cross-section capacity.

## 5.2 Cross-section optimization using genetic algorithm

To find the most optimized cross-sections a genetic algorithm, GA, is used and it is implemented in Matlab. The GA searches within a design space for the design parameters that results in the most optimized cross-section. The method is described in chapter 5.2.1 and chapter 5.2.2.

### 5.2.1 What is a genetic algorithm?

According to Pamfil, Palm (2021) the genetic algorithm optimization is used to find a number of design parameters,  $\mathbf{x}$ , which is a vector that contains the desired variables. The fitness function or also called objective function is dependent on these variables and is used to calculate the maximum or minimum of some properties, it can for example be the area or the price. The fitness function can be subjected to constraints such as utilization ratio or geometrical constraints. By introducing a lower and upper bound for each variable in the vector  $\mathbf{x}$ , the sought solution is narrowed to an interesting design range (Pamfil, Palm, 2021).

Pamfil, Palm (2021) further explains that the GA method can be compared to a biological evolution. Random values, within upper and lower bound, of the design parameters are picked and this creates a random population. For each individual the objective function is calculated and based on the result the GA selects some parents to reproduce children for the new generation. This is done through mutation and cross-breeding. There is an exception for the best individuals, so called elites, which have the lowest objective functions, these go straight to the next population. The new population is seen as the next generation based on the previous generations' properties (Pamfil, Palm, 2021).

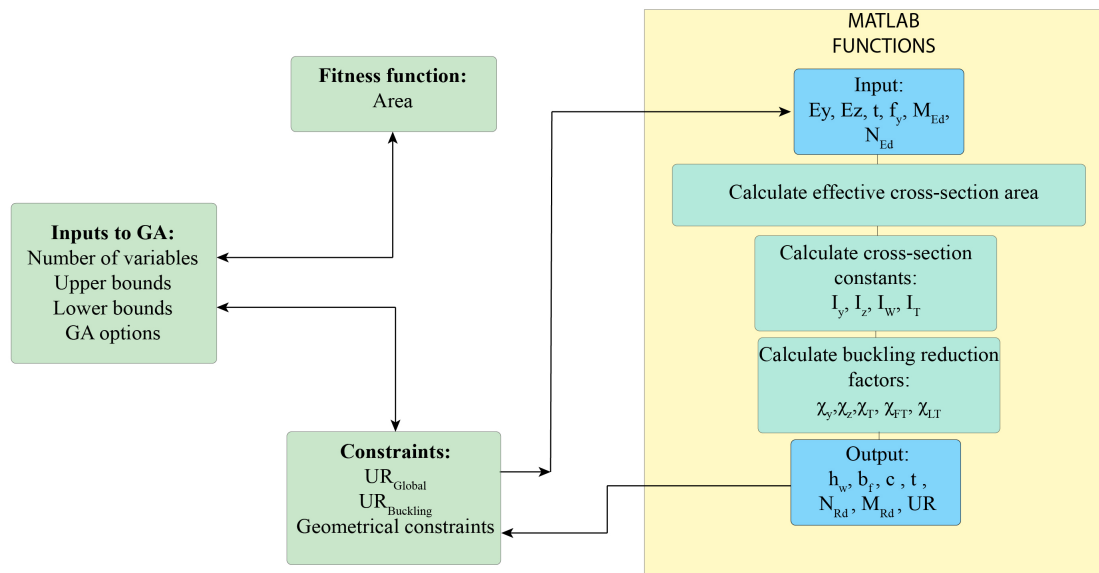
The purpose of the genetic algorithm is to generate more accurate solutions with high utilization for each new population and the GA will continue until convergence is reached. This happens when the function tolerance is reached. The function tolerance is the difference between two generations fitness functions. The termination criteria can also be the number of maximum generations and the GA will stop when this is reached.

### 5.2.2 Genetic algorithm implementation

The set-up of the genetic algorithm is seen in figure 5.7 and an example of the GA set up in `Matlab` is seen in Appendix C. As input for the GA the number of variables ( $N_{vars}$ ), the upper and lower bound and options for the GA are required. For the optimization of the C-section and double C-section the variables are the height, width, lip length and the thickness of the sections. As for the hollow square and hollow hexagon the variables are the height, width and thickness of the sections. The upper and lower bounds are kept the same for the different profiles and are presented in table 5.1. The geometrical dimensions are based on manufacturing constraints. However, the thickness is seen as a discrete variable which varies between  $2\text{ mm}$  and  $5\text{ mm}$  with an increment of  $0.1\text{ mm}$ . This is due to the standard thicknesses of the steel sheets.

**Table 5.1:** Lower and upper bounds for the variables.

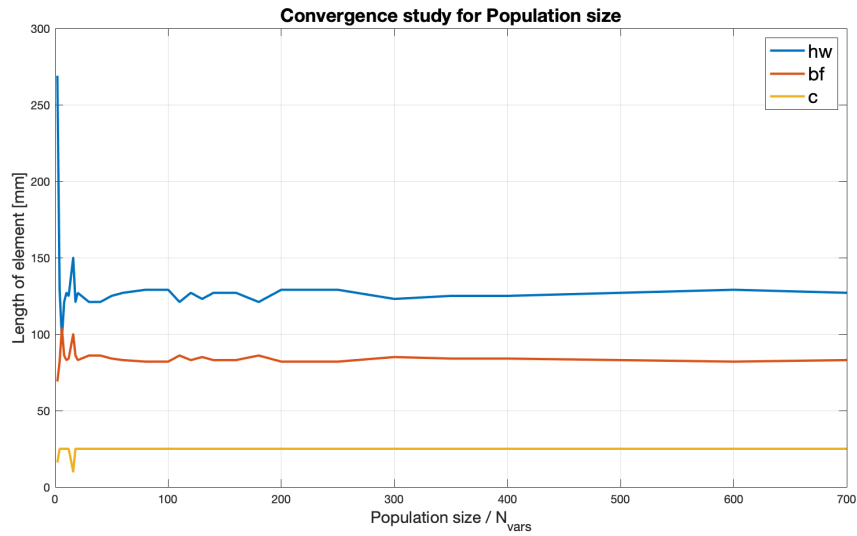
Variables	Lower bound [mm]	Upper bound [mm]
$h_w$	50	160
$b_f$	50	200
$c$	10	30
$t$	1	5


**Figure 5.7:** Flowchart for GA-optimization of cross-sections

The GA options shown in figure 5.7 are population size, max generations, elite count, function tolerance and initial population. A convergence study was performed to obtain the optimal population size to be used. The result of the study can be seen in figure 5.8 which shows that the variables converge after a population size of  $200 \cdot N_{vars}$ . The value for max generations is set to  $100 \cdot N_{vars}$ , this is the generation at which the optimization terminates. The optimization can also be terminated if the function tolerance is reached before the max generation.

**Table 5.2:** Input data for GA-options.

GA-Options	
Population size	$200 \cdot N_{vars}$
Max generation	$100 \cdot N_{vars}$
Elite count	50
Function tolerance	$1 \cdot 10^{-9}$

**Figure 5.8:** Convergence study for variables with different population sizes.

The constraints for the GA optimization are to achieve a high utilization ratio of the cross-sections load carrying capacity. The utilization ratio sought-after should be close to 100 %. Furthermore, there are some geometrical constraints that need to be fulfilled to imply the Eurocode analysis method. These constraints are shown in table 5.3.

**Table 5.3:** Geometrical constraints applied from Eurocode 1993-1-3 (2006).

Geometrical constraints	
$b/t$	$\leq 60$
$c/t$	$\leq 50$
$h/t$	$\leq 500$





# 6

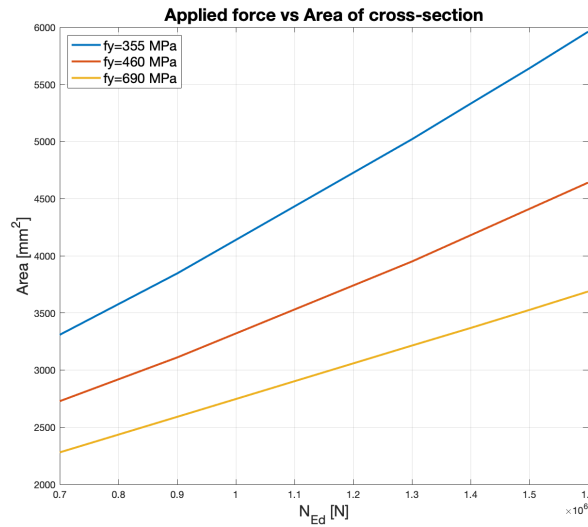
## Results and discussion

The analysed roof truss girders, as described in chapter 4, are to be optimized for a utilization ratio of 100 % using a genetic algorithm. The genetic algorithm is set to minimize the total area of each cross-section used in the relevant roof truss girder. For the upper chord of the roof truss only one cross-section is analysed, double back-to-back C-section. The upper chord can be subjected to different loads depending on the span of the roof truss, the applied evenly distributed loads and height of the roof truss girder as presented in table 4.1. The most common combinations are presented in table 4.2. For each compression force and applied moment an optimized cross-section is defined and presented in this chapter to create a library of cross-sections. Moreover, how these cross-sections are reached in the optimization is analysed.

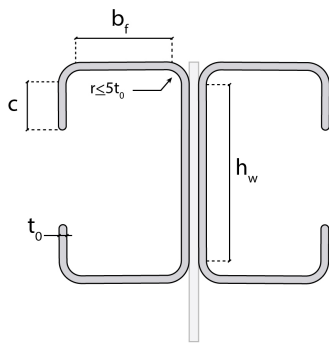
The compressed diagonals in the roof truss girders can be divided into two groups as seen in table 4.3. For each group of diagonals four possible cross-sections are analysed. The possible cross-sections are presented in chapter 4. A library of cross-sections for the compressed diagonals is presented in this chapter.

## 6.1 Upper chord

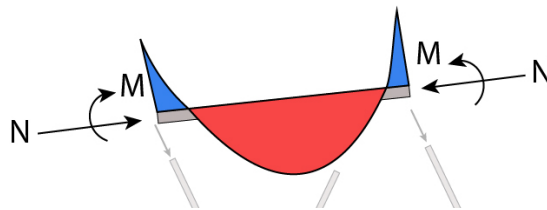
For the upper chord the cross-sectional area can be seen in figure 6.1. The results show that for higher applied force the cross-sectional area increases linearly for each steel yield strength. It can also be seen that the higher yield strength steel needs less cross-sectional area to achieve enough load carrying resistance. The ratios between areas needed to achieve enough load carrying resistance for different steel yield resistance for different steel yield strengths can be seen in figure 6.4. For the upper chord a fixed length of  $3\text{ m}$  is set. The cross-section analysed can be seen in figure 6.2 while the moment distribution with applied axial force and moment can be seen in figure 6.3.



**Figure 6.1:** Area needed to obtain enough load carrying resistance for different steel qualities; Upper chord  $L = 3\text{ m}$ .



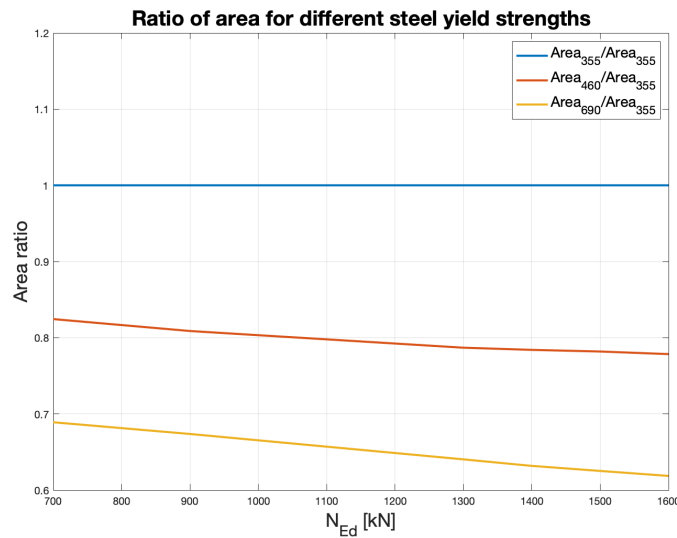
**Figure 6.2:** Cross-section of upper chord element.



**Figure 6.3:** Moment distribution over the upper chord.

It can also be seen from figure 6.1 that as the axial force increases the area needed to achieve enough load carrying resistance for different steel yield strength is not proportional. This behaviour is due to local buckling being more susceptible for higher

yield strength steel. To illustrate this behaviour the S355 steel is set as reference and the ratio of needed area for different yield strength steel can be compared as seen in figure 6.4. The figure presents the ratio of needed area when higher yield strength steel is used for increasing axial force. When S460 steel is used the upper chord needs between 18 % – 22 % less area, while for S690 steel needs between 32 % – 39 % less area. Considering that the difference in cost between S355 and S460 steel is minimal with savings of 18 % – 22 % in weight the S460 steel is more efficient to use. For S690 steel there is even more weight savings to be done, however, this comes with an added cost. For S690 steel the cost saved in material weight will be added back by higher steel yield strength cost. The cross-section library for the upper chord can be seen in table 6.1 with steel yield strength of 460 MPa.

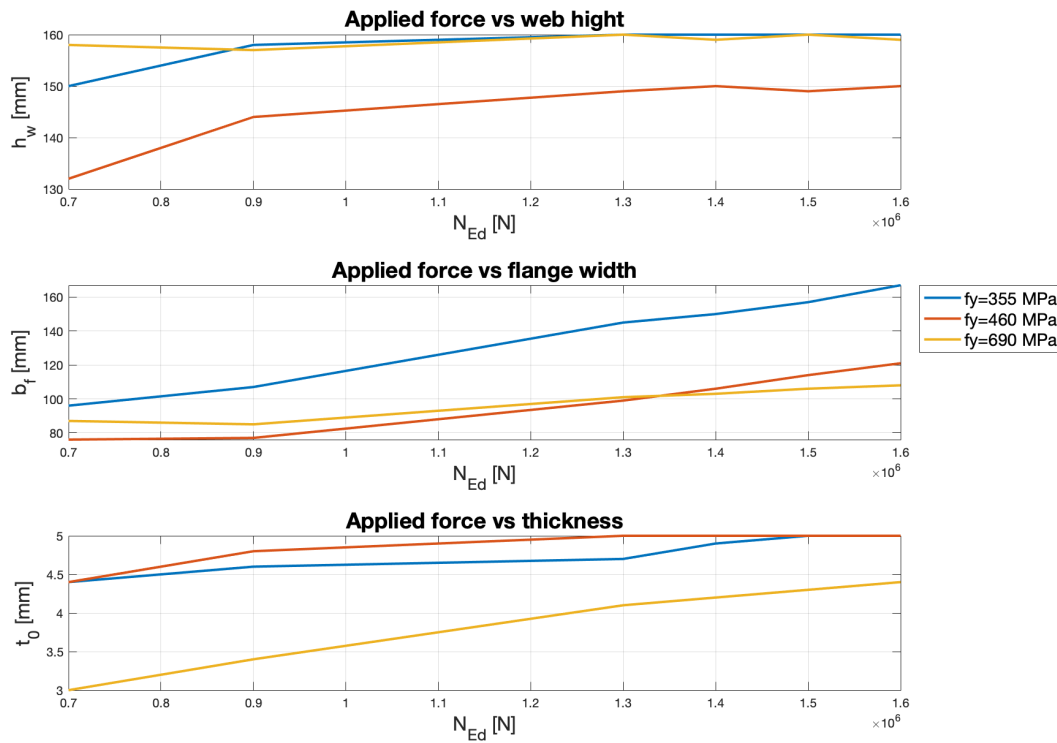


**Figure 6.4:** Ratios between areas needed to obtain enough load carrying resistance for different steel yield strengths; Upper chord  $L = 3\text{ m}$ .

**Table 6.1:** Optimized cross-sections for different applied loads; upper chord  $f_y = 460\text{ MPa}$ .

$N_{Ed}$ [kN]	$h_w$ [mm]	$b_f$ [mm]	$c$ [mm]	$t_0$ [mm]	$Area$ [mm <sup>2</sup> ]	$UR$ Cross-section	$UR$ Buckling
700	132	76	13	4,4	2728	0,9622	0,9756
900	144	77	13	4,8	3110	0,9734	0,9806
1300	149	99	24	5	3950	0,9719	0,9809
1400	150	106	28	5	4148	0,9687	0,9782
1500	149	114	32	5	4410	0,9726	0,9804
1600	150	121	36	5	4640	0,9736	0,9795

An interesting observation for the upper chord is that the web height first reaches the upper limit set in the GA optimization followed by the flange width as seen in figure 6.5. This is due to the fact that the upper chord design is governed by bending/buckling around y-y axis and the most optimum utilization of material in the cross-section is obtained by, first increasing the web height, and when the upper limit value is reached, by increasing the flange width. It can also be seen that the thickness reaches the upper limit for S355 and S460 steel to increase the buckling resistance for higher loads.



**Figure 6.5:** Dimensions of upper chord cross-section vs applied force.

In this study only a minimal area of the cross-section is set as a fitness function for the GA. However, looking at different steel strengths for a given applied force of 700 kN the lower strength steel achieves higher utilization ratios, especially cross-section resistance utilization ratio, in comparison to S690 steel. For the upper chord it can also be seen that for S460 steel both the cross-section resistance utilization ratio and buckling resistance utilization ratio reaches nearly 100 %. The difference in area of the cross-section can be seen in table 6.2. If the goal is to achieve the highest utilization ratios than the lower yield strength steel is too be used. It can be argued that the greater area for the lower yield strength steel can be justified by the cost of higher-grade steel. Considering that S460 steel also reaches full utilization ratios with almost no difference in price compered to S355 steel indicates that S460 steel is the best alternative for the upper chord. However, the least area will be achieved by using S690 steel. The library is created using S460 steel as it reaches

full utilization ratio and needs less area compared to S355 steel with no major added cost.

**Table 6.2:** Cross-section dimensions for applied normal force  $N_{Ed} = 700 \text{ kN}$  and different steel strengths.

$N_{Ed}$	$h_w$	$b_f$	$c$	$t_0$	$Area$	$f_y$	$UR$	$UR$	$Difference \text{ in area}$
$[kN]$	$[mm]$	$[mm]$	$[mm]$	$[mm]$	$[mm^2]$	$[MPa]$	Cross-section	Buckling	$[\%]$
700	158	87	24	3	2280	690	0,7834	0,9806	-
700	132	76	13	4	2728	460	0,9622	0,9755	18
700	150	96	17	4	3309	355	0,9798	0,9790	31

## 6.2 Compressed diagonals

The optimized cross-sections for the two diagonal groups will be presented in two separate sub-chapters to easily distinguish the result. The outcome of the GA is presented in figures and tables and some load and spans are analysed to gain further understanding of how the optimization is obtained. When analysing the result of for different lengths of the diagonals mainly analyses of diagonal 1 is presented. However, it should be mentioned that the same behaviour was seen for diagonal 2 in the cases that has been looked analyzed.

### 6.2.1 Diagonal group 1

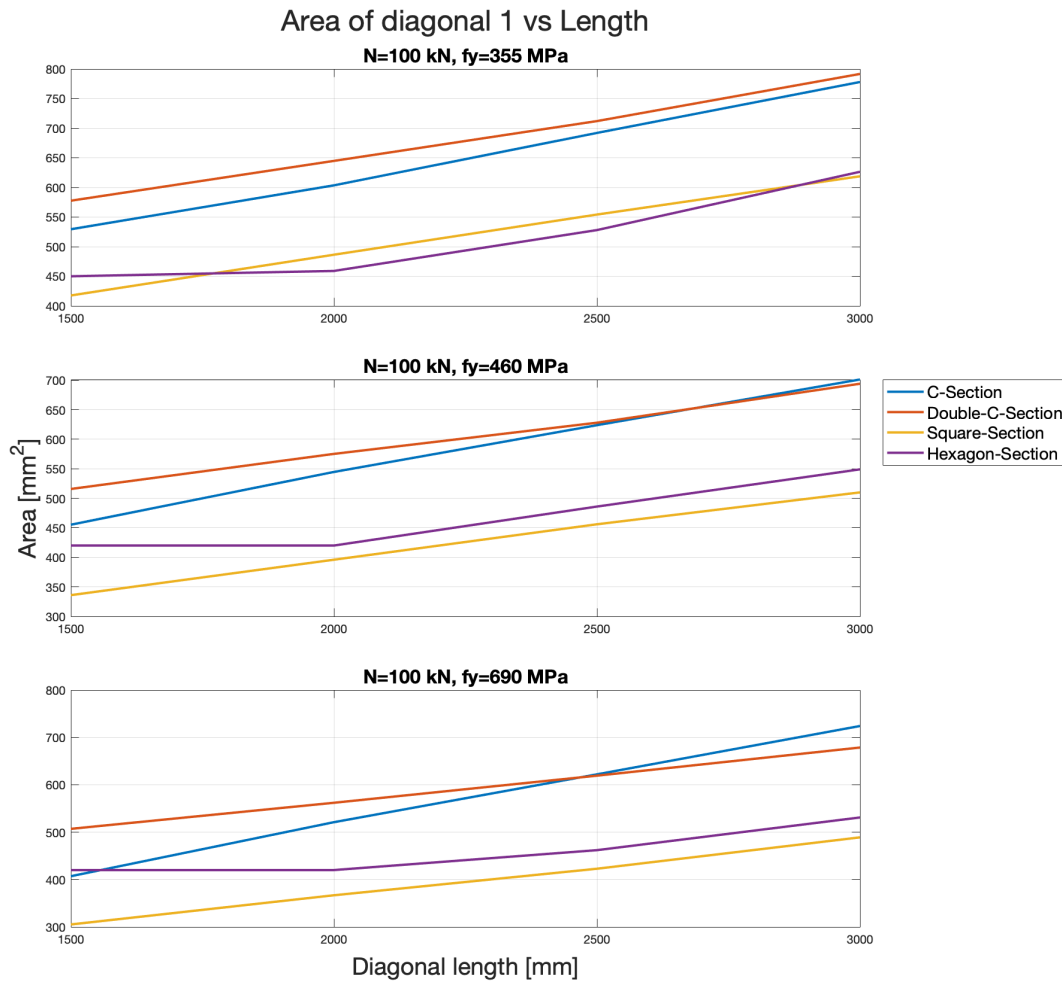
The results of diagonal 1, which is subjected to 100 kN, is presented in figure 6.6 where the area and length of the diagonal is displayed. The four cross-sections were optimized, and the first graph represents the yield strength  $f_y = 355 \text{ MPa}$ , the middle graph  $f_y = 460 \text{ MPa}$  and the last  $f_y = 690 \text{ MPa}$ .

For the S355, the most optimized section for diagonals longer than 1.75 m is obtained for the hexagon cross-sections. It was expected to reach a lower area for the hollow square- and hexagon-sections compared to C- and double C-sections since these closed sections have higher stiffness, less torsion and distorsional buckling effects.

It is interesting that the C-section is a better choice, when it comes to area, than the double C-section for different lengths of the diagonal when S355 or S460 are used. For S690, double C-sections give a slightly lower cross-sectional area for longer diagonals. This is mainly due to the effects of local buckling. For double C-section there are two webs located on the natural axis giving less effect for the second moment of area. This will result in greater area compared to a C-section. This behaviour is further explained in chapter 6.2.1.2. However, a hypothesis is that the double C-section can have higher buckling resistance for the limits set in the GA compared

to a C-section.

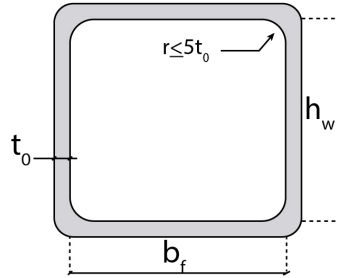
Another interesting observation from figure 6.6 is that the area of the hexagon cross-section does not change for the first two lengths. This is due to the lower limits set in the GA optimization for width and height. It is concluded that widths and height smaller than  $50\text{ mm}$  are not in the scope of this study. However, changing the lower limit will not affect the results in a major way as the hexagon cross-section area is linear. The hexagon cross-section area will therefore be parallel line with the square cross-section line seen in figure 6.6.



**Figure 6.6:** Area needed to obtain enough load carrying capacity for different cross-sections; diagonal 1.

For all cross-sections used as diagonals the utilization ratio is close to 100 %. The comparison between the different cross-sections is therefore only dependent on the area. For the optimization done in this study only the buckling resistance utilization ratio is of interest for the compressed diagonals. This results in high utilization ratio for different steel yield strengths. For the cross-section analysed the most effective

cross-section is square cross-section as seen in figure 6.7 and the dimensions are presented in table 6.3.



**Figure 6.7:** Cross-section of diagonal 1.

**Table 6.3:** Optimized cross-sections for different length of diagonal elements with applied force  $N_{Ed} = 100 \text{ kN}$ ; diagonal 1  $f_y = 690 \text{ MPa}$  (square cross-section).

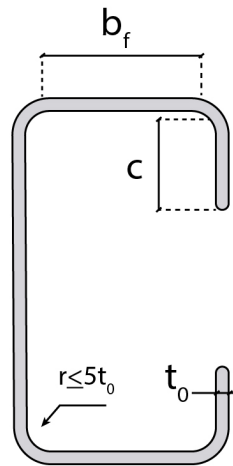
$L$ [m]	$h_w$ [mm]	$b_f$ [mm]	$t_0$ [mm]	$A_{gross}$ [mm <sup>2</sup> ]	UR Buckling
1,5	54	55	1,4	305	0,9771
2	65	66	1,4	367	0,9741
2,5	76	75	1,4	423	0,9764
3	81	82	1,5	489	0,9802

For the full roof truss girder concept the square and hexagon cross-section will practically not work as diagonals. This is due to the connection between the upper chord (back-to-back double C-section) and the diagonals being difficult to manufacture for closed sections. From a manufacturing and construction point of view, open section will be feasible with regards to connection between the upper chord and diagonals. The library for both groups of diagonals will therefore consist of C-sections as seen in figure 6.8. For diagonal 1 the final library is presented in table 6.4.

**Table 6.4:** Library for diagonal group 1 with applied force  $N_{Ed} = 100 \text{ kN}$  consisting of C-section with S690 steel ( $f_y = 690 \text{ MPa}$ ).

$L$ [m]	$h_w$ [mm]	$b_f$ [mm]	$c$ [mm]	$t_0$ [mm]	$A_{gross}$ [mm <sup>2</sup> ]	UR Buckling
1,5	50	50	22	2,1	407	0,9536
2	151	86	12	1,5	521	0,9807
2,5	158	94	10	1,7	622	0,9759
3	160	108	13	1,8	724	0,9790

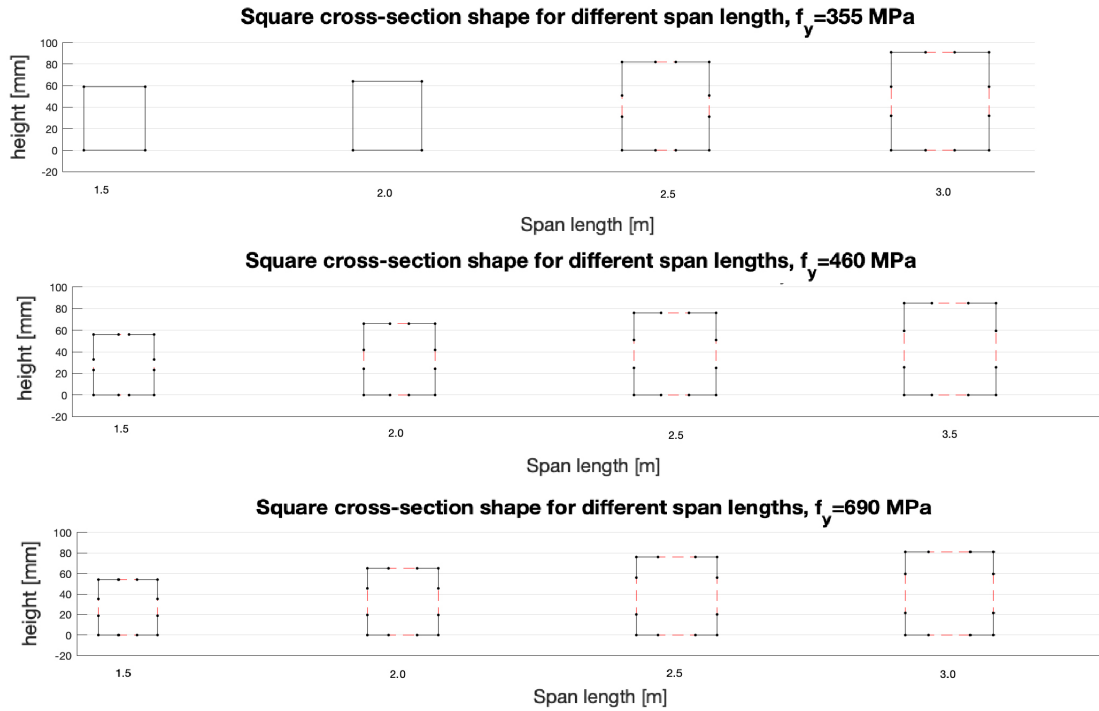




**Figure 6.8:** Back-to-back C-section used as diagonal.

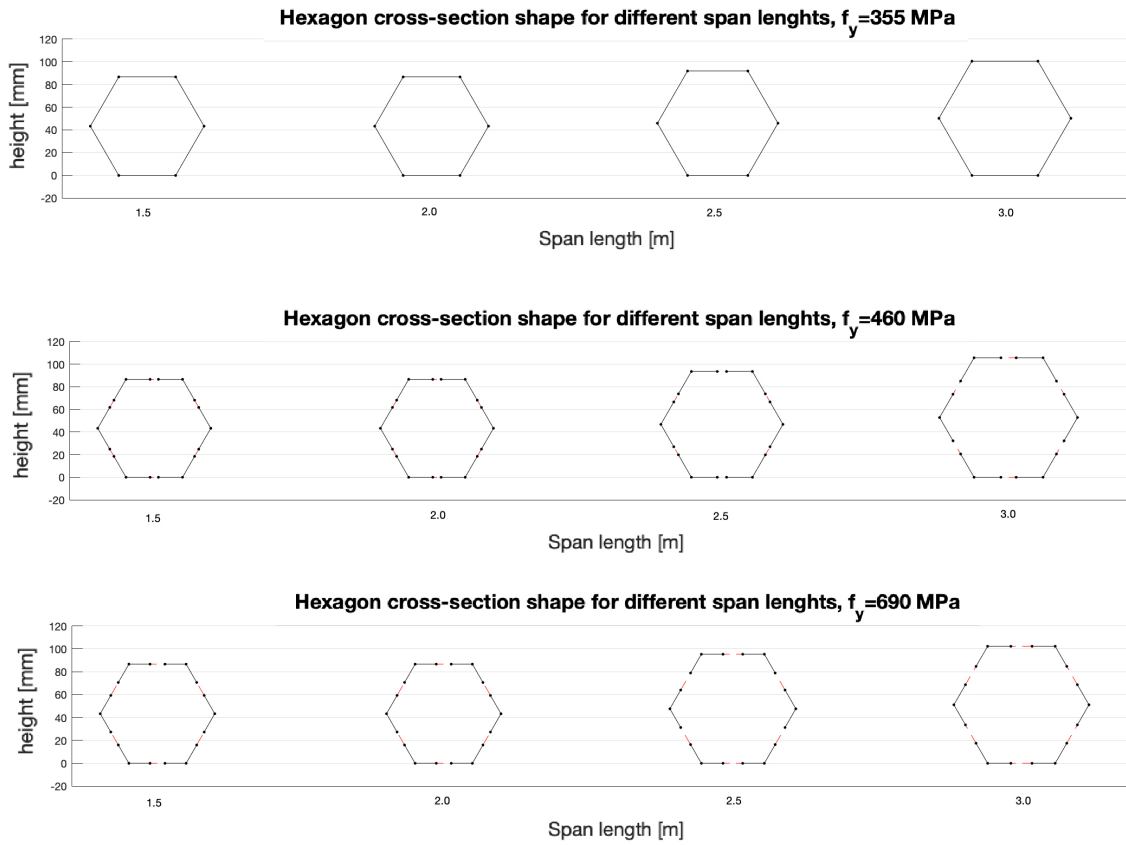
### 6.2.1.1 Square cross-section vs hexagon cross-section

When the higher yield strengths are analysed, it can be seen in figure 6.6 that the most optimized cross-section is the hollow-square section both for the case where  $f_y = 460 \text{ MPa}$  and  $f_y = 690 \text{ MPa}$ . The reason for that is that the square-section needs to be reduced for  $f_y = 355 \text{ MPa}$  and when  $f_y$  is increased the section can be more compact (with shorter wall height) and thus the effective width (area) is increased. For lower yield strength steel ( $f_y = 355 \text{ MPa}$ ) it can also be seen that the hexagon cross-section will need less area compared to the square cross-section. This is due to that the slenderness of the walls in the hexagon cross-section is less than that for a square cross-section with the same area. This is mainly due to the bends in the hexagons cross-sections webs acting as stiffeners or dividers to reduce the effects of local buckling. This can be seen in figure 6.9 and figure 6.10 where the square cross-section strength will be determined by buckling strength while hexagon cross-section by yield strength for  $f_y = 355 \text{ MPa}$ . The reduction of area of the cross-section due to local buckling is seen in figure 6.9 and figure 6.10 as red dotted lines.



**Figure 6.9:** Square cross-section shape for different span lengths in group diagonal 1. Cross-section capacity determined by local buckling if cross-section area is reduced (class 4).

## 6. Results and discussion



**Figure 6.10:** Hexagon cross-section shape for different span lengths in group diagonal 1. Cross-section capacity determined by local buckling if cross-section area is reduced (class 4).

To better understand what happens when comparing the hollow square and hollow hexagon section the effective areas, along with the second moment of areas, for the two cross-sections are presented in table 6.5. The values represent the yield strength  $f_y = 690$  MPa and different lengths of the diagonal.

**Table 6.5:** Square cross-section vs hexagon cross-section effective area and second moment of area for different length of diagonals  $f_y = 690$  MPa.

	Square cross-section			Hexagon cross-section		
$L$ [m]	$A_{eff}$ [mm <sup>2</sup> ]	$I_y$ [mm <sup>4</sup> ]	$I_z$ [mm <sup>4</sup> ]	$A_{eff}$ [mm <sup>2</sup> ]	$I_y$ [mm <sup>4</sup> ]	$I_z$ [mm <sup>4</sup> ]
1,5	211	$1,532 \cdot 10^5$	$1,490 \cdot 10^5$	310	$3,355 \cdot 10^5$	$3,208 \cdot 10^5$
2	219	$2,653 \cdot 10^5$	$2,593 \cdot 10^5$	310	$3,355 \cdot 10^5$	$3,208 \cdot 10^5$
2,5	225	$3,977 \cdot 10^5$	$4,057 \cdot 10^5$	317	$5,436 \cdot 10^5$	$4,270 \cdot 10^5$
3	258	$5,464 \cdot 10^5$	$5,364 \cdot 10^5$	365	$7,189 \cdot 10^5$	$5,648 \cdot 10^5$

Despite that the hollow hexagon cross-section has a smaller effective area for the same diagonal length and yield strength, the buckling resistance of a hollow square is higher. This can be explained through equation 6.1, even if the effective area ( $A_{eff}$ ) is smaller for one case the buckling resistance can reach a higher value through a greater reduction factor ( $\chi$ ). The parameter  $N_{cr}$  in equation 6.2 is dependent on the second moment of area ( $I$ ) and a smaller  $I$  will result in a greater reduction factor, and this is the case here and thereby the buckling resistance is greater.

$$N_{b,Rd} = \chi A_{eff} f_y \quad (6.1)$$

Where:

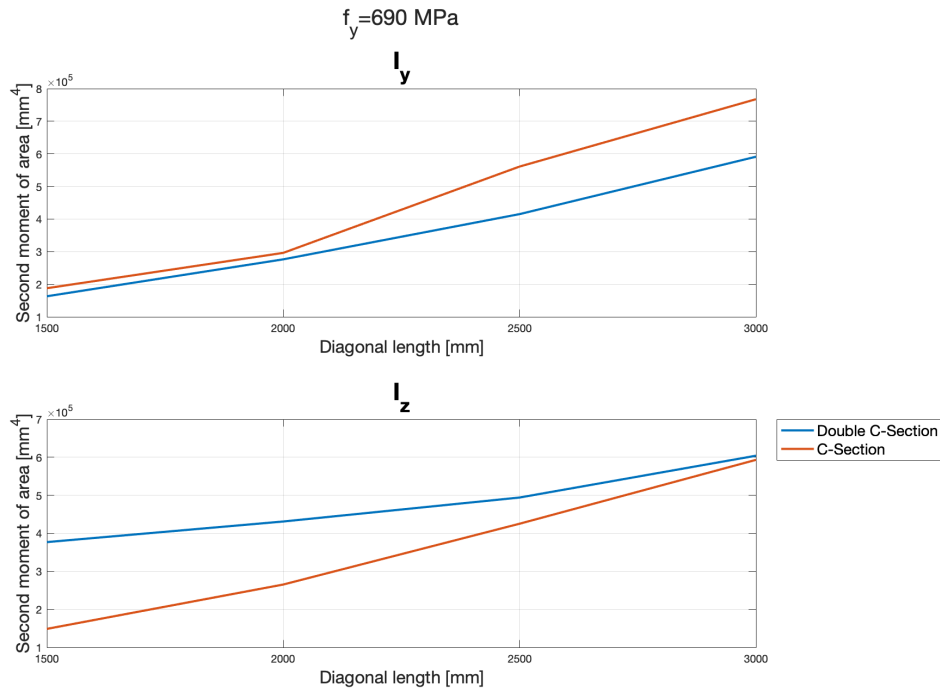
$$\chi = \sqrt{\frac{N_y}{N_{cr}}} \quad (6.2)$$

#### 6.2.1.2 Single C-section vs double C-section

From the results it can also be seen that the double C-section generally needs more area compared to a C-section for the same applied axial force on the diagonals. A hypothesis was that the double C-section will for most cases need less area when used as a diagonal.

The results shows that both the cross-sections have a similar height of the web which is most critical to have enough buckling resistance. On the other hand, the length of the flange is shorter for the double C-section as well as thinner nominal thickness. This results in a rather equal area of the two sections. This could be seen for other cases as well (other span lengths and yield strengths). For the double C-section that the flange is  $40\text{ mm}$  for most spans, which is the lower limit set in the GA. This will result in a double C-section with greater area than that for a C-section.

Compering the dimensions of a C-section and a double C-section the slenderness of the two cross-sections will be nearly the same. As the double C-section consists of two back-to-back C-section the natural axis in y-y plane will be where the two webs are connected. The results show that the global optimization wants to reach the same magnitude for the second moment of area in both the y-y and z-z plane. Both the cross-sections will also have very similar second moment of area, as the same buckling resistance is sought after. This can be seen in figure 6.11. As a result of this the web height for the two cross-sections will be nearly the same to achieve the same second moment of area in y-y plane. The distance from the natural axis to the flange centre of gravity for the double C-section will also yield in a smaller width for the flanges as compared to a C-section.



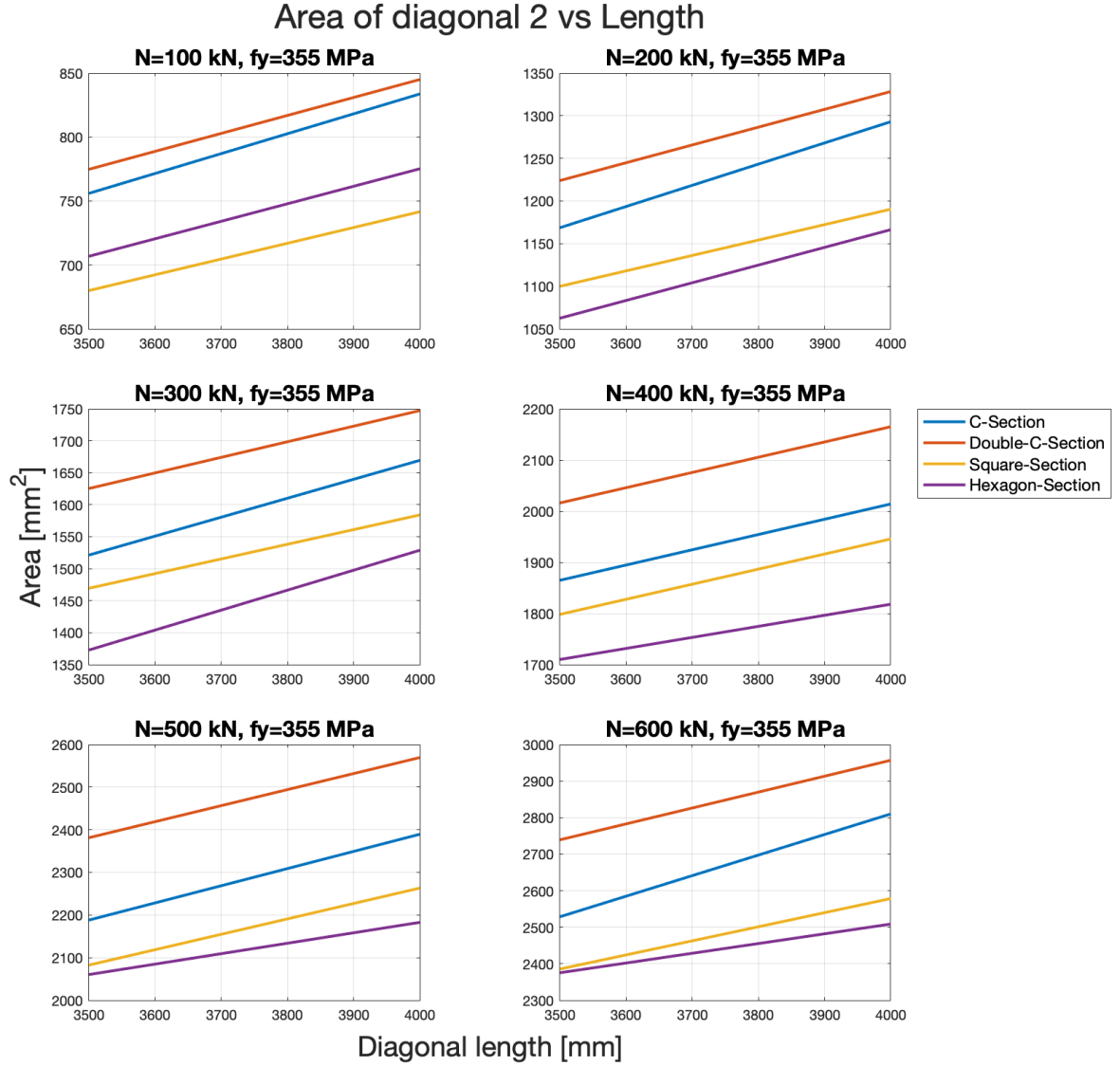
**Figure 6.11:** Second moment of area for C-section and double C-section.

## 6.2.2 Diagonal group 2

As mentioned previously the compressed diagonals are analysed in two groups that covers the most common lengths and applied forces for typical roof truss girders in the studied interval. The second group of diagonals, diagonal 2, are subjected to compression forces that varies between  $100\text{ kN}$  and  $600\text{ kN}$  with lengths between  $3,5\text{ m}$  and  $4\text{ m}$ , which is presented in table 4.3. For this group, an optimization is made to create a library of optimized cross-section for the different lengths and applied forces. The optimizations aim is to find the lowest area possible for a cross-section that is needed to have enough buckling resistance. For the four cross-sections analysed (see chapter 4) the area needed for each cross-section can be seen in figure 6.12 for steel yield strength of  $355\text{ MPa}$ , figure 6.13 for steel yield strength of  $460\text{ MPa}$  and figure 6.14 for yield steel strength of  $690\text{ MPa}$ .

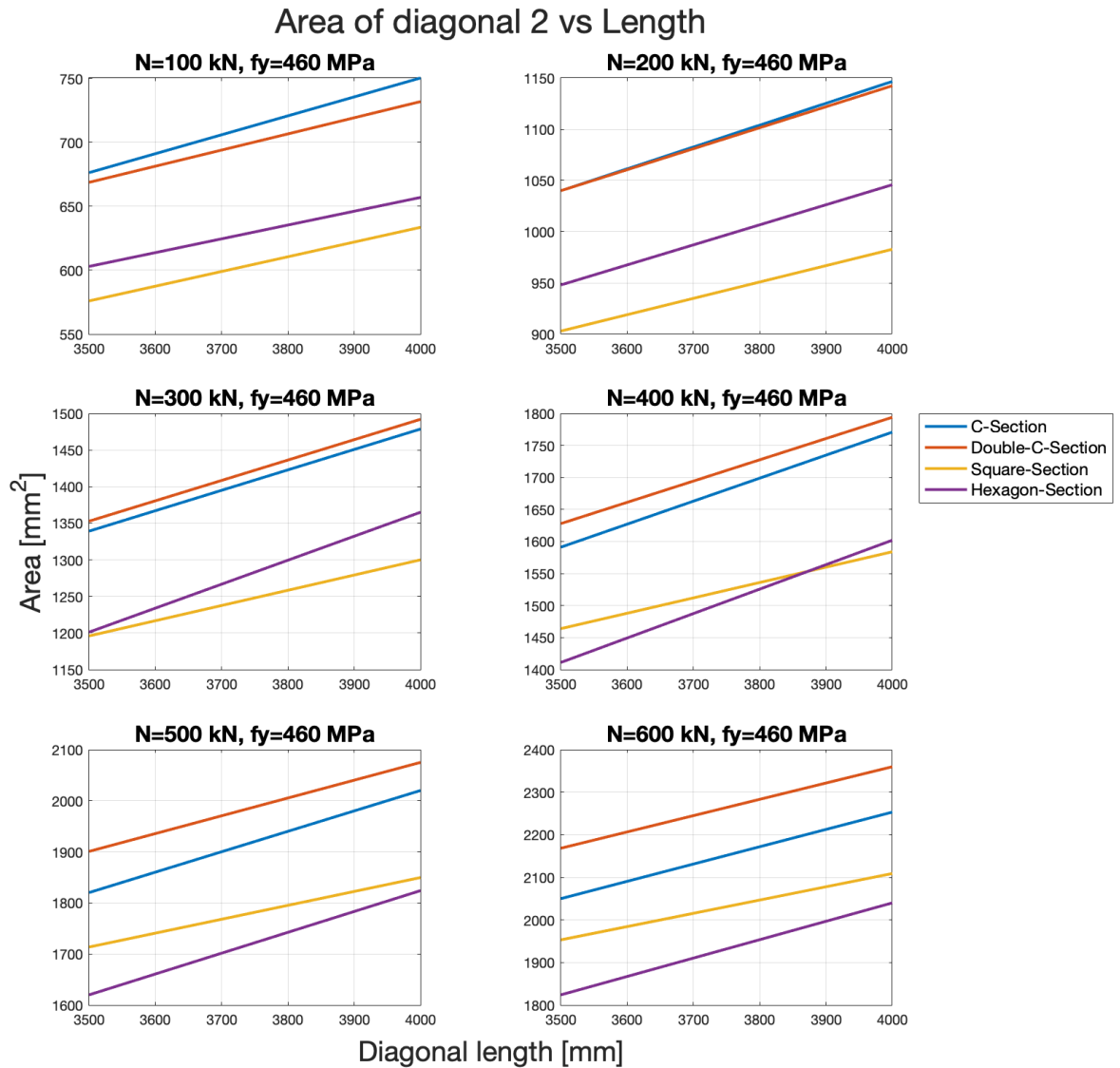
From the results the most optimized cross-section for steel yield strength of  $355\text{ MPa}$  is the hexagon cross-section for five out of six cases. However, for higher strength steel the square cross-section will need less area to achieve the same buckling resistance of the hexagon cross-section. This trend is in line with the results seen for diagonal group 1. An interesting observation is that for an applied load of  $600\text{ kN}$  on a diagonal with length of  $3,5\text{ m}$  the cross-section with lowest is hexagon cross-section with steel yield strength of  $460\text{ MPa}$ .

From figure 6.12 it is seen that for all applied forces greater then  $100\text{ kN}$  the hexagon cross-section with S355 steel is the best followed by square cross-section. It can also be seen that the double C-section is the least effective.



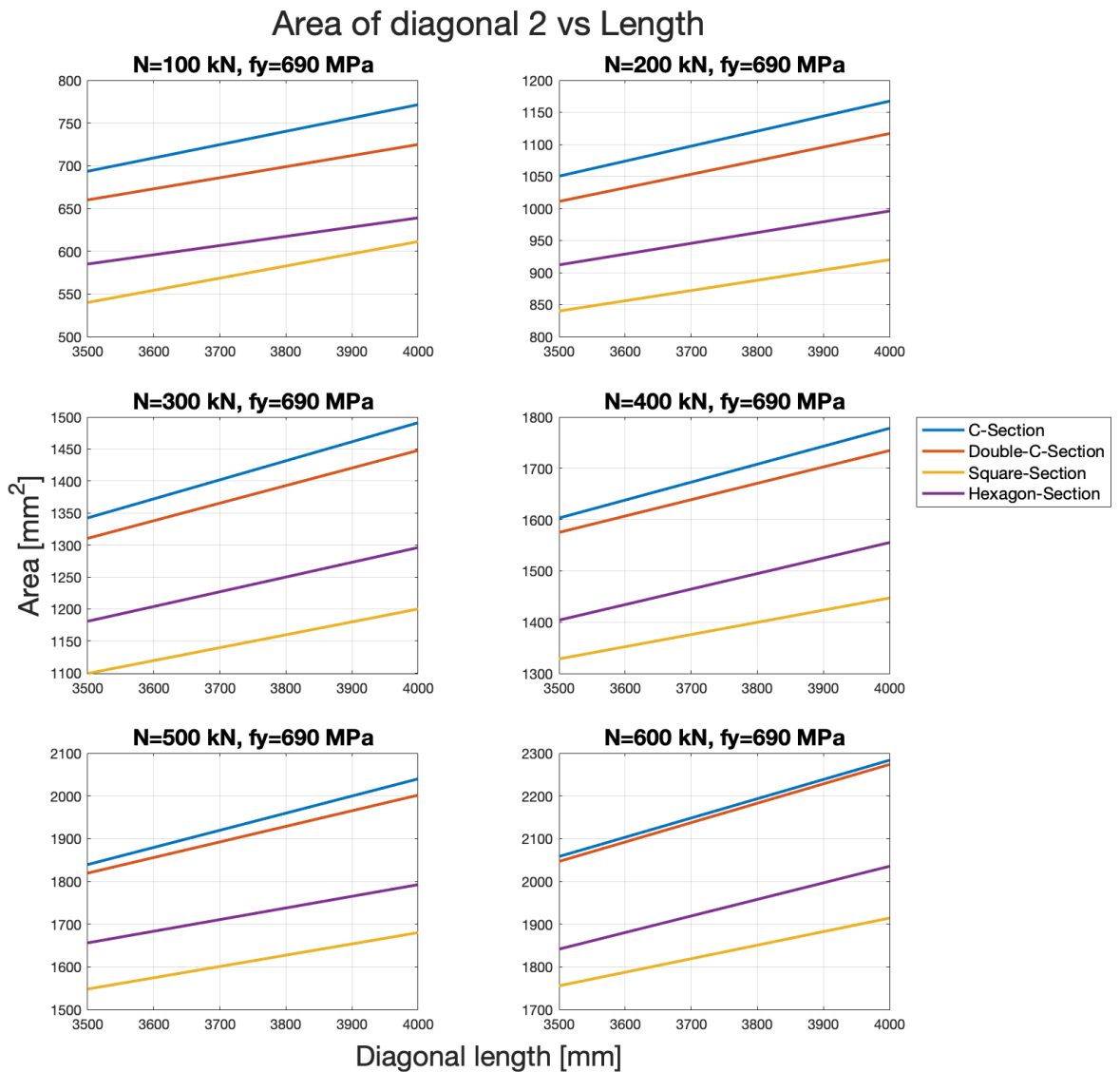
**Figure 6.12:** Area needed to obtain enough load carrying capacity for different cross-sections; diagonal 2,  $f_y = 355\text{ MPa}$ .

From figure 6.13 it is seen that single and double C-section requires almost the same area for S460 steel. The closed sections (hexagon and square sections) are closer in terms of area. However, hexagon cross-section becomes more efficient for higher axial forces.



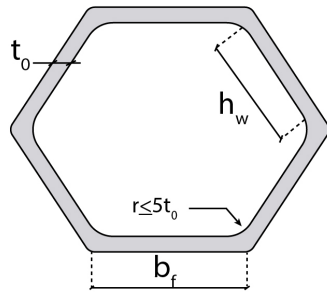
**Figure 6.13:** Area needed to obtain enough load carrying capacity for different cross-sections; diagonal 2,  $f_y = 460 \text{ MPa}$ .

From figure 6.14 it is seen that single C and double C-sections still have rather moderate difference in term of area for S690 steel, the double C-section becomes more efficient with steel yield strength of  $690\text{ MPa}$  compared to yield strength  $355\text{ MPa}$ . It can also be seen that the square cross-section is better in terms of less area than the hexagon cross-section for all applied forces and different diagonal lengths.

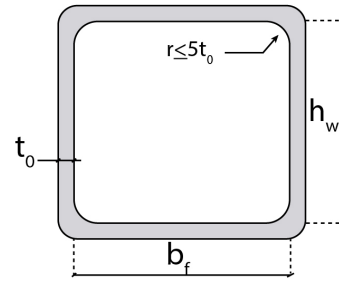


**Figure 6.14:** Area needed to obtain enough load carrying capacity for different cross-sections; diagonal 2,  $f_y = 690\text{ MPa}$ .





**Figure 6.15:** Hexagon cross-section for diagonal 2



**Figure 6.16:** Square cross-section for diagonal 2

The theoretical library created for diagonal group 2 can be seen in table 6.6. The most dominant cross-section is the square cross-section as seen in the table. For each cross-section shown in table 6.6 the dimensions are presented in table 6.7.

**Table 6.6:** Optimized cross-sections type for different length and applied forces of diagonal elements; diagonal 2.

$\begin{matrix} N_{Ed} \\ L \\ [m] \end{matrix}$	100	200	300	400	500	600
3,5	Square-1	Square-2	Square-3	Square-4	Square-5	Hexagon-1
4	Square-6	Square-7	Square-8	Square-9	Square-10	Square-11

**Table 6.7:** Dimension of optimized cross-sections described in table 6.6.

	$h_w$ [mm]	$b_f$ [mm]	$t_0$ [mm]	$f_y$ [MPa]	$A_{gross}$ [mm <sup>2</sup> ]	$UR$
Hexagon-1	95	95	3,2	460	1824	0,9741
Square-1	90	90	1,5	690	540	0,9779
Square-2	105	105	2	690	840	0,9724
Square-3	115	114	2,4	690	1099,2	0,9798
Square-4	123	123	2,7	690	1328,4	0,9785
Square-5	129	129	3	460	1548	0,9782
Square-6	96	95	1,6	690	611,2	0,9774
Square-7	114	116	2	690	920	0,9773
Square-8	126	124	2,4	690	1200	0,9795
Square-9	134	134	2,7	690	1447,2	0,9764
Square-10	140	140	3	690	1680	0,9806
Square-11	145	145	3,3	690	1914	0,9734

As stated previously the closed cross-section are theoretically better for use as diagonals, however, in the concept used for the roof truss girders in this thesis only open cross-section are feasible to use as diagonals. This is due to the connection between the upper chord and diagonals. For diagonal group 2 a C-section is used with the dimensions presented in table 6.8.

**Table 6.8:** Library for diagonal group 2 with consisting of C-section with S690 steel ( $f_y = 690 \text{ MPa}$ ).

$L$ [mm]	$h_w$ [mm]	$b_f$ [mm]	$c$ [mm]	$t_0$ [mm]	$A_{gross}$ [mm <sup>2</sup> ]	$N_{Ed}$ [kN]	$UR$ <i>Buckling</i>
3,5	67	72	21	3,3	835	100	0,9781
3,5	76	84	21	4,5	1287	200	0,9777
3,5	127	88	22	5	1735	300	0,9791
3,5	160	131	10	5	2210	400	0,9776
3,5	160	173	10	5	2630	500	0,9767
3,5	160	200	25	5	3050	600	0,9795
4	72	79	22	3,4	932	100	0,9800
4	85	91	22	4,6	1431	200	0,9797
4	160	97	22	5	1990	300	0,9793
4	160	165	10	5	2550	400	0,9783
4	160	200	27	5	3070	500	0,9828
4	160	200	56	5	3360	600	0,9829

# 7

## Conclusion

The genetic algorithm used for the optimization of steel cross-section analysed in this Master's thesis is set to reach a utilization ratio, for both cross-section resistance and buckling resistance, close to 100 %. The genetic algorithm test different values for web height, flange width and thickness through a number of generations until minimal area with high utilization ratio is reached. The sensitivity of the GA is susceptible to the population size and therefore a convergence study was performed to get the settings needed for high accuracy. The conclusions of the global optimization using the genetic algorithm are presented in this chapter.

### 7.1 Upper chord

For roof truss girders subjected to uniformly distributed loads with spans between 30 – 40 m the upper chord, back-to-back double C-section, has optimized cross-sections as seen in table 7.1.

For the upper chord the library created with back-to-back double C-section is seen in table 7.1 where S460 steel is used. The presented cross-sections are dimensioned for axial loads of 700 – 1600 kN with applied moment of 14 kNm. For S355 steel the cross-sections will have high utilization ratios, however, the area needed to achieve enough load carrying resistance is greater than that for S460 steel. Considering that S460 steel and S355 steel is within the same price range it is more efficient to use S460 steel. As for the S690 steel the needed area to achieve enough load carrying resistance is even less than that for S460 steel but the utilization ratio will be lower. Furthermore, the cost of S690 steel is not within the same price range as S355 and S460 steel and therefore S460 steel is chosen.

**Table 7.1:** Library for upper chord consisting of back-to-back double C-section,  $f_y = 460 \text{ MPa}$ .

	$h_w$	$b_f$	$c$	$t_0$	$A_{gross}$	$I_y$	$I_z$	$I_T$	$I_W$	$W$
	[mm]	[mm]	[mm]	[mm]	[mm <sup>2</sup> ]	[mm <sup>4</sup> ]	[mm <sup>4</sup> ]	[mm <sup>4</sup> ]	[mm <sup>6</sup> ]	[mm <sup>3</sup> ]
CC-145x80	145	80	15	5	3350	$1,223 \cdot 10^7$	$6,301 \cdot 10^6$	$2,792 \cdot 10^4$	$9,805 \cdot 10^9$	$1,687 \cdot 10^5$
CC-150x110	150	110	30	5	4300	$1,740 \cdot 10^7$	$1,812 \cdot 10^7$	$3,583 \cdot 10^4$	$3,376 \cdot 10^{10}$	$2,200 \cdot 10^5$
CC-150x120	150	120	40	5	4700	$1,884 \cdot 10^7$	$2,556 \cdot 10^7$	$3,917 \cdot 10^4$	$5,603 \cdot 10^{10}$	$2,556 \cdot 10^5$

## 7.2 Compressed diagonals

For the compressed diagonals the library created can be seen in the tables below. The hypothesis made for the diagonals was that the hexagon cross-section would be the optimal cross-section. This hypothesis was made as the hexagon cross-section has less risk for local buckling. Furthermore, closed cross-sections are less susceptible to torsional buckling. The results from this study show that the hexagon cross-section will have less risk for local buckling. However, the square cross-section needs less area, for most of the cases, to achieve the same buckling resistance as the hexagon cross-section when higher yield strength is used. For lower yield strength steel, the hexagon cross-section's better resistance to local buckling will result in less area compared to the square cross-section. For diagonal group two with length 3, 5m and applied axial force of 600kN the hexagon cross-section with yield strength of 460 MPa will have the smallest area. Due to manufacturing difficulties the closed cross-sections are not feasible to use as diagonals when the upper chord is a double C-section. An open C cross-section is therefore used and presented in the table 7.2 for diagonal group 1 and 2.

**Table 7.2:** Library for compressed diagonals consisting of C-section,  $f_y = 690 \text{ MPa}$

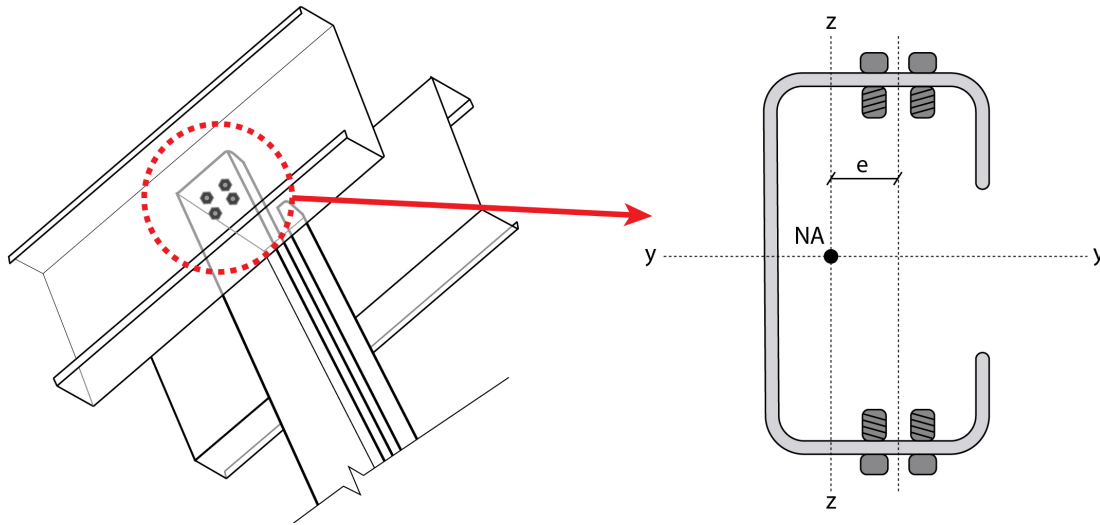
	$h_w$	$b_f$	$c$	$t_0$	$A_{gross}$	$I_y$	$I_z$	$I_T$	$I_W$	$W$
	[mm]	[mm]	[mm]	[mm]	[mm <sup>2</sup> ]	[mm <sup>4</sup> ]	[mm <sup>4</sup> ]	[mm <sup>4</sup> ]	[mm <sup>6</sup> ]	[mm <sup>3</sup> ]
<b>C-50x50x2</b>	50	50	25	2	400	$1,563 \cdot 10^5$	$1,667 \cdot 10^5$	533	$2,331 \cdot 10^8$	5854
<b>C-160x110x2</b>	160	110	15	2	820	$3,815 \cdot 10^6$	$1,344 \cdot 10^6$	1093	$5,347 \cdot 10^8$	28824
<b>C-75x80x4</b>	75	80	25	4	1140	$1,177 \cdot 10^6$	$1,128 \cdot 10^6$	6080	$1,816 \cdot 10^8$	26683
<b>C-85x90x5</b>	85	90	25	5	1575	$2,121 \cdot 10^6$	$1,936 \cdot 10^6$	13125	$3,486 \cdot 10^8$	42313
<b>C-130x90x5</b>	130	90	25	5	1800	$5,422 \cdot 10^6$	$2,252 \cdot 10^6$	15000	$6,987 \cdot 10^9$	67755
<b>C-160x110x5</b>	160	110	25	5	2150	$9,901 \cdot 10^6$	$3,862 \cdot 10^6$	17917	$1,665 \cdot 10^9$	83985
<b>C-160x170x5</b>	160	170	10	5	2600	$1,315 \cdot 10^7$	$9,237 \cdot 10^6$	21667	$3,877 \cdot 10^9$	132390
<b>C-160x200x5</b>	160	200	25	5	3050	$1,566 \cdot 10^7$	$1,618 \cdot 10^7$	25417	$7,268 \cdot 10^9$	144017

### 7.3 Further studies

Further studies can be to analyse other cold-formed profiles than those chosen in this project. This is to find if any other shape of a cross-section can be more optimal with respect to a smaller area and high utilization ratio.

In this study an assumption is that the diagonals are not subjected to any moment. In the real case the diagonals are subjected to a moment due to the eccentricity from point of force application (at bolt connection) to centre of gravity for the cross-section. Figure 7.1 shows a principal bolt connection between an upper chord (double C-section with a gap) and a diagonal (C-section). The eccentricity is seen as a distance  $e$ .

Further studies can analyse the extra moment due to eccentricity of the bolted connection and to have the diagonals placed in between the double C-sections of the upper chord. A hypothesis is that due to the extra moment the double C-section will have less needed area for the diagonals. In the results from this thesis the double C-section is not relevant for diagonals as the area is always bigger than that for a C-section.



**Figure 7.1:** Bolt connection between upper chord and diagonal. Upper chord consist of a double back-to-back C-section with a gap.

Another interesting aspect that can be analysed in further studies is using a double C-section with a gap (as seen in figure 7.1) for the upper chord and placing the diagonals between the two C-sections of the upper chord. As this study is to analyse optimization for both upper chord and diagonals the gap between the two C-section in the upper chord should not be set to width. For a set width for the gap the web height of the diagonals would also be set, and the optimization would be very limited. Further studies could include the optimization of the gap between the two C-section for the upper chord or optimization of web height for the diagonals.

## 7. Conclusion

---

Further investigation is to optimize the roof truss girder by running the optimization again with the obtained cross-sections. By using the double C-section as the upper chord and the square-section as the diagonals. As a result, other lengths of the diagonals, moments and axial forces will be obtained. That will further lead to other dimensions of the optimized cross-sections.

# Bibliography

- 1993-1-1 Eurocode.* Eurocode 3: Design of steel structures - Part 1-1: General rules and rules for buildings. EN 1993-1-1. 2005. 90 p.
- 1993-1-3 Eurocode.* Eurocode 3 - Design of steel structures - Part 1-3: General rules - Supplementary rules for cold-formed members and sheeting. EN 1993-1-3. 2006. 130 p.
- 1993-1-5 Eurocode.* Eurocode 3 - Design of steel structures - Part 1-5: Plated structural elements. 2006. 51 p.
- 1993-1-8 Eurocode.* Eurocode 3: Design of steel structures - Part 1-8: Design of joints. 2005. 130 p.
- Al-Emrani Mohammad, Eengström Börn, Johansson Marie, Johansson Peter.* Bärande konstruktioner - Del 1. 2013. 230 p.
- Dubina D., Ungureanu V., Landolfo R.* Design of Cold-formed Steel Structures. 2012. 646 p.
- Halmos George T.* High-production roll forming. Dearborn, Mich.: Society of Manufacturing Engineers, Marketing Services Dept., 1983. 1st. 258 p. (Manufacturing update series).
- Hansen T., Gath J., Nielsen M. P.* An Improved Effective Width Method Based on the Theory of Plasticity // Advanced Steel Construction. 2010. 6, 1. 515–547.
- Pamfil B., Palm R.* Design and Optimization of Nature-inspired Piezoelectric Generators: Fractal design. 2021. 81 p.
- Quach W. M., Teng J. G., Chung K. F.* Residual stresses in steel sheets due to coiling and uncoiling: a closed-form analytical solution // Engineering Structures. 2004. 26, 9. 1249–1259.
- Rhodes J.* Design of cold formed steel members. London ; New York: Elsevier Applied Science, 1991. 409 p.
- Rondal J.* Cold formed steel members and structures - General Report // Journal of Constructional Steel Research. 2000. 55, 1-3. 155–158.
- Tran T., Li L. Y.* Global optimization of cold-formed steel channel sections // Thin-Walled Structures. 2006. 44, 4. 399–406.



*Ungureanu V., Dubina D.* Single and interactive buckling modes for unstiffened thin-walled steel sections in compression // *Stability and Ductility of Steel Structures*. 1999. 2. 543–550.

*Yu Wei-Wen, LaBoube Roger A., , Yu Weiwen.* Cold-Formed Steel Design. 2010. 51 p.

*Zahn C. J., Iwankiw N. R.* Flexural-Torsional Buckling and Its Implications for Steel Compression Member Design // *Engineering Journal-American Institute of Steel Construction Inc.* 1989. 26, 4. 143–154.

# A

## Appendix: Matlab functions

### A.1 Cross-section classification

```
function [y_tp,class,epsilon]=CSC(Ex,Ey,t,fy,es)

% Written by: Mahdi Mahdi, Chalmers University of Technology
% Master's Thesis 2022
%-----
% PURPOSE
% Compute classification for each part in a cross-section.
%
% INPUT:  Ex = [x_1 x_2;
%              .
%              .
%              .
%              x_n x_m]
%
%         Ey = [y_1 y_2;
%              .
%              .
%              .
%              y_n y_m]      [n,2] Matrix, Element node coordinates
%                               Each row corresponds to a new part
%
%         t      Element thickness [n,1] matrix
%         fy      Yield strength
%
%         es = [StressDistribution_1 PartPosition_1 PartType_1;
%              .
%              .
%              .
%              StressDistribution_m PartPosition_n PartType_n]
%
%                               [n,3] Matrix, one row for each part
%
%         StressDistribution      1 for Compression only
%                                2 for Bending
```

```

%                               3 for Compression and Bending
%
% PartPosition                1 for Internal compression part
%                               2 for Outstand flange
%
% PartType                    1 Web
%                               2 Flange
%                               3 Edge fold
%
%
%
% OUTPUT: y_tp:                Distance from bottom of cross-section to
%                               centroid
%
%           class:              [n,1] Matrix
%                               n: Cross-section classification for each element
%
%           epsilon:            Strain relation
%-----
% LAST MODIFIED: 2022-03-01 by Mahdi Mahdi
%-----

%-----Gross section parameters-----

% Strain relation
epsilon=sqrt(235/fy);

% Function that calculates the distance from bottom of cross-section to
% centroid
y_tp=ytp(Ex,Ey,t);

%-----Cross-section classification-----

for i=1:length(Ex)

% Length of element
c=sqrt((Ex(i,2)-Ex(i,1))^2 + (Ey(i,2)-Ey(i,1))^2);

% Class limits for internal compression part subjected only to compression
if es(i,1)==1 && es(i,2)==1

```

```
class1=33*epsilon;

class2=38*epsilon;

class3=42*epsilon;

end

% Class limits for an outstand flange part subjected only to compression
if es(i,1)==1 && es(i,2)==2

class1=9*epsilon;

class2=10*epsilon;

class3=14*epsilon;

end

% Class limits for an internal compression part subjected to bending
if es(i,1)==2 && es(i,2)==1

class1=72*epsilon;

class2=83*epsilon;

class3=124*epsilon;

end

% Class limits for an outstand flange part subjected to bending
if es(i,1)==2 && es(i,2)==2

disp(['Outstand flange elements can only be subjected to' ...
      ' compression or compression and bending, not only bending'])

end

% Class limits for an internal compression part subjected to combined
% bending and compression

alpha=y_tp/(max(max(Ey)-y_tp));
```

```
% if part is in bending or bending & compression but the whole part
% is in the compression zone than zeta is expressed as the
% following:

if (es(i,1)==2 || es(i,1)==3) && Ey(i,1) >= y_tp

    zeta=-(Ey(i,1)-y_tp)/(Ey(i,2)-y_tp);

    % if part is in bending or bending & compression and the part is
    % not only in compression zone than zeta is expressed as the
    % following:
    elseif (es(i,1)==2 || es(i,1)==3) && Ey(i,1) < y_tp

        zeta=-(Ey(i,1))/(Ey(i,2)-y_tp);

end

% If part is in bending & compression than class limits are calculated as
% the following

if es(i,1)==3 && es(i,2)==1

    if alpha > 0.5

        class1=(396*epsilon)/(13*alpha-1);

    else
        class1=(36*epsilon)/alpha;
    end

    if alpha > 0.5

        class2=(456*epsilon)/(13*alpha-1);

    else
        class2=(41.5*epsilon)/alpha;
    end

    if zeta > -1
```

```
        class3=(42*epsilon)/(0.67+0.33*zeta);

    else
        class3=62*epsilon*(1-zeta)*sqrt(-zeta);

    end
end

% Class for part according to limits calculated above. The element is in
% class 4 if non of the limits are compatible.
if class1>= c/t(i)

    class(i,1)=1;

    elseif class2>= c/t(i)

    class(i,1)=2;

    elseif class3>= c/t(i)

    class(i,1)=3;

else

    class(i,1)=4;

end
end
end
```

## A.2 Distance to centroid

```
function [y_tp,A]=ytp(Ex,Ey,t)

% Written by: Mahdi Mahdi, Chalmers University of Technology
% Master's Thesis 2022
%-----
% PURPOSE
% Compute the distance from bottom of cross-section to centroid and the
% area of the cross-section
%
%
% INPUT:  Ex = [x_1 x_2;
%              .
%              .
```

```
%
%           .
%           x_n x_m]
%
%           Ey = [y_1 y_2;
%                 .
%                 .
%                 .
%                 y_n y_m]      [n,2] Matrix, Element node coordinates
%                               Each row corresponds to a new part
%
%           t                    Element thickness [n,1] matrix
%
% OUTPUT:
%           y_tp:                Distance from bottom of cross-section to
%                               centroid
%
%           A:                   Area of cross-section
%-----
%
% LAST MODIFIED: 2022-03-01 by Mahdi Mahdi
%-----
```

```
top=0;
for i=1:length(Ex)

    % Length of element
    c=sqrt((Ex(i,2)-Ex(i,1))^2 + (Ey(i,2)-Ey(i,1))^2);

    % If change in x-axis is zero than element is 90° to x-axis

    if (Ex(i,2)-Ex(i,1))==0

        % Angle of element from x-axis
        theta=pi/2;

    else

        theta=atan(sqrt((Ey(i,2)-Ey(i,1))^2/(Ex(i,2)-Ex(i,1))^2));

    end

    % If angle of element is 0° than midpoint of element is at
    % half thickness (where our x-axis is, therefore y_e=0).
    if theta==0
```

```
        y_e=0;

    else

        % Length from element mid point to element bottom
        y_e=sin(theta)*c/2;

    end

    % Length from x-axis of coordinate system to midpoint of element
    y_i(i)=Ey(i,1)+y_e;

    % Area of element
    A_i(i)=t(i)*c;

    % Sum of each part
    top=top+A_i(i)*y_i(i);
end

% Area of cross-section
A=sum(A_i);

% Distance from bottom of cross-section to centroid
y_tp=top/A;

end
```

### A.3 Second moment of area

```
function [I]=SecondMomentOfArea(Ex,Ey,t,y_tp)

% Written by: Sarah Aref & Mahdi Mahdi, Chalmers University of Technology
% Master's Thesis 2022
%-----
% PURPOSE
% Compute the second moment of area of a cross-section.
%
% INPUT:  Ex = [x_1 x_2;
%              .
%              .
%              .
%              x_n x_m]
%
%         Ey = [y_1 y_2;
%              .
%              .
%              .
%              y_n y_m]
```



```
%
%      .
%      .
%      y_n y_m]      [n,2] Matrix, Element node coordinates
%                      Each row corresponds to a new part, n is
%                      number of parts
%
%      t      Element thickness [n,1] Matrix
%
%      y_tp      Distance from bottom of cross-section to centroid
%
%
% OUTPUT:
%      I:      Second moment of area of cross-section
%-----
%
% LAST MODIFIED: 2022-03-26 by Sarah Aref
%-----

I_i=0;

for i=1:length(Ex)

    % Length of each element
    c=sqrt((Ex(i,2)-Ex(i,1))^2 + (Ey(i,2)-Ey(i,1))^2);

    % Calculating angle of element from x-axis
    theta=atan(sqrt((Ey(i,2)-Ey(i,1))^2/(Ex(i,2)-Ex(i,1))^2));

%-----If change in x-axis is zero-----
%-----the element is 90° to x-axis-----

    % If element is above the neutral axis
    if ((Ex(i,2)-Ex(i,1))==0) && (max(Ey(i,:)) > y_tp)

        theta=pi/2;

        % Distance from element midpoint to element bottom
        y_e=sin(theta)*c/2;

        % Calculating second moment of area for each element
        I_i(i)=t(i)*c^3/12+(t(i)*c*(y_tp-(Ey(i,1)+y_e))^2);

    % If element is below the neutral axis
    elseif ((Ex(i,2)-Ex(i,1))==0) && (max(Ey(i,:)) < y_tp)
```

```
theta=pi/2;

% Distance from element midpoint to element bottom
y_e=sin(theta)*c/2;

% Calculating second moment of area for each element
I_i(i)=t(i)*c^3/12+(t(i)*c*(y_tp-y_e)^2);

%-----If angle of element is 0°-----

% If the element is above the neutral axis
elseif (theta==0) && (max(Ey(i,:)) > y_tp)

    % Calculating second moment of area for each element
    I_i(i)=c*t(i)^3/12+(c*t(i)*(Ey(i,2)-y_tp)^2);

% If the element is below the neutral axis
elseif (theta==0) && (max(Ey(i,:)) < y_tp)

    % Calculating second moment of area for each element
    I_i(i)=c*t(i)^3/12+(c*t(i)*(y_tp-Ey(i,2))^2);

%-----If the element is inclined-----

% If element is above the neutral axis
elseif (max(Ey(i,:)) > y_tp)

    % Distance from element midpoint to element bottom
    y_e=sin(theta)*c/2;

    % Calculating second moment of area for each element
    I_i(i)=t(i)*c/12*(c^2*cos(theta)^2+t(i)^2*sin(theta)^2)...
        +(t(i)*c*(Ey(i,2)-y_tp-y_e)^2);

% If element is below the neutral axis
elseif (max(Ey(i,:)) < y_tp)

    % Distance from element midpoint to element bottom
    y_e=sin(theta)*c/2;

    % Calculating second moment of area for each element
    I_i(i)=t(i)*c/12*(c^2*cos(theta)^2+t(i)^2*sin(theta)^2)+...
        (t(i)*c*(Ey(i,1)+y_e-y_tp)^2);
```

```

end

% Total second moment of area
I=sum(I_i);

end

```

## A.4 Flange reduction

```

function [Ex_flange,Ey_flange,t_flange,es_flange]=...
    flangeEdgefoldReductionCompression(Ex,Ey,t,es,class,epsilon)

% Written by: Mahdi Mahdi, Chalmers University of Technology
% Master's Thesis 2022
%-----
% PURPOSE
% Reduce flanges and edge folds that are in cross-section class 4.
%
% INPUT:  Ex = [x_1 x_2;
%              .
%              .
%              .
%              x_n x_m]
%
%         Ey = [y_1 y_2;
%              .
%              .
%              .
%              y_n y_m]    [n,2] Matrix, Element node coordinates
%                           Each row corresponds to a new part
%
%         es = [StressDistribution_1 PartPosition_1 PartType_1;
%              .
%              .
%              .
%              StressDistribution_m PartPosition_n PartType_n]
%
%                           [n,2] Matrix, one row for each part
%
% StressDistribution      1 for Compression only
%                        2 for Bending
%                        3 for Compression and Bending
%
% PartPosition           1 for Internal compression part
%                        2 for Outstand flange
%

```

---

```

%      PartType          1 Web
%                        2 Flange
%                        3 Edge fold
%
%      t                  Element thickness [n,1] matrix
%
%      class              [n,1] Matrix for CSC of each part
%                        n: Cross-section class for each element
%
%      epsilon            Strain relation
%
%
% OUTPUT:
%
% Ex_flange & Ey_Flange:  Coordinates for reduced flange and edge folds
%
%      t_flange:          Thickness for reduced flange and edge fold
%                        elements
%
%      es_flange:         Element parameters for reduced flange and edge
%                        fold
%-----
%
% LAST MODIFIED: 2022-03-22 by Mahdi Mahdi
%-----

% Creating output matrices
Ex_flange=[];
Ey_flange=[];
t_flange=[];
es_flange=[];
class_flange=[];

%-----Reduction of flange-----

% Start values for reduction factor rho
rho=[1;1];

for i=1:length(class)

    % Length of element
    c(i)=sqrt((Ex(i,2)-Ex(i,1))^2 + (Ey(i,2)-Ey(i,1))^2);

```

```
% Reduction for all parts in class 4 if cross-section is in
% compression only
if (class(i)==4) && all(es(:,1)==1)

    % For compression zeta is always 1 for flanges
    zeta=1;

    % Reduce flange first
    if es(i,3)==2

        % K_sigma for internal compression element
        if es(i,2)==1

            K_sigma=4;

            % K_sigma for external compression element
            elseif es(i,2)==2

                K_sigma=0.43;

        end

        % Slenderness
        lambda_p=(c(i)/t(i))/(28.4*epsilon*sqrt(K_sigma));

        % Reduction factor rho for internal compression element
        if es(i,2)==1

            if lambda_p <= 0.673

                rho=1;

            else

                rho=(lambda_p - 0.055*(3+zeta))/(lambda_p^2);

            end

        % Reduction factor rho for external compression element
        elseif es(i,2)==2

            if (lambda_p <= 0.748) && (es(i,2)==2)

                rho=1;

            end

        end

    end

end
```

```
elseif (lambda_p > 0.748) && (es(i,2)==2)

    rho=(lambda_p - 0.188)/(lambda_p^2);

    end
end

% Reduction of internal compression element
if es(i,2)==1

    % Effective width
    b_eff=c(i)*rho;

    be1=0.5*b_eff;
    be2=0.5*b_eff;

    % New coordinates for reduced flange, the coordinates in y-axis
    % stays the same because the flange is always at 0° from x-axis

    Ex_flange(end+1,1)=Ex(i,1);
    Ex_flange(end,2)=(Ex(i,1)+be1);

    Ex_flange(end+1,1)=(Ex(i,2)-be2);
    Ex_flange(end,2)=Ex(i,2);

    Ey_flange(end+1,1)=Ey(i,1);
    Ey_flange(end,2)=Ey(i,2);

    Ey_flange(end+1,1)=Ey(i,1);
    Ey_flange(end,2)=Ey(i,2);

    % New thickness vector for reduced part
    t_flange(end+1)=t(i);
    t_flange(end+1)=t(i);

    % New class matrix that accounts for the new element of the
    % reduced flange and puts them in class 3
    class_flange(end+1)=3;
    class_flange(end+1)=3;

    % New part info matrix for added element in flange
    es_flange(end+1,:)=es(i,:);
    es_flange(end+1,:)=es(i,:);
```

```

% Reduction of external compression element
elseif es(i,2)==2

    % Effective width
    b_eff=c(i)*rho;

    % New coordinates for reduced flange, the coordinates in y-axis
    % stays the same because the flange is always at 0° from x-axis
    Ex_flange(end+1,1)=Ex(i,1);
    Ex_flange(end,2)=Ex(i,2);

    Ey_flange(end+1,1)=(Ey(i,2)-b_eff);
    Ey_flange(end,2)=Ey(i,2);

    % New thickness vector for reduced part
    t_flange(end+1)=t(i);

    % New class matrix that accounts for the new element of the
    % reduced flange and puts them in class 3
    class_flange(end+1)=3;

    % New part info matrix for added element in flange
    es_flange(end+1,:)=es(i,:);

end
end

%-----Reduction of edge fold-----

if es(i,3)==3

    % K_sigma for edge fold
    if (c(i)/c(i-1) <= 0.35)

        K_sigma=0.5;

    else

        K_sigma=0.5 + 0.83*(((c(i)/c(i-1))-0.35)^2)^(1/3);
    end
end

```

```
end

% Slenderness of edge fold
lambda_p=(c(i)/t(i))/(28.4*epsilon*sqrt(K_sigma));

% Reduction factor
rho=(lambda_p-0.188)/lambda_p^2;

% Reduction factor may not exceed 1
if rho > 1

    rho=1;

end

% Effective width
b_eff=c(i)*rho;

% New coordinates for reduced edge fold
Ex_flange(end+1,1)=Ex(i,1);
Ex_flange(end,2)=Ex(i,2);

Ey_flange(end+1,1)=(Ey(i,2)-b_eff);
Ey_flange(end,2)=Ey(i,2);

% New thickness vector for reduced edge fold
t_flange(end+1)=t(i);

% New class vector for reduced edge fold
class_flange(end+1)=3;

% New info matrix for reduced edge fold
es_flange(end+1,:)=es(i,:);

end
end
end
end
```

## A.5 Distorsional buckling

```
function [chi_d,t_n,t_flange]=...
    DistortionalBuckling(Ex_flange,Ey_flange,...
    Ex_n,Ey_n,es_flange,es_n,t_flange,t_n,b_f,h_w,c,E,fy,v)
```





```
%  
%  
%          StressDistribution_m PartPosition_n PartType_n]  
%  
%          [n,3] Matrix, one row for each part  
%  
% StressDistribution      1 for Compression only  
%                        2 for Bending  
%                        3 for Compression and Bending  
%  
% PartPosition           1 for Internal compression part  
%                        2 for Outstand flange  
%  
% PartType               1 Web  
%                        2 Flange  
%                        3 Edge fold  
%  
%  
% t_flange               Vector with edge stiffener thickness for  
%                        elements that needs to be reduced (class 4)  
%                        [n,1] matrix  
%  
% t_n                    Element thickness for elements not in class 4  
%                        [n,1] matrix  
%  
% b_f                    Flange width  
%  
% h_w                    Web hieght  
%  
% c                      Length of edge fold  
%  
% E                      Young's Modulus  
%  
% fy                     Yield strength  
%  
% v                      Poisson's ratio  
%  
%  
% OUTPUT:  
% chi_d:                 Reduction factor for thickness of edge stiffener  
%  
% t_n:                   Vector with edge stiffener  
%                        thickness for non reduced elements  
%  
% t_flange:              Vector with edge stiffener thickness for  
%                        reduced elements  
%
```

```
%-----  
%  
% LAST MODIFIED: 2022-04-26 by Mahdi Mahdi  
%-----  
  
% Output matrices  
chi_d=1;  
A_s=0;  
  
t_stiff=[];  
Ex_stiff=[];  
Ey_stiff=[];  
  
% Calculating the area of the edge stiffener (Edge fold + effective part of  
% flange)  
  
%-----If no flange or edge fold are in CSC 4-----  
    if isempty(Ex_flange)  
  
        t0=t_n(1);  
  
        for i=1:length(es_n)  
  
            % Length of each part  
            c_stiff(i)=sqrt((Ex_n(i,2)-Ex_n(i,1))^2 + (Ey_n(i,2)-Ey_n(i,1))^2);  
  
            if es_n(i,3)==3  
  
                % Area of edge stiffener  
                A_s(i)=t0*(c_stiff(i-1) + c_stiff(i));  
  
                % Coordinates for edge fold in stiffener  
                Ex_stiff(end+1,:)=Ex_n(i,:);  
                Ey_stiff(end+1,:)=Ey_n(i,:);  
  
                % Coordinates for flange in stiffener  
                Ex_stiff(end+1,:)=Ex_n(i-1,:);  
                Ey_stiff(end+1,:)=Ey_n(i-1,:);  
  
                % Thickness for edge fold and flange in stiffener  
                t_stiff(end+1)=t0;  
                t_stiff(end+1)=t0;  
  
                % Effective width of flange  
                be2=c_stiff(i-1);
```

```
end
end

else

    t0=t_flange(1);

    for i=1:length(Ex_flange)

        % Length of each part
        c_stiff(i)=sqrt((Ex_flange(i,2)-Ex_flange(i,1))^2 +...
            (Ey_flange(i,2)-Ey_flange(i,1))^2);

        if es_flange(i,3)==3

%-----If only the edge folds are in CSC 4-----

            if all(es_flange(:,3)==3)

                % Area of edge stiffener
                A_s(i)=t0*(b_f + c_stiff(i));

                % Coordinates for edge fold in stiffener
                Ex_stiff(end+1,:)=Ex_flange(i,:);
                Ey_stiff(end+1,:)=Ey_flange(i,:);

                % Coordinates for flange in stiffener
                Ex_stiff(end+1,1)=Ex_flange(i,1)-b_f;
                Ex_stiff(end,2)=Ex_flange(i,1);

                Ey_stiff(end+1,1)=Ey_flange(i,2);
                Ey_stiff(end,2)=Ey_flange(i,2);

                % Thickness for edge fold and flange in stiffener
                t_stiff(end+1)=t0;
                t_stiff(end+1)=t0;

                % Effective width of flange
                be2=b_f;
```

```
%-----If flange and edge fold are in CSC 4-----

    else

        % Area of edge stiffener
        A_s(i)=t0*(c_stiff(i-1) + c_stiff(i));

        % Coordinates for edge fold in stiffener
        Ex_stiff(end+1,:)=Ex_flange(i,:);
        Ey_stiff(end+1,:)=Ey_flange(i,:);

        % Coordinates for flange in stiffener
        Ex_stiff(end+1,:)=Ex_flange(i-1,:);
        Ey_stiff(end+1,:)=Ey_flange(i-1,:);

        % Thickness for edge fold and flange in stiffener
        t_stiff(end+1)=t0;
        t_stiff(end+1)=t0;

        % Effective width of flange
        be2=c_stiff(i-1);

    end
end
end
end

% Area of edge stiffener (only one edge stiffener)
if any(A_s~=0)
    A_s=nonzeros(A_s);
    A_s=A_s(end);
end

%-----if only flanges are in CSC 4-----

if isempty(Ex_stiff)

    % Coordinates for edge fold and flange in stiffener
    Ex_stiff(end+1,:)=Ex_flange(end,:);
    Ex_stiff(end+1,:)=Ex_flange(end,:);

    Ey_stiff(end+1,:)=Ey_flange(end,:);
    Ey_stiff(end+1,1)=Ey_flange(end,1)-c;
    Ey_stiff(end+1,2)=Ey_flange(end,2);
```

```
% Thickness for edge fold and flange in stiffener
t_stiff=[t0
        t0];

% Calculating y_tp for edge stiffener
y_tp_stiff=ytp(Ex_stiff,Ey_stiff,t_stiff);

% Calculating second moment of area for edge stiffener
I_s=SecondMomentOfArea(Ex_stiff,Ey_stiff,t_stiff,y_tp_stiff);

% Effective width of flange
be2=sqrt((Ex_flange(end,1)-Ex_flange(end,2))^2 +...
        (Ey_flange(end,1)-Ey_flange(end,2))^2);

% Area of edge stiffener
A_s=t0*(be2+c);

%-----Calculating ytp and I_s for edge stiffener-----

else
    % Calculating y_tp for edge stiffener
    y_tp_stiff=ytp(Ex_stiff(end-1:end,:),Ey_stiff(end-1:end,:),...
                  t_stiff(end-1:end));

    % Calculating Second moment of area for edge stiffener
    I_s=SecondMomentOfArea(Ex_stiff(end-1:end,:),...
                          Ey_stiff(end-1:end,:),t_stiff(end-1:end),y_tp_stiff);

end

%-----Checking for distorsional buckling-----

% For symmetrical sections in compression k_f=1
k_f=1;

% Distance from web to the centre of the effective area of edge stiffener
b_1=b_f - (be2*t0*(be2/2))/(A_s);
b_2=b_1;

% Spring stiffness, only for C and back to back C sections
K=((E*t0^3)/(4*(1-v^2)))*((1)/(b_1^2*h_w + b_1^3 + 0.5*b_1*b_2*h_w*k_f));
```

```
% Critical stress for edge stiffener
sigma_cr_s=(2*sqrt(K*E*I_s))/(A_s);

% Slenderness
lamnda_d=sqrt(fy/sigma_cr_s);

% Reduction factor
if lamnda_d <= 0.65

    chi_d=1.0;

elseif (0.65<lamnda_d) && (lamnda_d<1.38)

    chi_d=1.47 - 0.723*lamnda_d;

elseif lamnda_d > 1.38

    chi_d=0.66/lamnda_d;
end

% Reducing thickness of edge stiffener with reduction factor chi_d
if isempty(Ex_flange)

    for i=1:length(t_n)

        if es_n(i,3)==3

            t_n(i-1:i)=chi_d*t_n(i-1);

        end
    end
else

    for i=1:length(t_flange)

        if all(es_flange(:,3)==3)

            t_flange(i)=chi_d*t_flange(i);

        elseif es_flange(i,3)==3

            t_flange(i-1:i)=chi_d*t_flange(i-1:i);

        end
    end
end
```

```

    end
end

```

## A.6 Reduction of hexagon

```

function [Ex_web,Ey_web,t_web]=ReductionHexa(Ex,Ey,t,es,class,epsilon)

% Written by: Mahdi Mahdi & Sarah Aref, Chalmers University of Technology
% Master's Thesis 2022
%-----
% PURPOSE
% Reduce inclined webs that are in cross-section class 4.
%
% INPUT:  Ex = [x_1 x_2;
%              .
%              .
%              .
%              x_n x_m]
%
%         Ey = [y_1 y_2;
%              .
%              .
%              .
%              y_n y_m]      [n,2] Matrix, Element node coordinates
%                               Each row corresponds to a new part
%
%         es = [StressDistribution_1 PartPosition_1 PartType_1;
%              .
%              .
%              .
%              StressDistribution_m PartPosition_n PartType_n]
%
%                               [n,2] Matrix, one row for each part
%
% StressDistribution      1 for Compression only
%                        2 for Bending
%                        3 for Compression and Bending
%
% PartPosition           1 for Internal compression part
%                        2 for Outstand flange
%
% PartType               1 Web
%                        2 Flange
%                        3 Edge fold
%
% t                     Element thickness [n,1] matrix

```



```
%
%      class      [n,1] Matrix for CSC of each part
%                  n: Cross-section class for each element
%
%      epsilon      Strain relation
%
%
% OUTPUT:
%
% Ex_web & Ey_web:      Coordinates for reduced inclined webs
%
%      t_web:      Thickness for reduced inclined webs
%
%-----
%
% LAST MODIFIED: 2022-04-26 by Mahdi Mahdi
%-----

% Creating output matrices
Ex_web=[];
Ey_web=[];
t_web=[];

be1=[];
be2=[];

%-----Reduction of web-----

% Start values for reduction factor rho
rho=[1;1];

for i=1:length(class)

    % Length of element
    c(i)=sqrt((Ex(i,2)-Ex(i,1))^2 + (Ey(i,2)-Ey(i,1))^2);

    % Reduction for all parts in class 4 if cross-section is in compression
    % only
    if (class(i)==4) && es(i,3)==1

        % For compression zeta is always 1 for flanges
        zeta=1;
```

```
K_sigma=4;

% Slenderness
lambda_p=(c(i)/t(i))/(28.4*epsilon*sqrt(K_sigma));

% Reduction factor rho for internal compression element
if es(i,2)==1

    if lambda_p <= 0.673

        rho=1;

    else
        rho=(lambda_p - 0.055*(3+zeta))/(lambda_p^2);
    end

% Reduction of internal compression element

if es(i,2)==1

    % Effective width
    b_eff=c(i)*rho;

    be1(end+1)=0.5*b_eff;
    be2(end+1)=0.5*b_eff;

end
end
end

%-----New coordinates for reduced inclined web-----

% If no reduction is done
if isempty(be1)

% First element

% Part 1
Ex_web(end+1,:)=Ex(2,:);

Ey_web(end+1,:)=Ey(2,:);
```

```
t_web(end+1)=t(1);

% Second element

% Part 1
Ex_web(end+1,:)=Ex(3,:);

Ey_web(end+1,:)=Ey(3,:);

t_web(end+1)=t(1);

% Third element

% Part 1
Ex_web(end+1,:)=Ex(5,:);

Ey_web(end+1,:)=Ey(5,:);

t_web(end+1)=t(1);

% Fourth element

% Part 1
Ex_web(end+1,:)=Ex(6,:);

Ey_web(end+1,:)=Ey(6,:);

t_web(end+1)=t(1);

% If webs are reduced
else

% First element

% Part 1
Ex_web(end+1,1)=Ex(2,1);
Ex_web(end,2)=(Ex(2,1)-(be1(1)*cos(pi/3)));

Ey_web(end+1,1)=Ey(2,1);
Ey_web(end,2)=Ey(2,1) + (be1(1)*sin(pi/3));
```

```
% Part 2
Ex_web(end+1,1)=Ex(2,2) + (be2(1)*cos(pi/3));
Ex_web(end,2)=Ex(2,2);

Ey_web(end+1,1)=Ey(2,2) - (sin(pi/3)*be2(1)) ;
Ey_web(end,2)=Ey(2,2);

t_web(end+1)=t(1);
t_web(end+1)=t(1);

% Second element

% Part 1
Ex_web(end+1,1)=Ex(3,1);
Ex_web(end,2)=(Ex(3,1)+(be1(2)*cos(pi/3)));

Ey_web(end+1,1)=Ey(3,1);
Ey_web(end,2)=Ey(3,1) + (be1(2)*sin(pi/3));

% Part 2
Ex_web(end+1,1)=Ex(3,2) - (be2(2)*cos(pi/3));
Ex_web(end,2)=Ex(3,2);

Ey_web(end+1,1)=Ey(3,2) - (sin(pi/3)*be2(2)) ;
Ey_web(end,2)=Ey(3,2);

t_web(end+1)=t(1);
t_web(end+1)=t(1);

% Third element

% Part 1
Ex_web(end+1,1)=Ex(5,1);
Ex_web(end,2)=(Ex(5,1)-(be1(3)*cos(pi/3)));

Ey_web(end+1,1)=Ey(5,1);
Ey_web(end,2)=Ey(5,1) + (be1(3)*sin(pi/3));

% Part 2
Ex_web(end+1,1)=Ex(5,2) + (be2(3)*cos(pi/3));
Ex_web(end,2)=Ex(5,2);

Ey_web(end+1,1)=Ey(5,2) - (sin(pi/3)*be2(3)) ;
Ey_web(end,2)=Ey(5,2);

t_web(end+1)=t(1);
```

```
t_web(end+1)=t(1);

% Fourth element

% Part 1
Ex_web(end+1,1)=Ex(6,1);
Ex_web(end,2)=(Ex(6,1)+(be1(4)*cos(pi/3)));

Ey_web(end+1,1)=Ey(6,1);
Ey_web(end,2)=Ey(6,1) + (be1(4)*sin(pi/3));

% Part 2
Ex_web(end+1,1)=Ex(6,2) - (be2(4)*cos(pi/3));
Ex_web(end,2)=Ex(6,2);

Ey_web(end+1,1)=Ey(6,2) - (sin(pi/3)*be2(4)) ;
Ey_web(end,2)=Ey(6,2);

t_web(end+1)=t(1);
t_web(end+1)=t(1);

end
end
```

## A.7 Web reduction

```
function [Ex_web,Ey_web,t_web]=WebReduction(Ex,Ey,t,es,y_tp,class,...
                                             epsilon,M,N,I_gross,A_gross)

% Written by: Mahdi Mahdi, Chalmers University of Technology
% Master's Thesis 2022
%-----
% PURPOSE
% Reduce web that are in cross-section class 4
%
% INPUT:  Ex = [x_1 x_2;
%              .
%              .
%              .
%              x_n x_m]
%
%         Ey = [y_1 y_2;
%              .
%              .
%              .
%              y_n y_m]      [n,2] Matrix, Element node coordinates
```

```
%                               Each row corresponds to a new part
%
%       es = [StressDistribution_1 PartPosition_1 PartType_1;
%             .
%             .
%             .
%             StressDistribution_m PartPosition_n PartType_n]
%
%                               [n,2] Matrix, one row for each part
%
% StressDistribution      1 for Compression only
%                       2 for Bending
%                       3 for Compression and Bending
%
% PartPosition           1 for Internal compression part
%                       2 for Outstand flange
%
% PartType               1 Web
%                       2 Flange
%                       3 Edge fold
%
%       t                Element thickness [n,1] matrix
%
%       y_tp             Distance from bottom of cross-section to
%                       centroid
%
%       class            [n,1] Matrix for CSC of each part
%                       n: cross-section classification
%                       for each element
%
%       epsilon          Strain relation
%
%       M                Moment
%
%       N                Normal force
%
%       I_gross          Gross second moment of area
%
%       A_gross          Gross sectional area
%
% OUTPUT:
%
%       Ex_web & Ey_web  Coordinates for reduced web
%
%       t_web            Thickness for reduced web
%
```

```
%-----  
%  
% LAST MODIFIED: 2022-03-22 by Mahdi Mahdi  
%-----  
  
% Output matrices  
Ex_web=[];  
Ey_web=[];  
t_web=[];  
es_web=[];  
class_web=[];  
  
%-----Stress relation: psi-----  
  
for i=1:length(Ex)  
  
    % Length of element  
    c=sqrt((Ex(i,2)-Ex(i,1))^2 + (Ey(i,2)-Ey(i,1))^2);  
  
    % If part is in class 4 than area needs to be reduced  
    if (class(i)==4) && (max(Ey(i,:)) > y_tp) && (es(i,3)==1)  
  
        % If part is in compression only the stress ratio is equal on both  
        % sides of the part, psi=1  
        if es(i,1)==1  
  
            psi=1;  
  
            % If part is in bending but the whole part  
            % is in the compression zone than psi is expressed as the  
            % following:  
            elseif (es(i,1)==2) && Ey(i,1) >= y_tp  
  
                psi=(Ey(i,1)-y_tp)/(Ey(i,2)-y_tp);  
  
            % If part is in bending and the part is both in the  
            % compression zone and the tension zone than psi is  
            % expressed as the following:  
            elseif (es(i,1)==2) && Ey(i,1) < y_tp  
  
                h_c=max(max(Ey))-y_tp;  
  
                psi=(h_c-max(max(Ey)))/h_c;  
  
            % If part is in bending & compression than psi is expressed as  
            % following:
```

```
elseif (es(i,1)==3)

    % Section modulus
    W_bottom=I_gross/y_tp;
    W_top=I_gross/(max(max(Ey)) - y_tp);

    W=min(W_bottom,W_top);

    % Stress for moment and normal force
    sigma_M=M/W;
    sigma_N=N*A_gross;

    psi=(sigma_M - sigma_N) / (sigma_M + sigma_N);
end

%-----Buckling factor, K_sigma-----

% Internal compression elements
if es(i,2)==1

    if psi==1
        K_sigma=4;

    elseif (1>psi) && (psi>0)

        K_sigma=8.2/(1.05+psi);

    elseif psi==0

        K_sigma=7.81;

    elseif (0>psi) && (psi>-1)

        K_sigma=7.81 - 6.29*psi + 9.78*psi^2;

    elseif psi==-1

        K_sigma=23.9;

    elseif (-1>psi) && (psi>-3)

        K_sigma=5.98*(1-psi)^2;
```



```

        end
    end

    % Slenderness
    lambda_p=(c/t(i))/(28.4*epsilon*sqrt(K_sigma));

    if (lambda_p <= 0.673) && (es(i,2)==1)

        rho=1.0;

%-----Reduction factor-----

        elseif (lambda_p > 0.673) && (es(i,2)==1)

            rho=(lambda_p - 0.055*(3+psi))/(lambda_p^2);

        elseif (lambda_p <= 0.748) && (es(i,2)==2)

            rho=1;

        elseif (lambda_p > 0.748) && (es(i,2)==2)

            rho=(lambda_p - 0.188)/(lambda_p^2);

        end

    if psi<0

%-----New coordinates for reduced web elements-----

        % Effective width
        b_eff=(rho*c)/(1-psi);

        be1=0.4*b_eff;
        be2=0.6*b_eff;

        % New x coordinates for reduced web elements
        Ex_web(end+1,1)=Ex(i,1);
        Ex_web(end,2)=Ex(i,1);

        Ex_web(end+1,1)=Ex(i,2);
        Ex_web(end,2)=Ex(i,2);

        % New y coordinates for reduced web elements
        Ey_web(end+1,1)=Ey(i,1) ;
        Ey_web(end,2)=y_tp + be2;
    
```

```
Ey_web(end+1,1)=Ey(i,2) - be1;
Ey_web(end,2)=Ey(i,2);

% New thickness vector
t_web(end+1)=t(i);
t_web(end+1)=t(i);

% New class matrix that accounts for the new element of the
% reduced web
class_web(end+1)=3;
class_web(end+1)=3;

% New part info matrix for added element in web
es_web(end+1,:)=es(i,:);
es_web(end+1,:)=es(i,:);

elseif psi==1

% Effective width
b_eff=c*rho;

be1=0.5*b_eff;
be2=0.5*b_eff;

% New x coordinates for reduced web elements
Ex_web(end+1,1)=Ex(i,1);
Ex_web(end,2)=Ex(i,1);

Ex_web(end+1,1)=Ex(i,2);
Ex_web(end,2)=Ex(i,2);

% New y coordinates for reduced web elements
Ey_web(end+1,1)=Ey(i,1) ;
Ey_web(end,2)=Ey(i,1) + be1;

Ey_web(end+1,1)=Ey(i,2) - be2;
Ey_web(end,2)=Ey(i,2);

% New thickness vector
t_web(end+1)=t(i);
t_web(end+1)=t(i);
```

```

        % New class matrix that accounts for the new element of the
        % reduced web
        class_web(end+1)=3;
        class_web(end+1)=3;

        % New part info matrix for added element in web
        es_web(end+1,:)=es(i,:);
        es_web(end+1,:)=es(i,:);

    end
end
end
end

```

## A.8 Torsion constant

```

function [I_T]=TorsionConstant(Ex,Ey,t,m,A)

% Written by: Sarah Aref, Chalmers University of Technology
% Master's Thesis 2022
%-----
% PURPOSE
% Compute the torsion constant of a cross-section.
%
% INPUT:   Ex = [x_1 x_2;
%               .
%               .
%               .
%               x_n x_m]
%
%          Ey = [y_1 y_2;
%               .
%               .
%               .
%               y_n y_m]    [n,2] Matrix, Element node coordinates
%                           Each row corresponds to a new part, n is
%                           number of parts
%
%          t      Element thickness [n,1] matrix
%
%          m      Type of cross-section
%                  m=1 open cross-section
%                  m=2 closed cross-section
%
%

```

```
%          A          Area of the gross cross-section
%
%
% OUTPUT:
%          I_T:      Torsion constant
%-----
%
% LAST MODIFIED: 2022-04-26 by Sarah Aref
%-----

I_Ti=0;

%-----Open cross-section-----
if m==1

for i=1:length(Ex)

    % Length of each element
    c=sqrt((Ex(i,2)-Ex(i,1))^2 + (Ey(i,2)-Ey(i,1))^2);

    % Calculating torsion constant for each element
    I_Ti(i)=(c*t(i)^3)/3;

end
    % Total torsion constant for open sections
    I_T=sum(I_Ti);

%-----Closed cross-section-----
else

P=0;
for i=1:length(Ex)

    % Length of each element
    c=sqrt((Ex(i,2)-Ex(i,1))^2 + (Ey(i,2)-Ey(i,1))^2);

    % Total length of all elements
    P=P+c;

end

    % Torsion constant for a closed section
    I_T=4*A^2*t(i)/P;

end
```

## A.9 Warping constant

```
function [I_w]=WarpingConstant(Ex,Ey,t,c,bf,hw,s)

% Written by: Sarah Aref, Chalmers University of Technology
% Master's Thesis 2022
%-----
% PURPOSE
% Compute the warping constant of a cross-section.
%
% INPUT:  Ex = [x_1 x_2;
%              .
%              .
%              .
%              x_n x_m]
%
%          Ey = [y_1 y_2;
%              .
%              .
%              .
%              y_n y_m]    [n,2] Matrix, Element node coordinates
%                          Each row corresponds to a new part, n is
%                          number of parts
%
%          t      Element thickness [n,1] matrix
%
%          c      Length of edge fold
%
%          bf     Length of flange
%
%          hw     Height of cross-section
%
%          s      Type of cross-section
%                  s=1 Lipped c-section
%                  s=2 back-to-back lipped c-section
%                  s=3 Closed sections
%
% OUTPUT:
%          I_w:    Warping constant
%-----
%
% LAST MODIFIED: 2022-04-26 by Sarah Aref
%-----

%Distance to centroid, from the bottom of cross-section
```

```
y_tp=ytp(Ex,Ey,t);

%Second moment of area around y-axis
I_y=SecondMomentOfArea(Ex,Ey,t,y_tp);

alpha=0.69;

%Shear centre coordinates with respect to the centroid of the gross
%cross-section
e=(bf*hw^2/I_y)*c*t(1)*(1/2+bf/(4*c)-(2/3*c^2/hw^2));

if s==1          %Lipped c-section

    % Warping constant
    I_w=((hw^2*bf^2*t(1))/12)*((2*hw^3*bf + 3*hw^2*bf^2 ...
        + alpha*(48*c^4 + 112*bf*c^3 + 8*hw*c^3 + 48*hw*bf*c^2 ...
        + 12*hw^2*c^2 + 12*hw*bf*c + 6*hw^3*c))/(6*hw^2*bf + ...
        (hw + alpha*2*c)^3 - alpha*24*hw*c^2));

elseif s==2      %Back-to-back lipped c-section

    % Warping constant for a c-section
    I_w=((hw^2*bf^2*t(1))/12)*((2*hw^3*bf + 3*hw^2*bf^2 ...
        + alpha*(48*c^4 + 112*bf*c^3 + 8*hw*c^3 + 48*hw*bf*c^2 ...
        + 12*hw^2*c^2 + 12*hw*bf*c + 6*hw^3*c))/(6*hw^2*bf + ...
        (hw + alpha*2*c)^3 - alpha*24*hw*c^2));

    % Total warping constant of the cross-section
    I_w=I_w*2;

elseif s==3      % Closed sections

    % Warping constant
    I_w=0;

end
end
```

## A.10 Flexural buckling

```
function [Chi_Fy, Chi_Fz, Lambda_y, Lambda_z]=...
    FlexuralBuckling(Ex,Ey,t,A_eff,E,fy,L_cr)

% Written by: Mahdi Mahdi, Chalmers University of Technology
```

```
% Master's Thesis 2022
%-----
% PURPOSE
% Calculate the reduction factors for flexural buckling in the two main
% planes, y-y and z-z.
%
% INPUT:  Ex = [x_1 x_2;
%              .
%              .
%              .
%              x_n x_m]
%
%         Ey = [y_1 y_2;
%              .
%              .
%              .
%              y_n y_m]    [n,2] Matrix, Element node coordinates
%                          Each row corresponds to a new part
%
%         t      Element thickness [n,1] matrix
%
%         A_eff  Effective area of cross-section
%
%         E      Young's modulus
%
%         fy     Yield strength
%
%         L_cr   Critical buckling length
%
% OUTPUT:
%
%         Chi_Fy: Reduction factor for buckling around the y-y plane
%
%         Chi_Fz: Reduction factor for buckling around the z-z plane
%
%         Lambda_y: Slenderness of y-y plane
%
%         Lambda_z: Slenderness of z-z plane
%
%-----
%
% LAST MODIFIED: 2022-03-29 by Mahdi Mahdi
%-----
```

```
% Calculate the distance from centroid to bottom of cross-section
% (y-y and z-z plane) and gross cross-sectional area
[y_tp,A_gross]=ytp(Ex,Ey,t);
z_tp=ytp(Ey,Ex,t);

% Calculate the second moment of area around y-y and z-z plane
I_y=SecondMomentOfArea(Ex,Ey,t,y_tp);
I_z=SecondMomentOfArea(Ey,Ex,t,z_tp);

%-----Flexural buckling calculations-----
Lambda_1=pi*sqrt(E/fy);

% Radii of gyration
i_y=sqrt(I_y/A_gross);
i_z=sqrt(I_z/A_gross);

% Slenderness
Lambda_y=(L_cr/i_y) * (sqrt(A_eff/A_gross)/Lambda_1);
Lambda_z=(L_cr/i_z) * (sqrt(A_eff/A_gross)/Lambda_1);

% Imperfection factors

if fy >= 460 % Yield strength greater than 460 MPa

    alpha_y=0.13;
    alpha_z=0.13;

else % Steel with yield strength less than 420 MPa

    alpha_y=0.21;
    alpha_z=0.34;

end

theta_y=0.5*(1 + alpha_y*(Lambda_y - 0.2) + Lambda_y^2 );
theta_z=0.5*(1 + alpha_z*(Lambda_z - 0.2) + Lambda_z^2 );

% Reduction factors
Chi_Fy= 1 / (theta_y + sqrt(theta_y^2 - Lambda_y^2 ));
Chi_Fz= 1 / (theta_z + sqrt(theta_z^2 - Lambda_z^2 ));
```



```
% Reduction factors should not be greater than 1.0
if Chi_Fy > 1

    Chi_Fy=1;

elseif Chi_Fz > 1

    Chi_Fz=1;

end
end
```

## A.11 Torsional buckling

```
function [chi_T,Ncr_T]=TorsionalBuckling(Ex,Ey,t,A_eff,I_w,...
                                         I_T,E,v,L_cr,n,fy,b_f,h_w,c_p)

% Written by: Sarah Aref, Chalmers University of Technology
% Master's Thesis 2022
%-----
% PURPOSE
% Compute the reduction factor for torsional buckling
%
% INPUT:
%     Ex = [x_1 x_2;
%           .
%           .
%           .
%           x_n x_m]
%
%     Ey = [y_1 y_2;
%           .
%           .
%           .
%           y_n y_m]      [n,2] Matrix, Element node coordinates
%                           Each row corresponds to a new part
%
%     t      Element thickness [n,1] matrix
%
%     A_eff   Effective area of the cross-section
%
%     I_w     Warping constant
%
%     I_T     Torsion constant
%
```

```
%      E      Modulus of elasticity
%
%      v      Poisson's ratio
%
%      L_cr    Buckling length of the member
%
%      n      Type of cross-section      n=1    Lipped c-section
%                                           n=2    Symmetrical section
%      fy      Yield strength
%
% OUTPUT:
%
%      chi_T:   Reduction factor for torsional buckling
%      Ncr_T:   Elastic critical force for torsional buckling
%-----
%
% LAST MODIFIED: 2022-04-26 by Sarah Aref
%-----
```

```
% Shear modulus
G=E/(2*(1+v));

% Distance to centroid, calculated from the bottom of the cross-section
[y_tp,A]=ytp(Ex,Ey,t);
z_tp=ytp(Ey,Ex,t);

% Second moment of area around y-axis
I_y=SecondMomentOfArea(Ex,Ey,t,y_tp);

% Second moment of area around z-axis
I_z=SecondMomentOfArea(Ey,Ex,t,z_tp);

% Radius of gyration of the gross cross-section about the y-y axis
i_y=sqrt(I_y/A);

%Radius of gyration of the gross cross-section about the z-z axis
i_z=sqrt(I_z/A);

if n==1 %Lipped c-section

% Shear centre co-ordinates with respect to the centroid of the gross
% cross-section
y_o=0;
z_o=(b_f*h_w^2/I_y)*c_p*t*(1/2+b_f/(4*c_p)-(2/3*c_p^2/h_w^2));
```

```
elseif n==2 %Symmetric cross-section

% Shear centre co-ordinates with respect to the centroid of the gross
% cross-section
y_o=0;
z_o=0;

end

i_o=i_y^2+i_z^2+y_o^2+z_o^2;

% Elastic critical force for torsional buckling
Ncr_T=(1/i_o)*(G*I_T+((pi^2*E*I_w)/L_cr^2));

% Non-dimensional slenderness
lambda_T=sqrt(A_eff*fy/Ncr_T);

% Imperfection factors

if fy<=420      % Yield strength less than 420 MPa
alpha_T=0.34;   % Buckling curve b

elseif fy>=460  % Yield strength greater than 460 MPa
alpha_T=0.13;   % Buckling curve a0

end

phi_T=0.5*(1+alpha_T*(lambda_T-0.2)+lambda_T^2);

% Reduction factor for torsional buckling
chi_T=1/(phi_T+sqrt(phi_T^2-lambda_T^2));

% Reduction factors should not be greater than 1.0
if chi_T > 1

    chi_T=1;

end
end
```

## A.12 Flexural-torsional buckling

```
function [chi_FT]=FTBuckling(Ex,Ey,t,A_eff,fy,E,L_cr,Ncr_T,n,b_f,h_w,c_p)

% Written by: Sarah Aref, Chalmers University of Technology
```

```
% Master's Thesis 2022
%-----
% PURPOSE
% Compute the reduction factor for flexural-torsional buckling
%
% INPUT:
%     Ex = [x_1 x_2;
%           .
%           .
%           .
%           x_n x_m]
%
%     Ey = [y_1 y_2;
%           .
%           .
%           .
%           y_n y_m]      [n,2] Matrix, Element node coordinates
%                           Each row corresponds to a new part
%
%     t      Element thickness [n,1] Matrix
%
%     A_eff   Effective area of the cross-section
%
%     fy      Yield strength
%
%     E       Modulus of elasticity
%
%     L_cr    Buckling length of the member
%
%     Ncr_T   Elastic critical force for torsional buckling
%
%     n       Type of cross-section      n=1   Lipped c-section
%                                           n=2   Symmetrical section
%
%     b_f     Width of flange
%
%     h_w     Height of web
%
%     c_p     Height of edge fold
%
% OUTPUT:
%
%     chi_FT:  Reduction factor for flexural-torsional buckling
%-----
%
% LAST MODIFIED: 2022-04-26 by Sarah Aref
```

```
%-----

% Distance to centroid, calculated from the bottom the cross-section
[y_tp,A]=ytp(Ex,Ey,t);
z_tp=ytp(Ey,Ex,t);

% Second moment of area around y-axis
I_y=SecondMomentOfArea(Ex,Ey,t,y_tp);

% Second moment of area around z-axis
I_z=SecondMomentOfArea(Ey,Ex,t,z_tp);

% Radius of gyration of the gross cross.section about the y-y axis
i_y=sqrt(I_y/A);

% Radius of gyration of the gross cross.section about the z-z axis
i_z=sqrt(I_z/A);

if n==1 %Lipped c-section

%Shear centre co-ordinates with respect to the centroid of the gross
%cross-section
y_o=0;
z_o=(b_f*h_w^2/I_y)*c_p*t(1)*(1/2+b_f/(4*c_p)-(2/3*c_p^2/h_w^2));

elseif n==2 %Symmetric cross-section

% Shear centre co-ordinates with respect to the centroid of the gross
% cross-section
y_o=0;
z_o=0;

end

i_o=i_y^2+i_z^2+y_o^2+z_o^2;

% Elastic critical force
Ncr_y=(I_y*pi^2*E)/L_cr^2;

beta=1-(y_o/sqrt(i_o))^2;

% Elastic critical force for flexural-torsional buckling
Ncr_FT=Ncr_y/(2*beta)*(1+(Ncr_T/Ncr_y)-sqrt((1+(Ncr_T/Ncr_y))^2-...
    4*beta*(Ncr_T/Ncr_y)));

% Non-dimensional slenderness
```

```
lambda_FT=sqrt(A_eff*fy/Ncr_FT);

% Imperfection factor

if fy<=420      % Yield strength less than 420 MPa
alpha_FT=0.34;  % Buckling curve b

elseif fy>=460 % Yield strength greater than 460 MPa
alpha_FT=0.13;  % Buckling curve a0
end

phi_FT=0.5*(1+alpha_FT*(lambda_FT-0.2)+lambda_FT^2);

% Reduction factor for flexural-torsional buckling
chi_FT=1/(phi_FT+sqrt(phi_FT^2-lambda_FT^2));

% Reduction factors should not be greater than 1.0
if chi_FT > 1

    chi_FT=1;

end
end
```

## A.13 Lateral-torsional buckling

```
function [chi_LT]=LTBuckling(Ex,Ey,hw,bf,c,t,I_eff,I_w,I_T,E,v,...
                             L_cr,n,fy,ytp_eff)
```

```
% Written by: Sarah Aref, Chalmers University of Technology
% Master's Thesis 2022
%-----
% PURPOSE
%   Compute the reduction factor for lateral-torsional buckling
%
% INPUT:
%       Ex = [x_1 x_2;
%             .
%             .
%             .
%             x_n x_m]
%
%       Ey = [y_1 y_2;
%             .
%             .
%             .
%             y_n y_m]
```

```
%
%      .
%      .
%      y_n y_m]      [n,2] Matrix, Element node coordinates
%                      Each row corresponds to a new part
%
%      t      Element thickness [n,1] matrix
%
%      A_eff   Effective area of the cross-section
%
%      I_w     Warping constant
%
%      I_T     Torsion constant
%
%      E       Modulus of elasticity
%
%      v       Poisson's ratio
%
%      L_cr    Buckling length of the member
%
%      n       Type of cross-section      n=1    Lipped c-section
%                                           n=2    Symmetrical section
%      fy      Yield strength
%
%
%
% OUTPUT:
%      chi_LT:      Reduction factor for lateral-torsional buckling
%
%-----
%
% LAST MODIFIED: 2022-04-26 by Sarah Aref
%-----
```

```
%Shear modulus
G=E/(2*(1+v));
```

```
%Distance to centroid, calculated from the bottom of the cross-section
y_tp=ytp(Ex,Ey,t);
z_tp=ytp(Ey,Ex,t);
```

```
%Second moment of area around y-axis
I_y=SecondMomentOfArea(Ex,Ey,t,y_tp);
```

```
%Second moment of area around z-axis
I_z=SecondMomentOfArea(Ey,Ex,t,z_tp);
```

```
if n==1 %Lipped c-section

%Shear centre co-ordinates with respect to the centroid of the gross
%cross-section

z_o=(bf*hw^2/I_y)*c*t(1)*(1/2+bf/(4*c)-(2/3*c^2/hw^2));

elseif n==2 %Symmetric cross-section

%Shear centre co-ordinates with respect to the centroid of the gross
%cross-section

z_o=0;

end

zj=z_o;

C1=1.127;
C3=0.525;
kz=1;

% Elastic critical force for torsional buckling
M_cr=C1*((pi^2*I_z*E)/(kz*L_cr)^2)*(((I_w/I_z)+((kz*L_cr)^2*...
    G*I_T)/(pi^2*E*I_z)))+(C3*zj)^2)^0.5+C3*zj);

% Section modulus
W_eff_t=I_eff/ytp_eff;

W_eff_c=I_eff/(max(max(Ey))-ytp_eff);

W_eff_min=min(W_eff_t,W_eff_c);

% Non-dimensional slenderness
lambda_LT=sqrt(W_eff_min*fy/M_cr);

% Imperfection factor

if fy<=420      % Yield strength less than 420 MPa
alpha_LT=0.34;  % Buckling curve b

elseif fy>=460  % Yield strength greater than 460 MPa
alpha_LT=0.13;  % Buckling curve a0
```



```

end

phi_LT=0.5*(1+alpha_LT*(lambda_LT-0.2)+lambda_LT^2);

%Reduction factor for torsional buckling
chi_LT=1/(phi_LT+sqrt(phi_LT^2-lambda_LT^2));

% Reduction factors should not be greater than 1.0
if chi_LT > 1

    chi_LT=1;

end
end

```

## A.14 Interaction of combined bending and axial compression

```

function [eta_y,eta_z]=Interaction(N_Ed,chi_y,chi_z,chi_LT,...
    M_Ed,fy,z_tp_eff,z_tp,class,A_gross,A_eff,W_eff,W,M_s,M_h,...
    lambda_y,lambda_z)

% Written by: Sarah Aref & Mahdi Mahdi, Chalmers University of Technology
% Master's Thesis 2022
%-----
% PURPOSE
% Interaction criteria for bending and axial compression of an element
%
% INPUT:
%
%     N_Ed      Design value of the compression force
%     chi_y     Reduction factor due to flexural buckling (y-y plane)
%     chi_z     Reduction factor due to flexural buckling (z-z plane)
%     chi_LT    Reduction factor due to lateral torsional buckling
%     M_Ed      Design value of the maximum moment along the member
%     fy        Yield strength
%     z_tp_eff  Distance to centroid (z-axis) of effective
%               cross-section
%     z_tp      Distance to centroid (z-axis)
%     class     Cross-section class
%     A_gross   Area of gross cross-section
%     A_eff     Effective area
%     W_eff     Effective section modulus

```

```
%      W      Section modulus
%      M_s     Moment in the span
%      M_h     Moment at the support
%      lambda_y Slenderness (y-y plane)
%      lambda_z Slenderness (z-z plane)
%
%
% OUTPUT:
%
%      eta_y:   Requirement 1 for members subjected to bending and axial
%               compression, should be less than 1
%
%      eta_z:   Requirement 2 for members subjected to bending and axial
%               compression, should be less than 1
%-----
% LAST MODIFIED: 2022-04-26 by Sarah Aref
%-----

%Partial factor
gamma_M1=1;

%Shift in z-axis
e_Ny=z_tp_eff-z_tp;

%Moment due to shift in centroidal axis
deltaM_Ed=N_Ed*e_Ny;

if any(class==4)

    N_Rk=fy*A_eff;

    M_Rk=fy*W_eff;

else

    N_Rk=fy*A_gross;

    M_Rk=fy*W;

end

%Moment ratio in span vs support
alpha_s=M_s/M_h;

if alpha_s<0
%Assuming that Psi is constant(Psi=1)
if 0.1-0.8*alpha_s>=0.4
```

## A. Appendix: Matlab functions

---

```
%Moment factors
C_my=0.1-0.8*alpha_s;
C_mLT=C_my;

else
    %Moment factors
    C_my=0.4;
    C_mLT=C_my;
end

elseif alpha_s>0

    %Assuming that Psi is constant(Psi=1)
    if 0.2+0.8*alpha_s>=0.4

        %Moment factors
        C_my=0.2+0.8*alpha_s;
        C_mLT=C_my;

    else
        %Moment factors
        C_my=0.4;
        C_mLT=C_my;
    end
end

L=C_my*(1+0.6*lambda_y*(N_Ed/(chi_y*N_Rk/gamma_M1)));
R=C_my*(1+0.6*(N_Ed/(chi_y*N_Rk/gamma_M1)));

if L<=R

    %Interaction factor
    k_yy=L;

else
    %Interaction factor
    k_yy=R;
end

LH=1-((0.05*lambda_z/(C_mLT-0.25))*(N_Ed/(chi_z*N_Rk/gamma_M1)));
RH=1-((0.05/(C_mLT-0.25))*(N_Ed/(chi_z*N_Rk/gamma_M1)));

if LH>=RH

L
```

```
%Interaction factor
k_zy=LH;

else
    %Interaction factor
    k_zy=RH;
end

%Check 1
eta_y=(N_Ed/(chi_y*(N_Rk/gamma_M1)))+...
    (k_yy*((M_Ed+deltaM_Ed)/(chi_LT*(M_Rk/gamma_M1))));

%Check 2
eta_z=(N_Ed/(chi_z*(N_Rk/gamma_M1)))+...
    (k_zy*((M_Ed+deltaM_Ed)/(chi_LT*(M_Rk/gamma_M1))));

end
```



# B

## Appendix: Example of cross-section resistance calculations

```
%-----INPUTS-----

% Geomatrix inputs
h_w=125; %mm;
b_f=100; %mm;
c_p=20; %mm
t0=2.4; %mm

% Distance of gap between webs
d=10; %mm

% Mastrial parameters
E=210000; %N/mm^2
v=0.3;

% Coordinate matrix for y-axis
Ey=[0 b_f
    0 0
    b_f+d b_f+d+b_f
    b_f+d+b_f b_f+d+b_f
    0 b_f
    0 0
    b_f+d b_f+d+b_f
    b_f+d+b_f b_f+d+b_f
    b_f b_f
    b_f+d b_f+d];

% Coordinate matrix for z-axis
Ez=[0 0
    0 c_p
    0 0]
```

## B. Appendix: Example of cross-section resistance calculations

---

```
0 c_p
h_w h_w
h_w-c_p h_w
h_w h_w
h_w-c_p h_w
0 h_w
0 h_w];

% Thickness vector
t=t0*ones(length(Ey),1);

% Properties of each element
es=[1 1 2
    1 2 3
    1 1 2
    1 2 3
    1 1 2
    1 2 3
    1 1 2
    1 2 3
    1 1 1
    1 1 1];

%-----CSC-----

[~,class,epsilon]=CSC(Ey,Ez,t,fy,es);

%-----Ytp-----
[y_tp,A_gross]=ytp(Ey,Ez,t);

%-----REDUCTION OF CROSS-SECTION-----

% Finding coordinates for all elements that are not in class 4
Ex_n=[];
Ey_n=[];
t_n=[];
class_n=[];
es_n=[];

for i=1:length(class)

    c(i)=sqrt((Ey(i,2)-Ey(i,1))^2 + (Ez(i,2)-Ez(i,1))^2);
```

```

    if class(i)~=4

        Ex_n(end+1,:)=Ey(i,:);
        Ey_n(end+1,:)=Ez(i,:);

        t_n(end+1)=t(i);

        class_n(end+1)=class(i);

        es_n(end+1,:)=es(i,:);

    end

end

% Finding coordinates for all web elements that are not in class 4
Ex_n_webb=[];
Ey_n_webb=[];
t_n_webb=[];
class_n_webb=[];
es_n_webb=[];

for i=1:length(class)

    c(i)=sqrt((Ey(i,2)-Ey(i,1))^2 + (Ez(i,2)-Ez(i,1))^2);

    if (class(i)==4) && (es(i,3)==1)

        Ex_n_webb(end+1,:)=Ey(i,:);
        Ey_n_webb(end+1,:)=Ez(i,:);

        t_n_webb(end+1)=t(i);

        class_n_webb(end+1)=class(i);

        es_n_webb(end+1,:)=es(i,:);

    end

end

end

```



```
% Moment of area for gross cross-section
[I_gross]=SecondMomentOfArea(Ey,Ez,t,y_tp);

% Finding coordinates for reduced flange elements
t_flange=[];
[Ex_flange,Ey_flange,t_flange,es_flange]=...
    flangeReduction(Ey,Ez,t,es,y_tp,class,epsilon);

% Checking distortional buckling and reducing edge stiffeners thickness
[chi_d,t_n,t_flange]=...
    DistortionalBuckling(Ex_flange,Ey_flange,...
        Ex_n,Ey_n,es_flange,es_n,t_flange,t_n,b_f,h_w,c_p,E,fy,v);

% Effective coordinates of the cross-section with reduced flanges and edge
% folds
Ex_eff=[Ex_n; Ex_flange; Ex_n_webb];
Ey_eff=[Ey_n; Ey_flange; Ey_n_webb];

% Effective thickness vector of the cross-section with reduced flanges and
% edge folds
t_eff=[t_n'; t_flange'; t_n_webb'];

% finding y_tp for reduced flange system
[y_tp_eff]=ytp(Ex_eff,Ey_eff,t_eff);

% Reduce the web if in class 4
[Ex_web,Ey_web,t_web]=...
    WebReduction(Ey,Ez,t,es,y_tp_eff,class,epsilon,M_Ed,N_Ed,I_gross,A_gross);

% Effective coordinates of the cross-section with reduced web and flanges
Ex_eff=[Ex_n; Ex_flange; Ex_web];
Ey_eff=[Ey_n; Ey_flange; Ey_web];

% Effective thickness vector of the cross-section with reduced web and
% flanges
t_eff=[t_n'; t_flange'; t_web'];

%-----Cross-section parameters-----

% Y_tp for effective cross-section
[y_tp_eff,A_eff]=ytp(Ex_eff,Ey_eff,t_eff);
```

```
% Effective moment of area
[I_eff]=SecondMomentOfArea(Ex_eff,Ey_eff,t_eff,y_tp_eff);

% Section modulus
w_eff_c=I_eff/(max(max(Ez))-y_tp_eff);
w_eff_t=I_eff/(y_tp_eff);

W_eff=min(w_eff_c,w_eff_t);

w_c=I_gross/(max(max(Ez))-y_tp);
w_t=I_gross/y_tp;

W=min(w_c,w_t);

m=1; % Open cross-section
n=2; % Symmetrical cross-section
s=2; % Liped back-to-back C-section

% Torsional constant
[I_T]=TorsionConstant(Ey,Ez,t,m,A_gross);

% Warping constant
[I_w]=WarpingConstant(Ey,Ez,t,c_p,b_f,h_w,s);

%-----Buckling analysis-----

% Fluxural buckling reduction factors
[Chi_Fy, Chi_Fz, lambda_y, lambda_z]=FlexuralBuckling(Ey,Ez...
,t,A_eff,E,fy,L_cr);

% Torsional buckling reduction factor
[chi_T,Ncr_T]=TorsionalBuckling(Ey,Ez,t,A_eff,I_w,I_T,E,v,L_cr,n,...
fy,b_f,h_w,c_p);

% Torsional-Fluxural buckling reduction factor
[chi_FT]=FTBuckling(Ey,Ez,t,A_eff,fy,E,L_cr,Ncr_T,n);

% LT-Buckling reduction factor
[chi_LT]=LTBuckling(Ey,Ez,h_w,b_f,c_p,t,I_eff,I_w,I_T,E,v,L_cr,...
n,fy,y_tp_eff);

% Shift in centroid
```

```
z_tp=ytp(Ez,Ey,t);
z_tp_eff=ytp(Ey_eff,Ex_eff,t_eff);

e_ny=abs(z_tp-z_tp_eff);

% Utilization ratios for interaction of moment and compressive forces
% (buckling resistance)

[UR2,UR3]=Interaction(N_Ed,Chi_Fy,Chi_Fz,chi_LT,...
    M_Ed,fy,z_tp_eff,z_tp,class,A_gross,A_eff,W_eff,W,M_s,M_h,...
    lambda_y,lambda_z);

% % Design buckling resistance for elements in compression
N_Rd=A_eff*fy;

% Global utilization ratio for bending and compression
UR1=(N_Ed/N_Rd) + ((M_Ed+e_ny*N_Ed)/(W_eff*fy));
```

# C

## Appendix: Genetic Algorithm

### Optimization of double back-to-back C-section; Genetic algorithm upper chord

```
clc
clear

% Applied compression forecs and moments
N_ed=[700 800 900 1300 1400 1600]*1e3; % N
M_ed=14*1e6; % Nmm
m_s=14*1e6; % Nmm
m_h=-14*1e6; % Nmm

% Length of upper chord element
l_cr=3000; % mm

% Steel strenght
f_y=[350 460 690]; %MPa

% All possible combantaions of forces and steel strengths
Comb=combvec(N_ed,f_y);

for j=1:length(Comb)

%Input global variables
global fy
global N_Ed
global M_Ed
global M_s
global M_h
global L_cr

%Output global variables
global UR1
global UR2
```

```
global UR3
global N_bRd

%where we save our variable range

global hw %global hw
global bf %global bf
global c %global c
global t0 %global t0

% choosing relevent forces and steel strenghts for each combination
fy=Comb(2,j);
N_Ed = Comb(1,j);
M_Ed=M_ed;
M_s=m_s;
M_h=m_h;
L_cr=l_cr; %mm

% 4 GA variables, Hw, bf, c and t0
nvars=4;

% Discrete variables
t0=1:0.1:5;

% Lower bounds for variables
LB=ones(1,nvars);

LB(1)=50; % hw
LB(2)=50; % bf
LB(3)=10; % c

% Upper bounds for variables
UB=ones(1,nvars);

UB(1)=160; % hw
UB(2)=200; % bf
UB(3)=60; % c
UB(4)=numel(t0); % t0

% Initial guesses
```

```
for i=1:nvars
    X0(i)=1;
end

% options for GA
options = optimoptions(@ga, ...
    'PopulationSize', nvars*20, ...%should be 100x
    'MaxGenerations', nvars*100, ...
    'EliteCount', 50, ...%50
    'FunctionTolerance', 1e-9, ...
    'PlotFcn', @gaplotbestf); ...
InitialPopulationMatrix = X0;

% Fitness function for area
ObjFcn= @FitnessFunc_Area;

% Constraints function
ConsFcn= @constraints ;

[x,fval,exitflag]= ga (ObjFcn, nvars, [], [], [], [], LB, UB, ConsFcn, 1:nvars, opt
    %x is vector containg the values of optimum solution
    %fval is the value of the fitness function
    %existflag tells if the solution converged & if the constraints are
    %satisfied
    %1:nvars tells GA to use integers only

    ["hw" "bf" "c" "t0"]
    [x(1) x(2) x(3) t0(x(4))])

% Saving all variables
Area(j)=fval;

h_w(j)=x(1);
b_f(j)=x(2);
c_p(j)=x(3);
t_0(j)=t0(x(4));
```

```
N_applied(j)=Comb(1,j);  
fy_used(j)=Comb(2,j);  
L_used(j)=3000;  
  
Ur_global(j)=UR1;  
Ur_interaction_y(j)=UR2;  
  
end
```

DEPARTMENT OF ARCHITECTURE AND CIVIL ENGINEERING  
CHALMERS UNIVERSITY OF TECHNOLOGY  
Gothenburg, Sweden  
[www.chalmers.se](http://www.chalmers.se)



**CHALMERS**  
UNIVERSITY OF TECHNOLOGY